Supplementary materials for:

Anne Aagaard, Jesper Bechsgaard, Jesper Givskov Sørensen, Tobias Sandfeld, Virginia Settepani, Tharina L. Bird, Marie Braad Lund, Kirsten Gade Malmos, Kasper Falck-Rasmussen, Iulia Darolti, Kirstine Lykke Nielsen, Mogens Johannsen, Thomas Vosegaard, Tom Tregenza, Koen J.F. Verhoeven, Judith E. Mank, Andreas Schramm and Trine Bilde

Molecular mechanisms of temperature tolerance plasticity in a social spider.

Contents

Figure S1: Realized ramping temperatures for CTmax and CCRTemp experiments

The relationship between time and temperature for determining a) CTmax and b) CCRTemp.

Coloured circles are measurements of temperature at a given time during ramping, while black circles indicate the mean with standard deviation. A linear model has been fitted on the average: lm = 0.098x + 42.99 for CTmax, and lm = 0.5x + 0.254 for CCRTemp. The number of measurements per timepoint are in table below graphs.

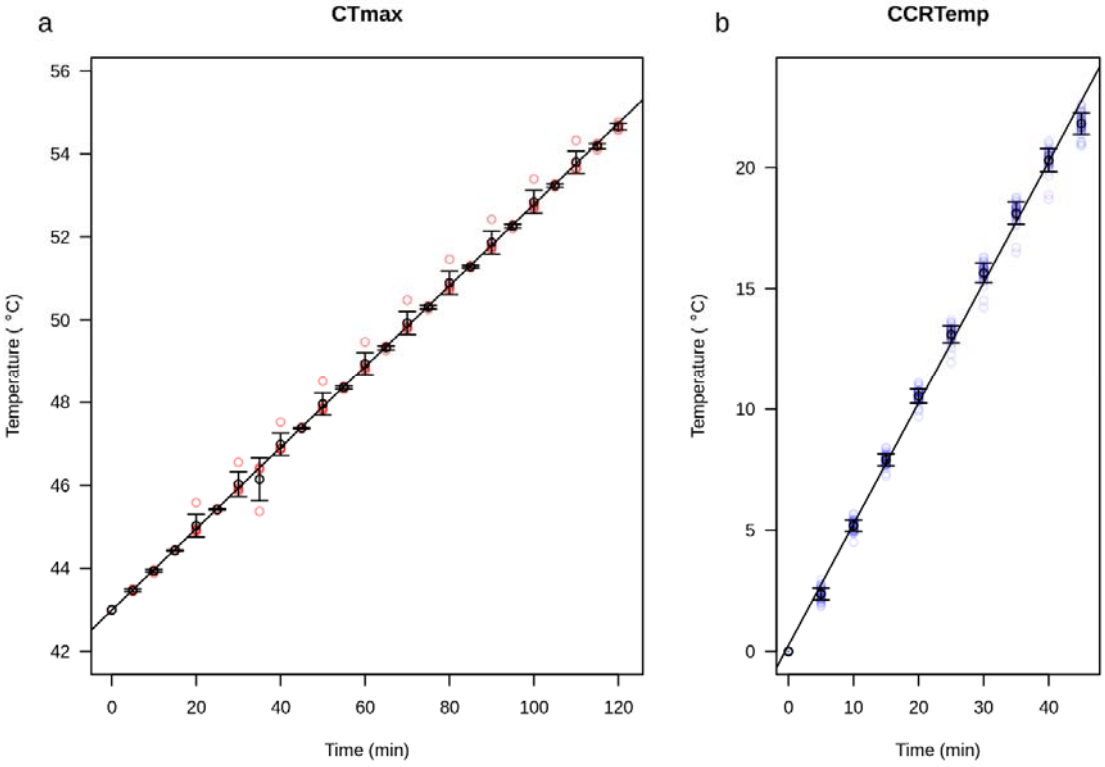

time	N measurements CTmax	N measurements CCRTemp
0	6	38
5	4	38
10	6	38
15	4	38
20	6	38
25	4	38
30	5	38
35	4	38
40	6	37

45	4	36
50	6	
55	4	
60	6	
65	4	
70	6	
75	4	
80	6	
85	4	
90	6	
95	4	
100	6	
105	4	
110	6	
115	4	
120	5	

Figure S2: Growth and survival of spiders in acclimation treatments

Growth rate and survival data of *S. dumicola* spiders as a function of acclimation temperature. Linear models and trend lines have been added to growth rate (a) while binomial models and smoothed lines have been applied to survival data (b).

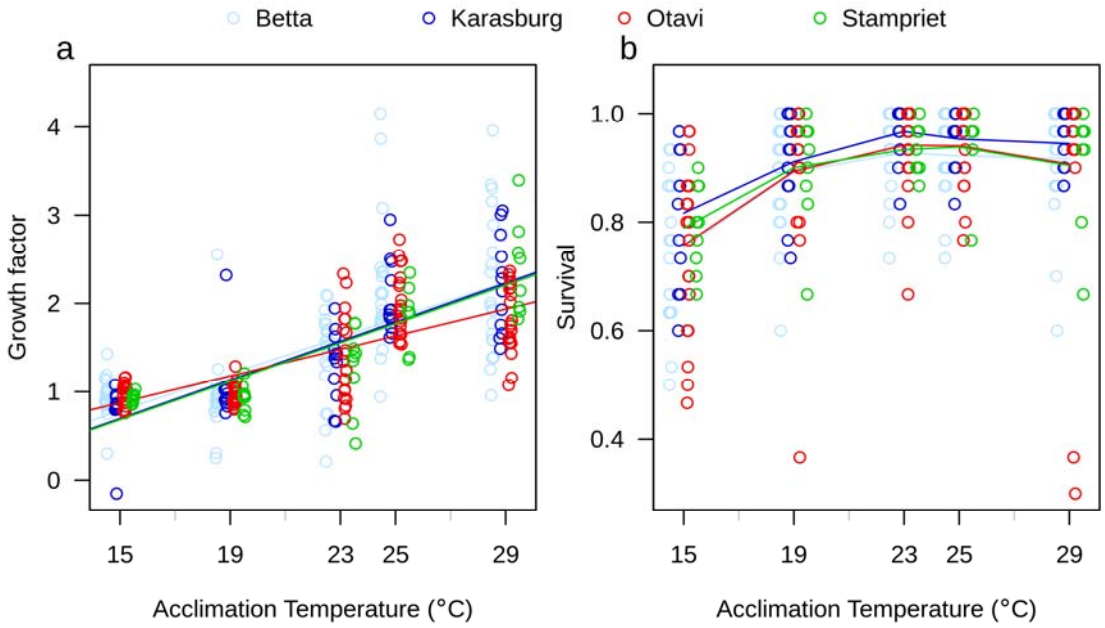

	HSD.tests on models				
		Growth rate (HSD.test)		Survival (emmeans)	
Acclimation temperature effect	**Temperature**	**Estimate**	**Group**	**Estimate (logit)**	**Group**
	15	0.9221065	c	1.48	a
	19	0.9705685	c	1.92	b
	23	1.3633561	b	2.35	c
	25	2.0595457	a	2.57	d
	29	2.0895684	a	3.01	e
Population effect	**Population**	**Estimate**	**Group**	**Estimate (logit)**	**Group**
	Betta	1.534714	a	2.11	a
	Karasburg	1.484138	a	2.53	b
	Otavi	1.411240	a	2.17	a
	Stampriet	1.434181	a	2.23	ab

Figure S3: Plots of additional explanatory variables for CTmax treated spiders

Plots of CTmax as a function of a) body mass (mg), (b) days since feeding, and (c) preacclimation duration (days at 21°C). A linear trend line has been added to the plots for easier interpretation.

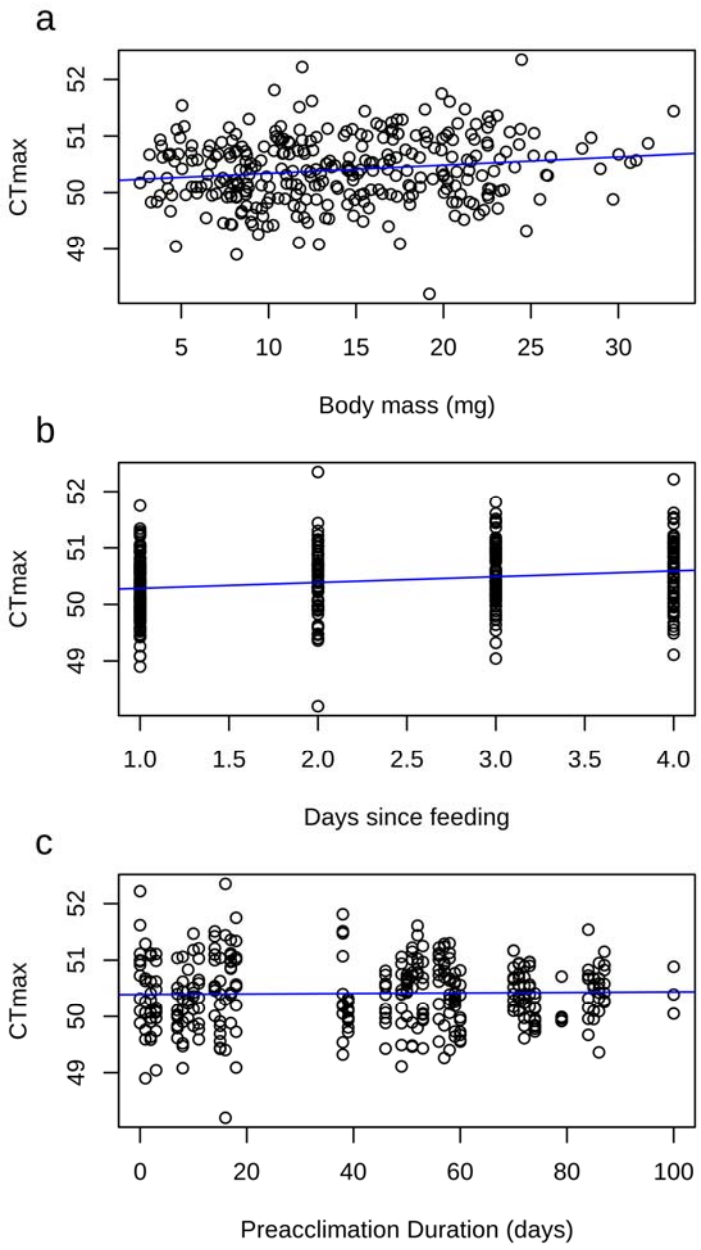

Figure S4: Plots of additional explanatory variables for CCRTemp treated spiders

Plots of CCRTemp as a function of a) body mass (mg), (b) time since feeding, and (c) preacclimation duration (days at 21 °C). A linear trend line has been added to the plots for easier interpretation.

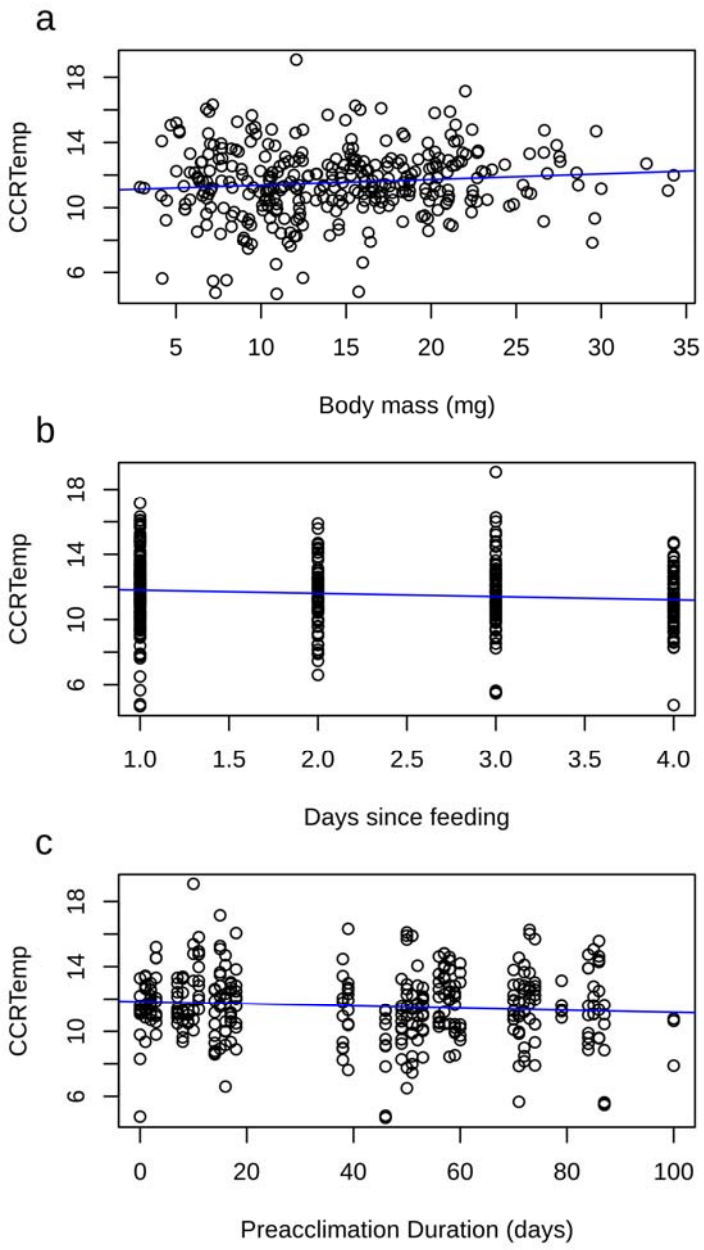

Figure S5: Details on body mass differences in acclimation treatments and populations

Boxplots showing a, c) spider body mass (mg) and population, or b,d) acclimation temperature for spiders used in a, b) CTmax and c, d) CCRTemp assays. For both CTmax and CCRTemp, Betta and Karasburg spider body mass are not statistically different, while both Otavi and Stampriet spider body mass are significantly different from Betta and Karasburg (significance groups annotated on boxplots,). Body mass increases with acclimation temperature (b, d).

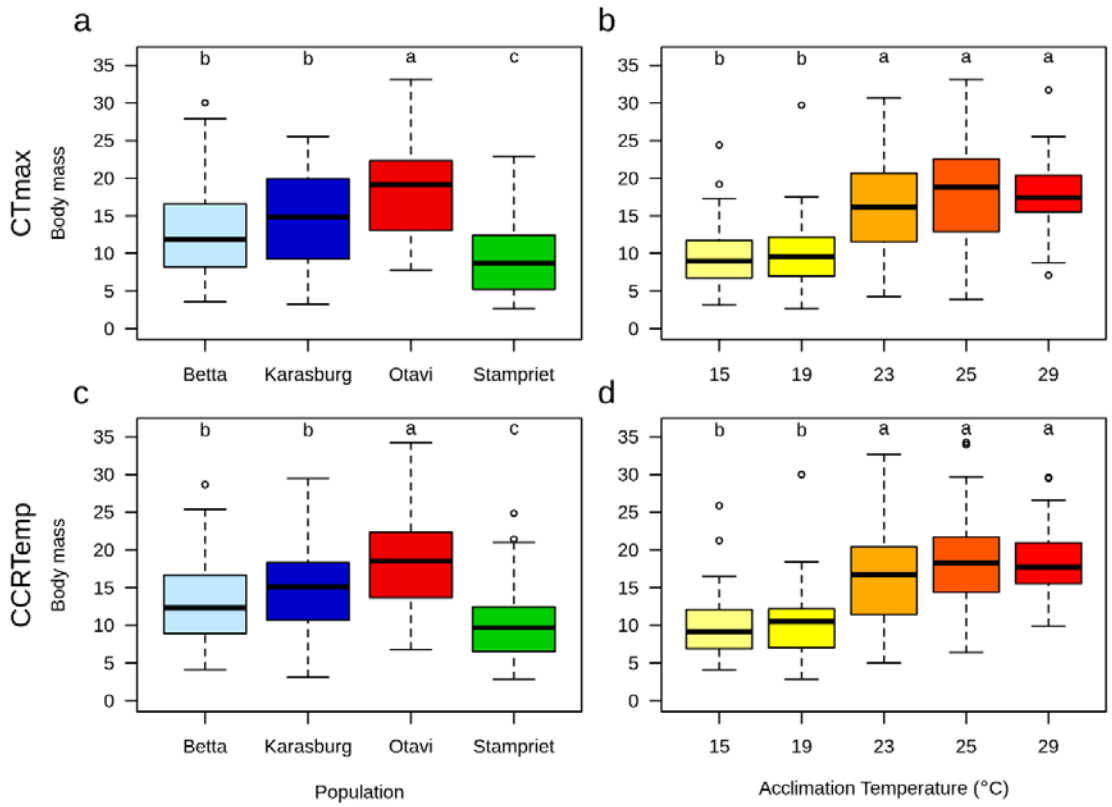

Figure S6: Number of genes with responses to population and temperature in gene expression and DNA methylation

Barplots with the number of genes showing population and temperature responses in gene-wise a) gene expression and b) DNA methylation data. The y axis represents genes showing population responses (Population), acclimation temperature responses (Temperature), both population and temperature responses (Pop+Temp) and an interaction between population and temperature (Interaction). The hashed lines indicate the number of genes with a population response in both DNA methylation and gene expression. The arrow indicates the number of genes we expect to show a population response in both expression (DEG) and methylation (DMG) at random (N $DMGs_{pop}$ / N all genes * N $DEGs_{pop}$).

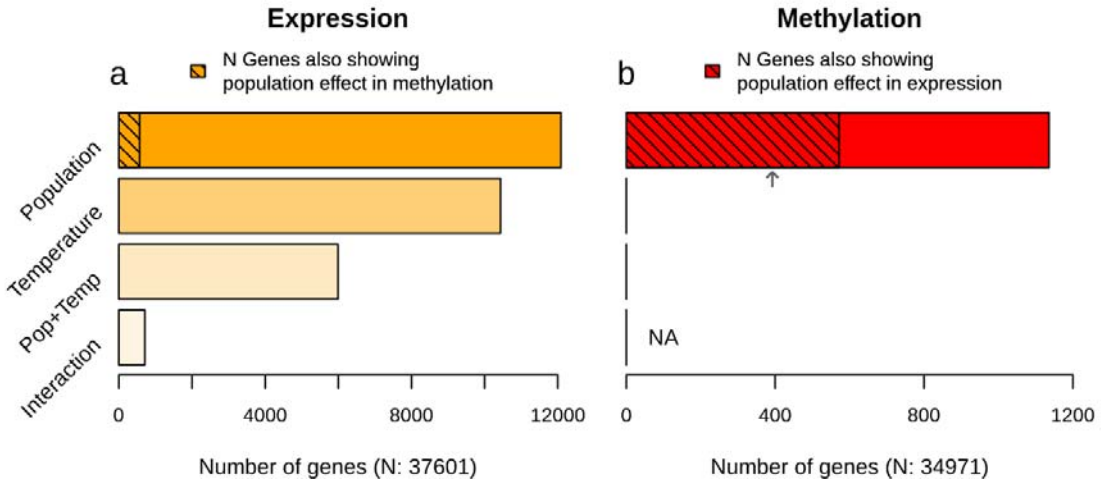

Figure S7: PCA of genes with effect of population and temperature in expression level

Principal component analyses of differentially expressed genes between populations (a, c) and temperature acclimation (b, d). Here, three principal components are plotted. There is a tendency for Otavi (red) and Betta (light blue) to separate from Karasburg (blue) and Stampriet (green).

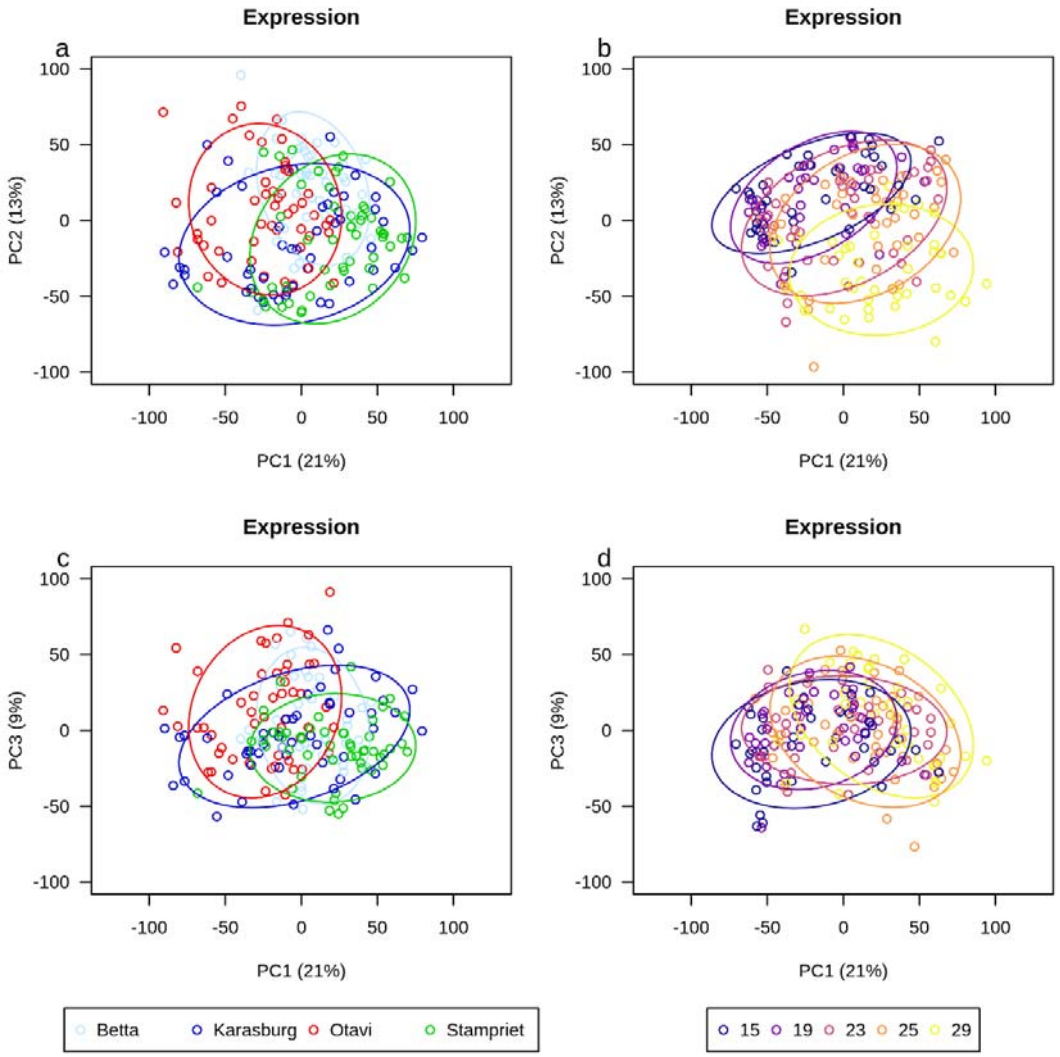

Figure S8: PCA of genes with interaction effect in expression level

Principal component analyses of differentially expressed genes with interaction. Here, three principal components are plotted, along with a screeplot and a biplot. There is a tendency for Otavi (red) and Betta (light blue) to separate from Karasburg (blue) and Stampriet (green) on PC2.

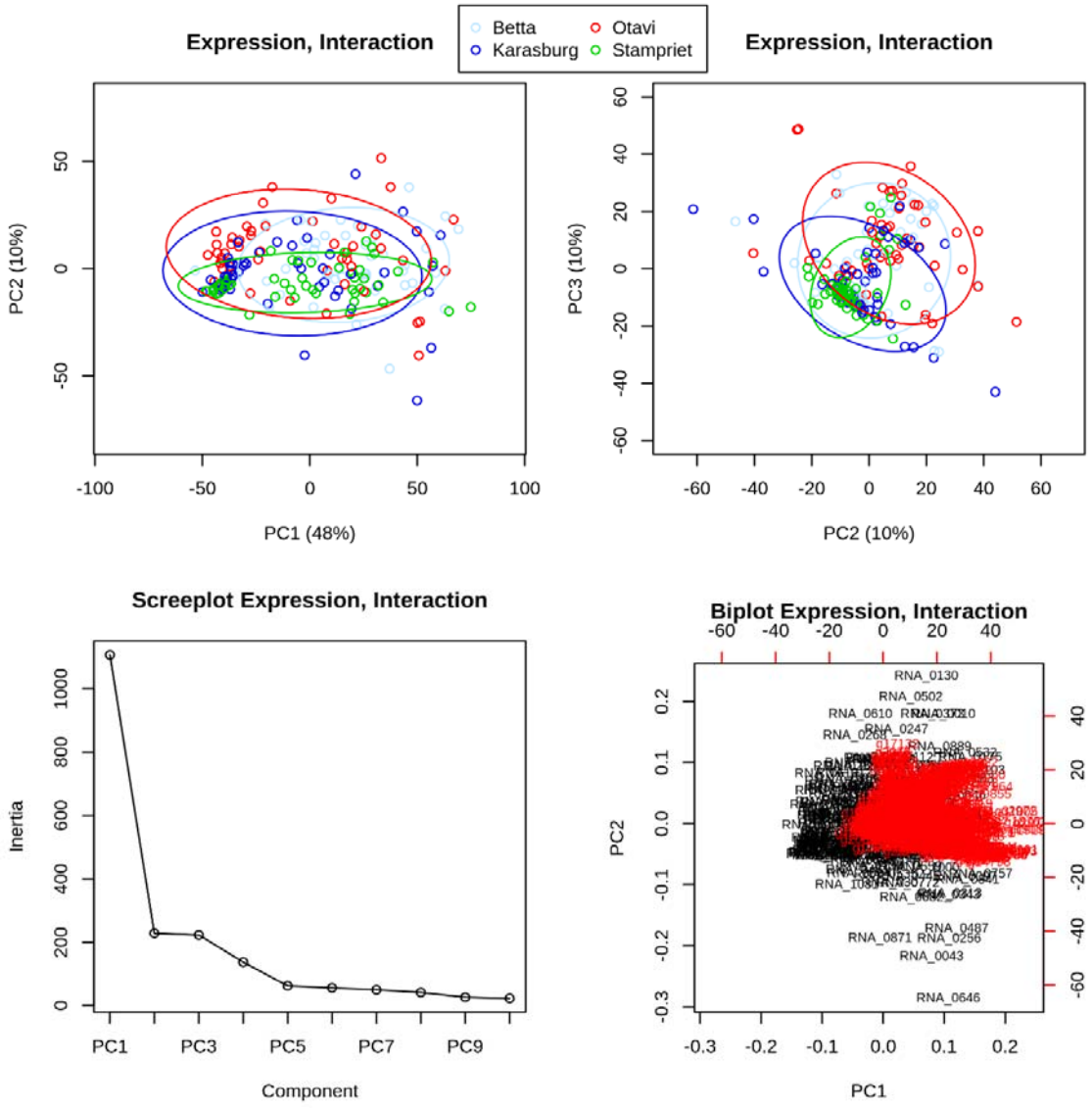

Figure S9: PCA of genes with population effect in weighted methylation level

Principal component analyses of DNA Methylation and population of origin, including Scree- and biplot. Here, three principal components are plotted, along with a screeplot and a biplot. Otavi (red) and Betta (light blue) separate from Karasburg (blue) and Stampriet (green) on PC1.

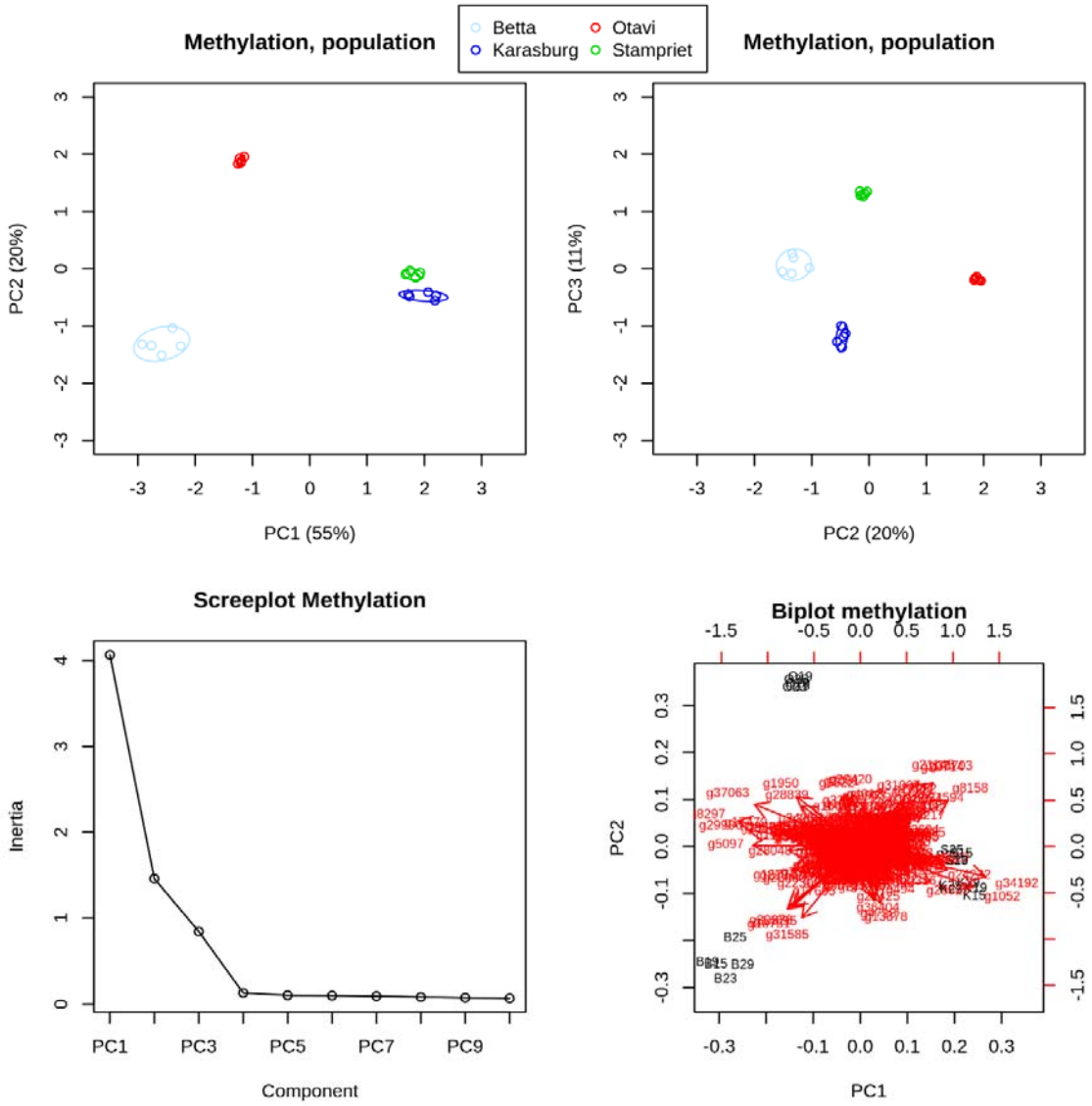

Figure S10: Histogram of correlation coefficients between methylation and gene expression

Histogram of correlation coefficients between gene-wise weighted methylation level and vst transformed normalized gene expression level. All correlated genes showed a population response in both DNA methylation and gene expression. If the distribution is left skewed, then differences in methylation level between populations could be associated with population differences in gene expression. However, this seem to not be the case.

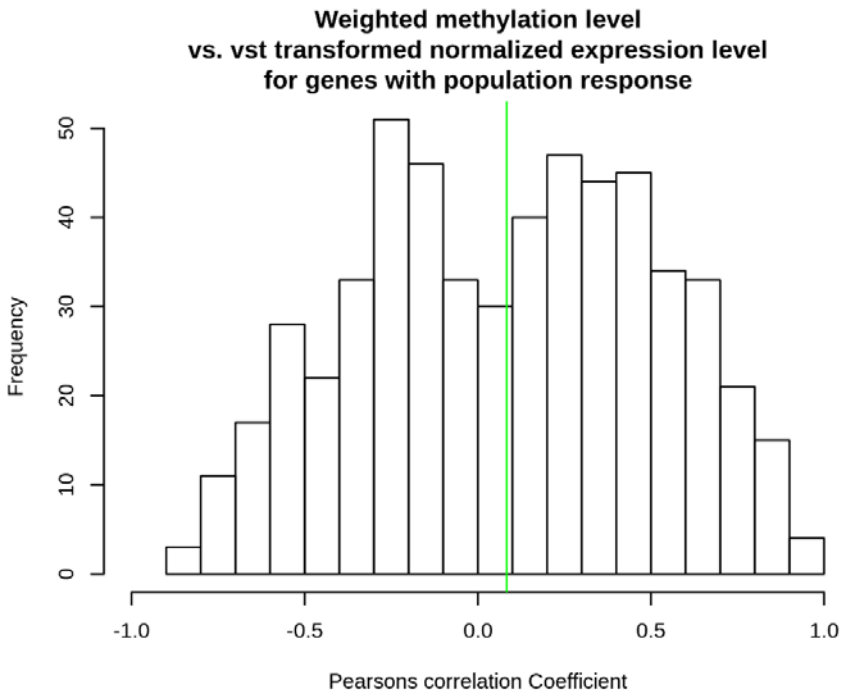

Figure S11: Histogram of correlation coeficients between methylation and stability of gene expression

Histogram of correlation coefficients between weighted methylation level and Standard deviation of vst transformed normalized expression level. All correlated genes showed a population response in both DNA methylation and gene expression. If population specific higher methylation yield a more stable expression level, we would expect a right skew on the distribution. A very subtle right skew can be seen, indicating that such relation is not applicable across all genes.

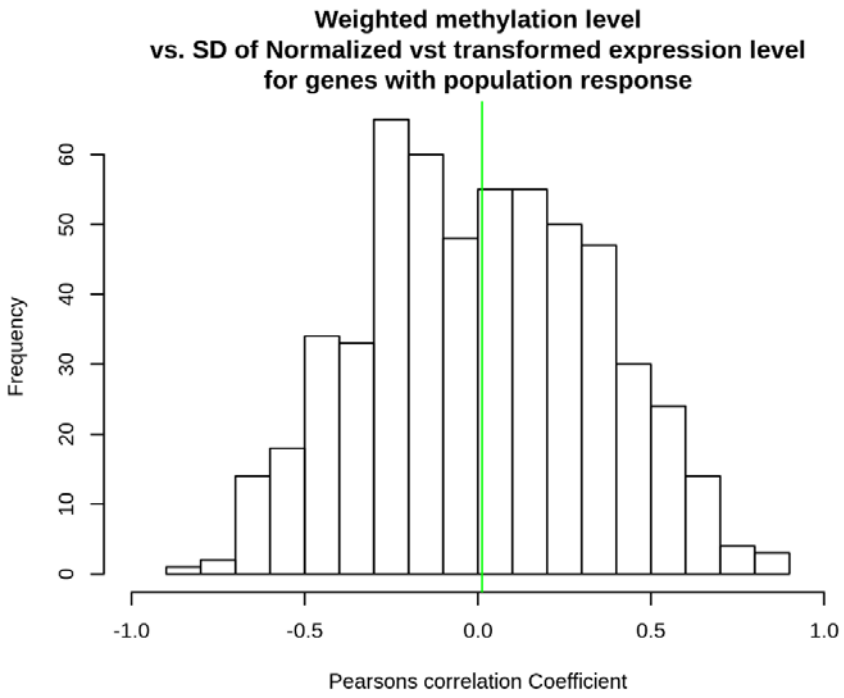

Figure S12: Scatter- and violin plot of gene-wise stability of gene expression as a function of methylation level

Standard deviation in expression (vst transformed for visualisation) in individual genes as a function of weighted methylation level plotted as a) scatterplot and b) violin plot with categorized x axis. Only genes showing effects of population in methylation level was included. Each gene has 20 points on the dot plot (a), one from each acclimation/treatment groups, and colours indicate population. Violin plot (b) shows the stability of gene expression grouped by methylation level. Group limits were based on Liu et al., (2019). Low methylation level has a significantly larger standard deviation than medium and high methylation level (tested on normalised counts). The same result was found using all genes (not shown).

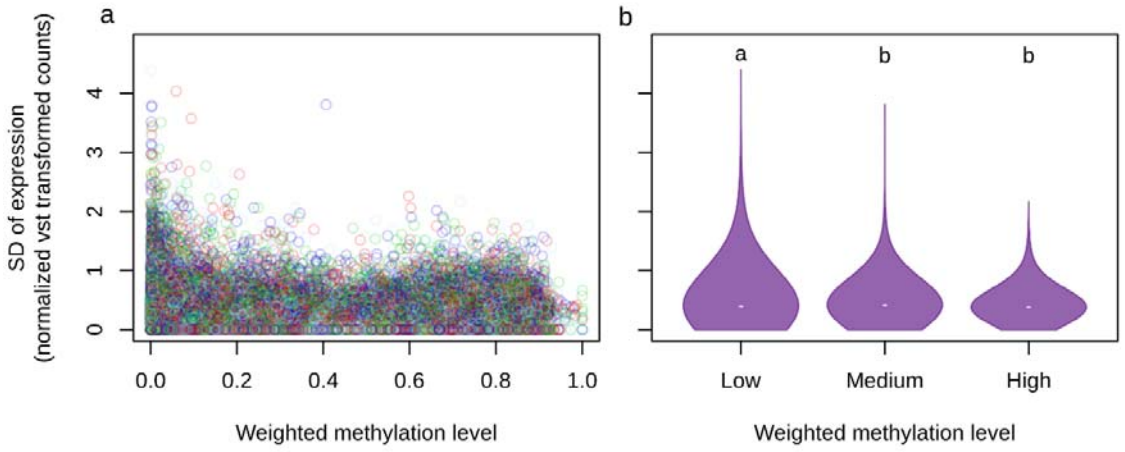

Figure S13: Number of metabolites with responses to population and temperature in LCMS and NMR analyses

Barplots with metabolome data for spiders having undergone CTmax and CCRTemp assays after common garden acclimation. a,b) LC-MS identified metabolites of spiders after a) CTmax assays and b) CCRTemp assays. c,d) NMR peaks of spiders extracted by aquatic solution (AQ, solid bars) or organic solution (ORG, hashed bars), after c) CTmax assay and d) CCRTemp assay. The total number of metabolites or peaks identified can be seen on the x axis label (a,b) or the legend (c,d).

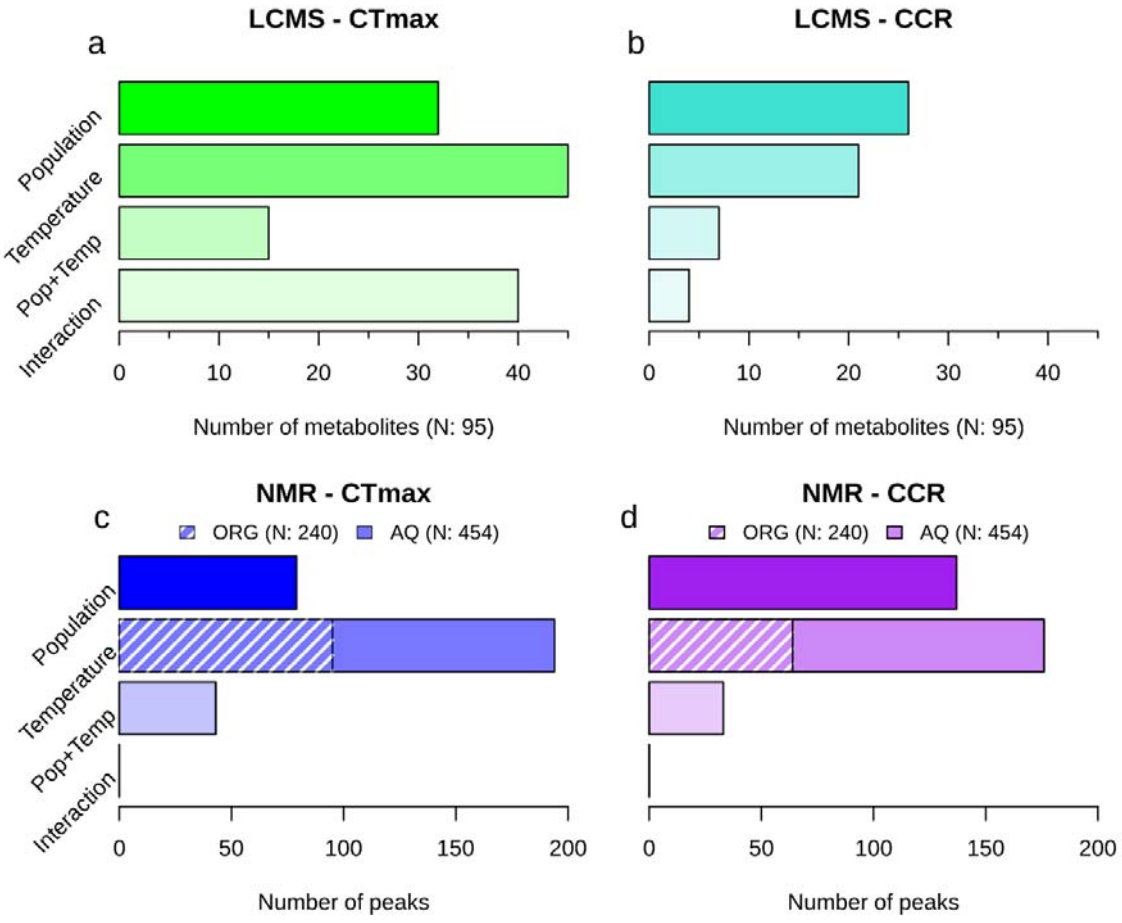

Figure S14: PCA of metabolite LCMS data from the CTmax treatment

Principal component analysis of metabolites from the LC-MS analysis for spiders having undergone CTmax treatment, colored according to population and temperature acclimation. Only metabolites that showed population effects (a, c) or temperature effect (b,d) are plotted. Here the first three principal components are plottet. There is a tendency for Otavi (red) and Betta (light blue) to separate from Karasburg (blue) and Stampriet (green).

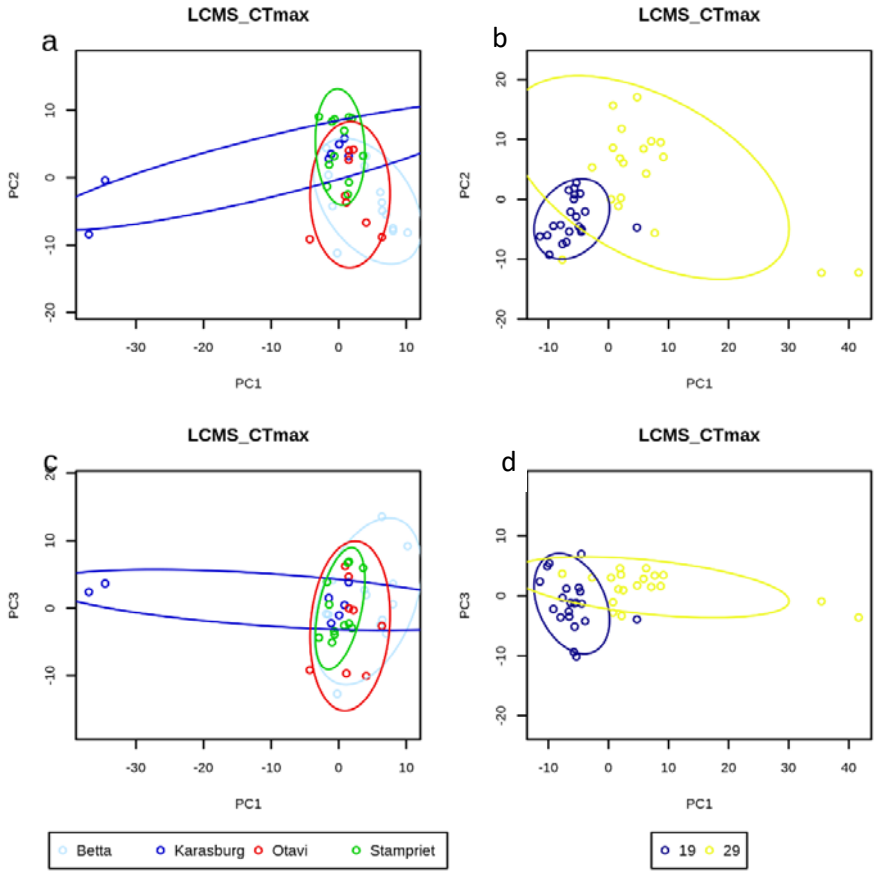

Figure S15: PLS-DA analysis of metabolite data from the CTmax treatment

PLS-DA analysis of metabolites from the NMR analysis of spiders having been through CTmax testing. Points are metabolite intensities that show effect of either population (a, d) or temperature (b, c, e). Rows indicate metabolite extraction and analysis type: a, b) NMR aquatic extraction, c) NMR organic extraction and d, e) LC-MS.

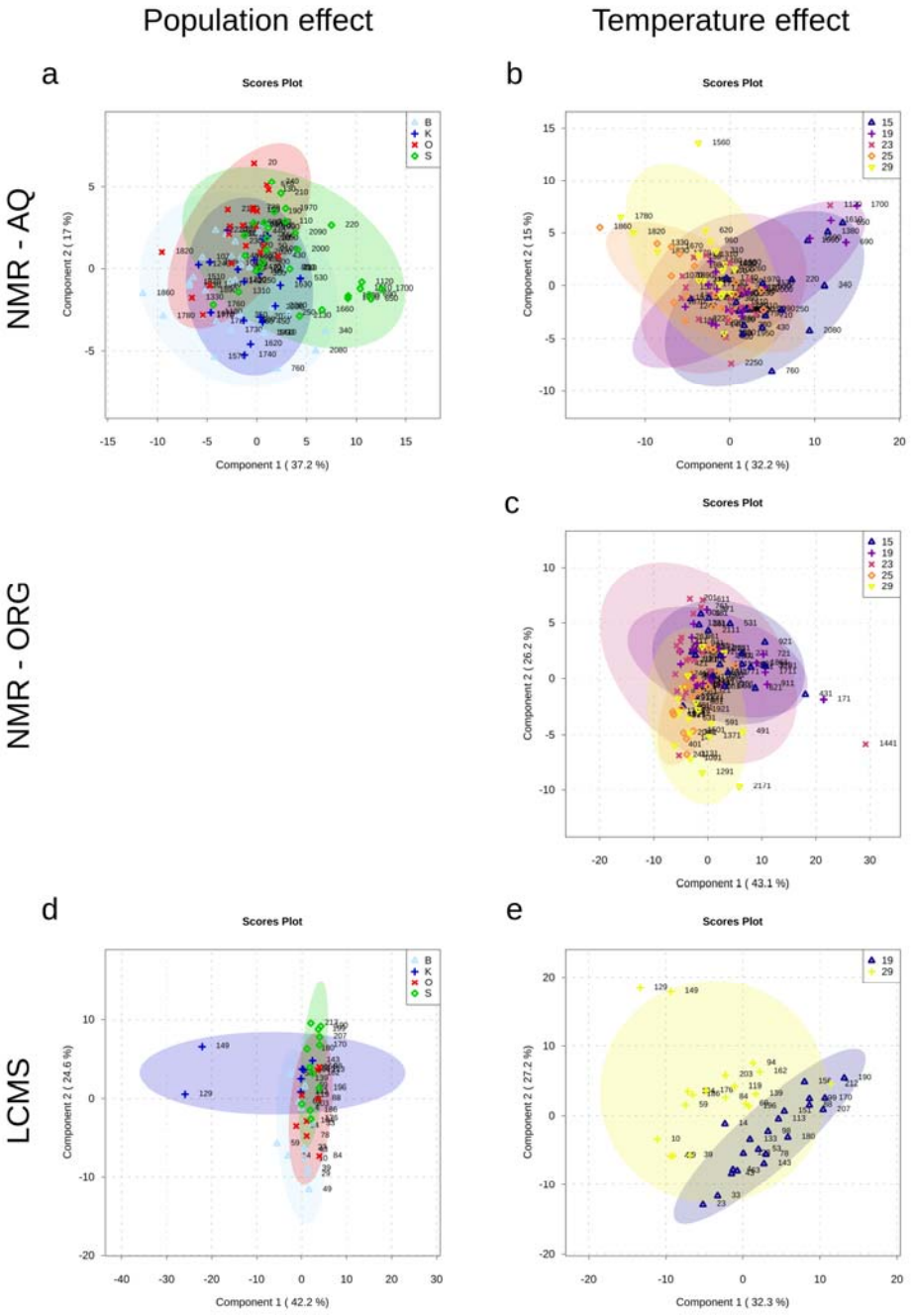

Figure S16: Metabolite intensities for named LC-MS metabolites for CTmax tested spiders.

Metabolite intensities of all named LC-MS metabolites in CTmax performance tested spiders, giving a visualization of direction of change with temperature and difference between populations. Trendlines have been added for ease of interpretation.

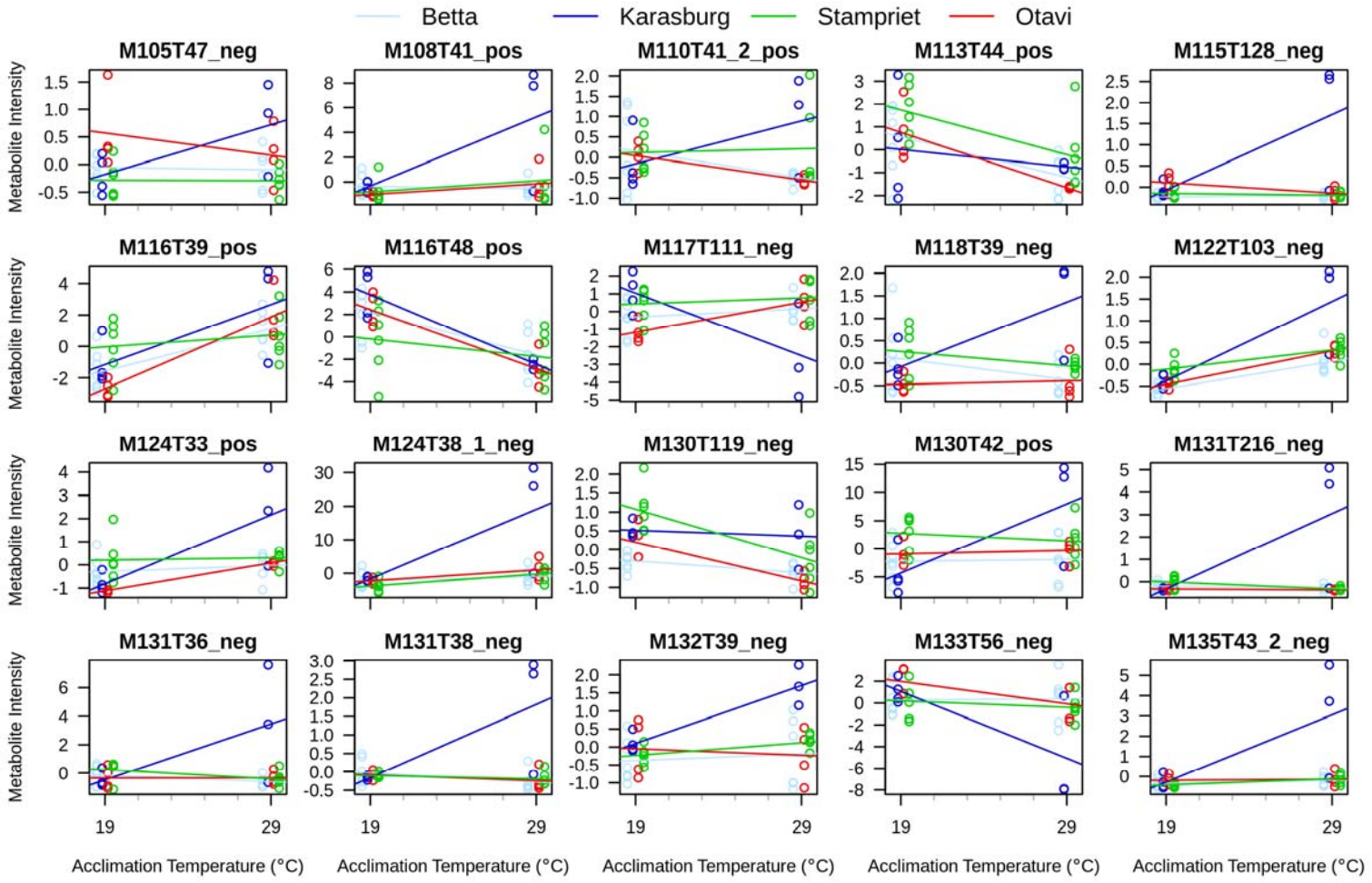

Figure S16 – continued: Metabolite intensities for named LC-MS metabolites for CTmax tested spiders.

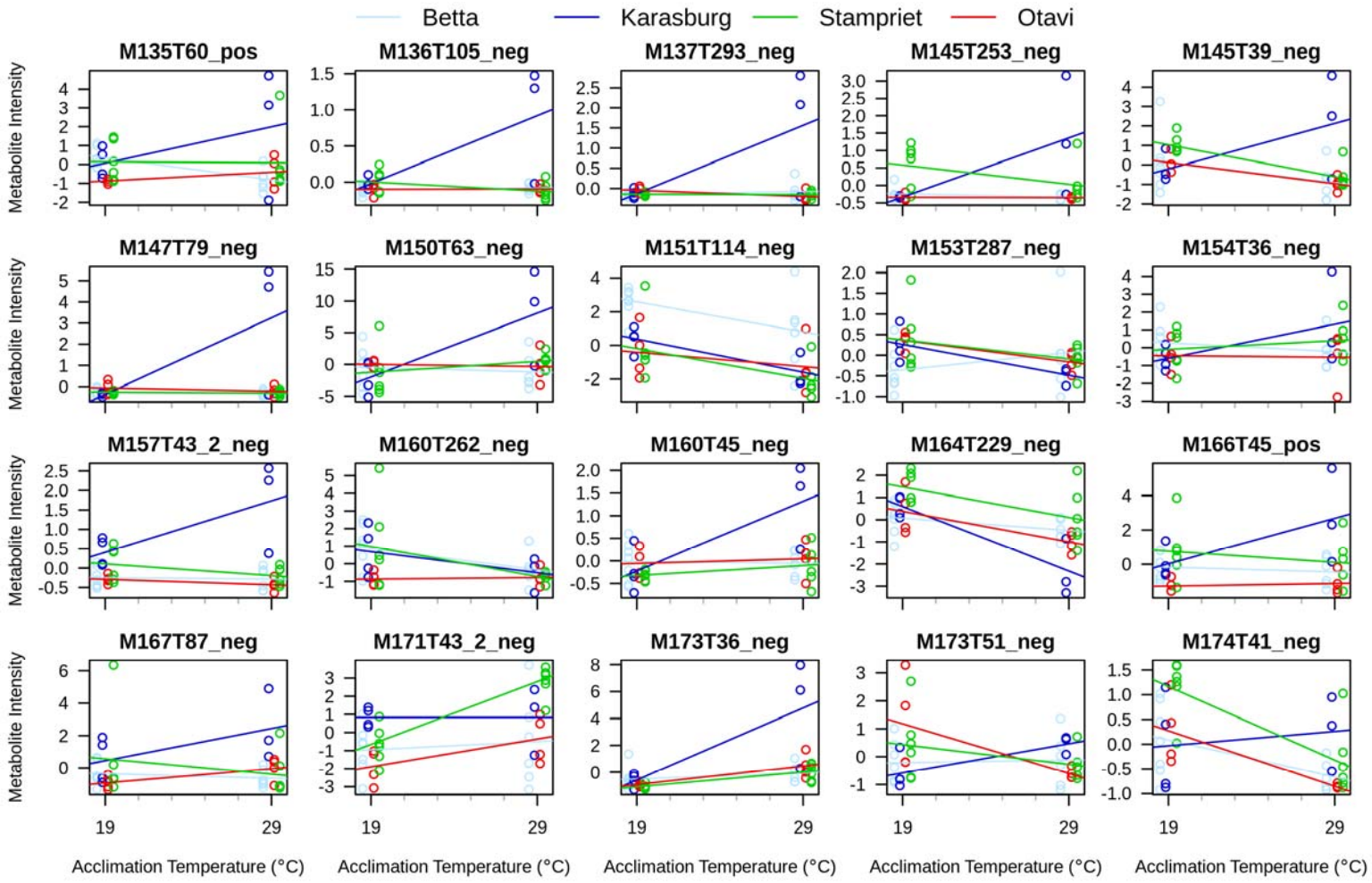

Figure S16 – continued: Metabolite intensities for named LC-MS metabolites for CTmax tested spiders.

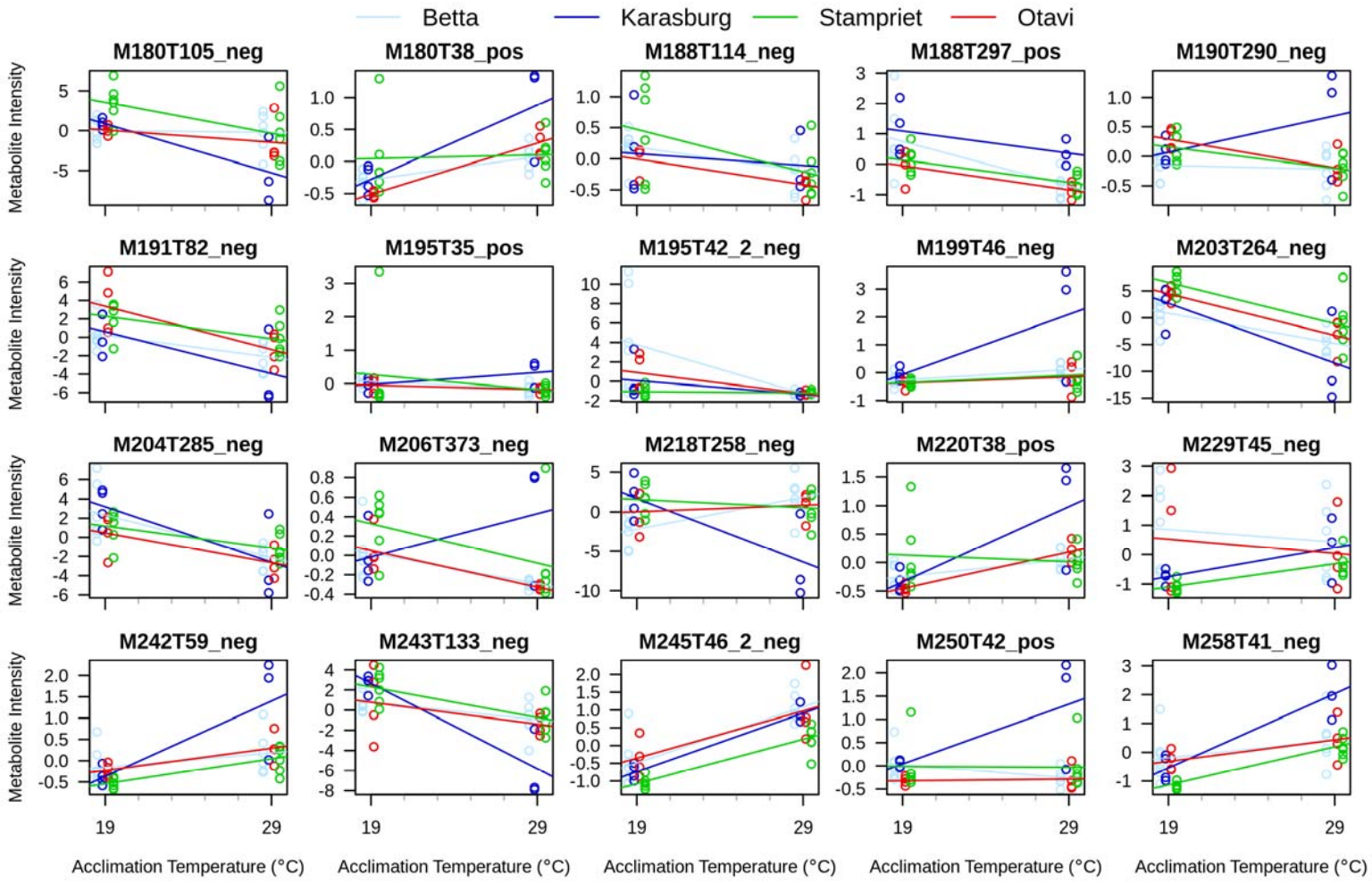

Figure S16 – continued: Metabolite intensities for named LC-MS metabolites for CTmax tested spiders.

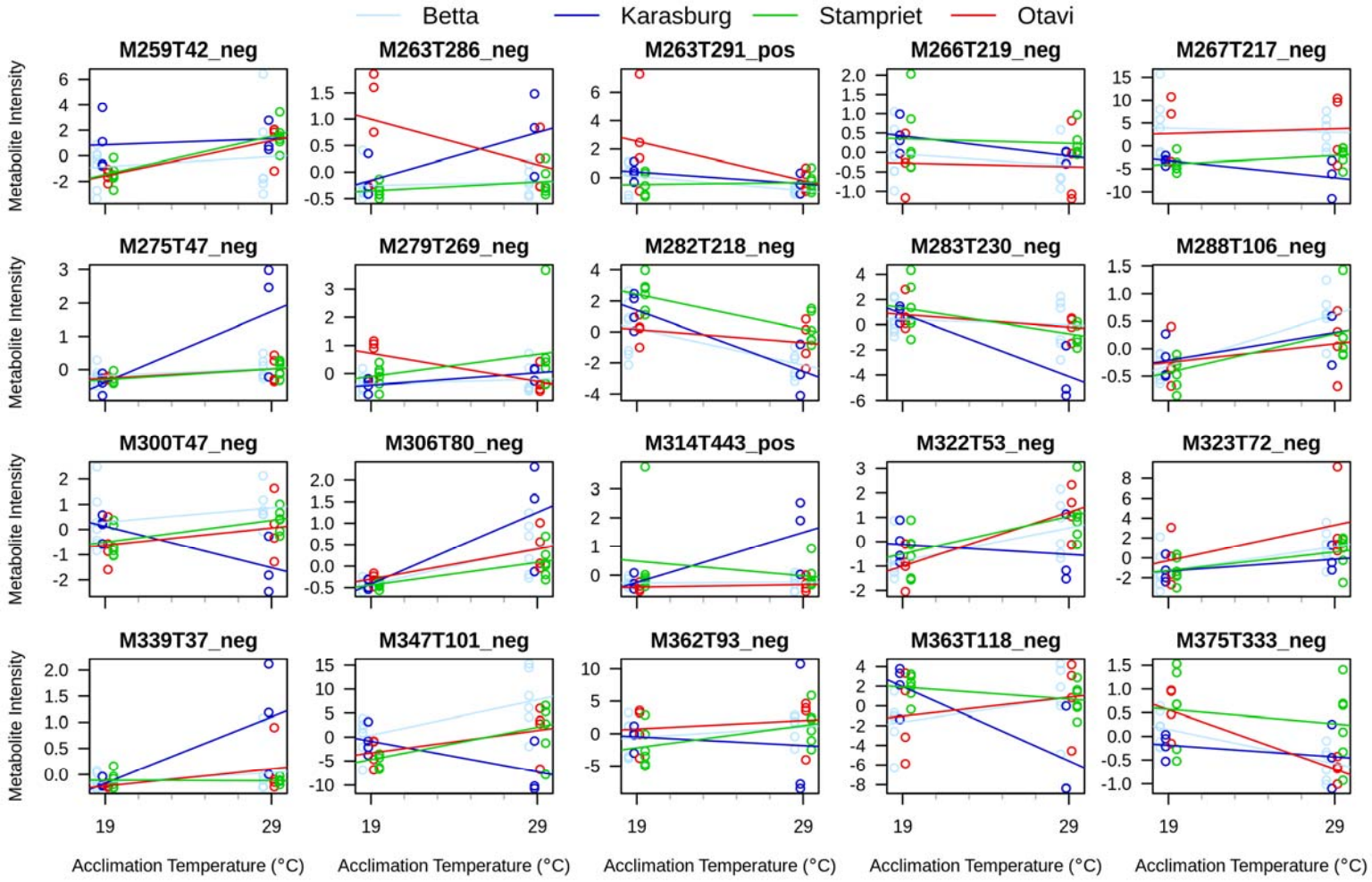

Figure S16 – continued: Metabolite intensities for named LC-MS metabolites for CTmax tested spiders.

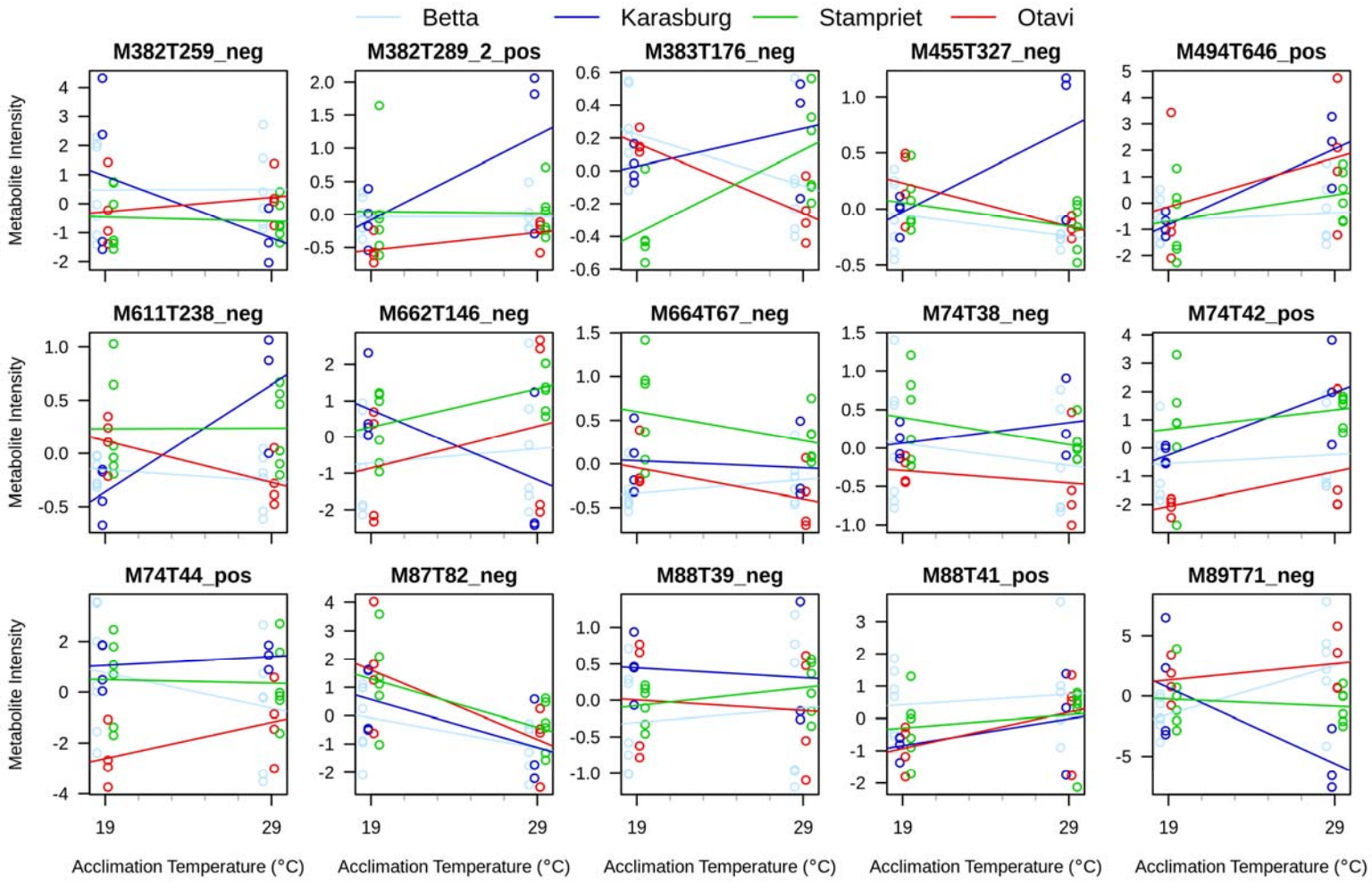

Figure S17: PCA of metabolite LCMS data from the CCRTemp treatment

Principal component analysis of metabolites from the LC-MS analysis for spiders having undergone CCRTemp treatment, colored according to population and temperature acclimation. Only metabolites that showed population effects (a, c) or temperature effect (b,d) are plotted. Here the first three principal components are plottet. There is a tendency for Otavi (red) and Betta (light blue) to separate from Karasburg (blue) and Stampriet (green).

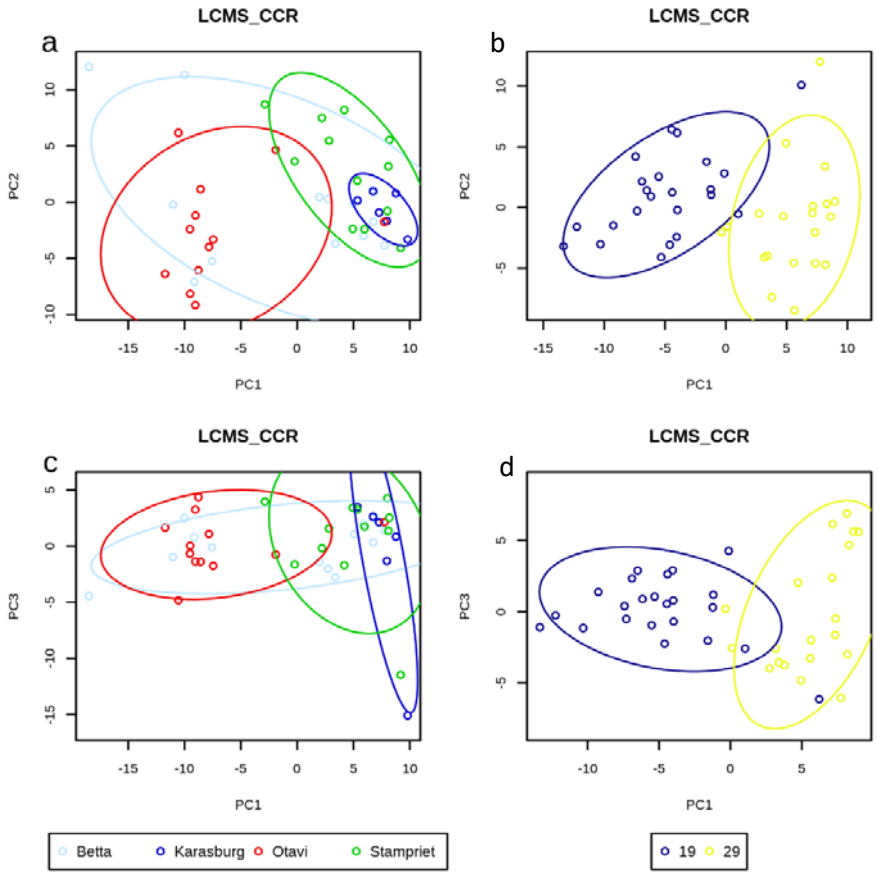

Figure S18: PLS-DA analysis of metabolite data from the CCRTemp treatment

PLS-DA analysis of metabolites from the NMR analysis of spiders having been through CCRTemp testing. Points are metabolite intensities that show effect of either population (a, d) or temperature (b, c, e). Rows indicate metabolite extraction and analysis type: a, b) NMR aquatic extraction, c) NMR organic extraction and d, e) LC-MS.

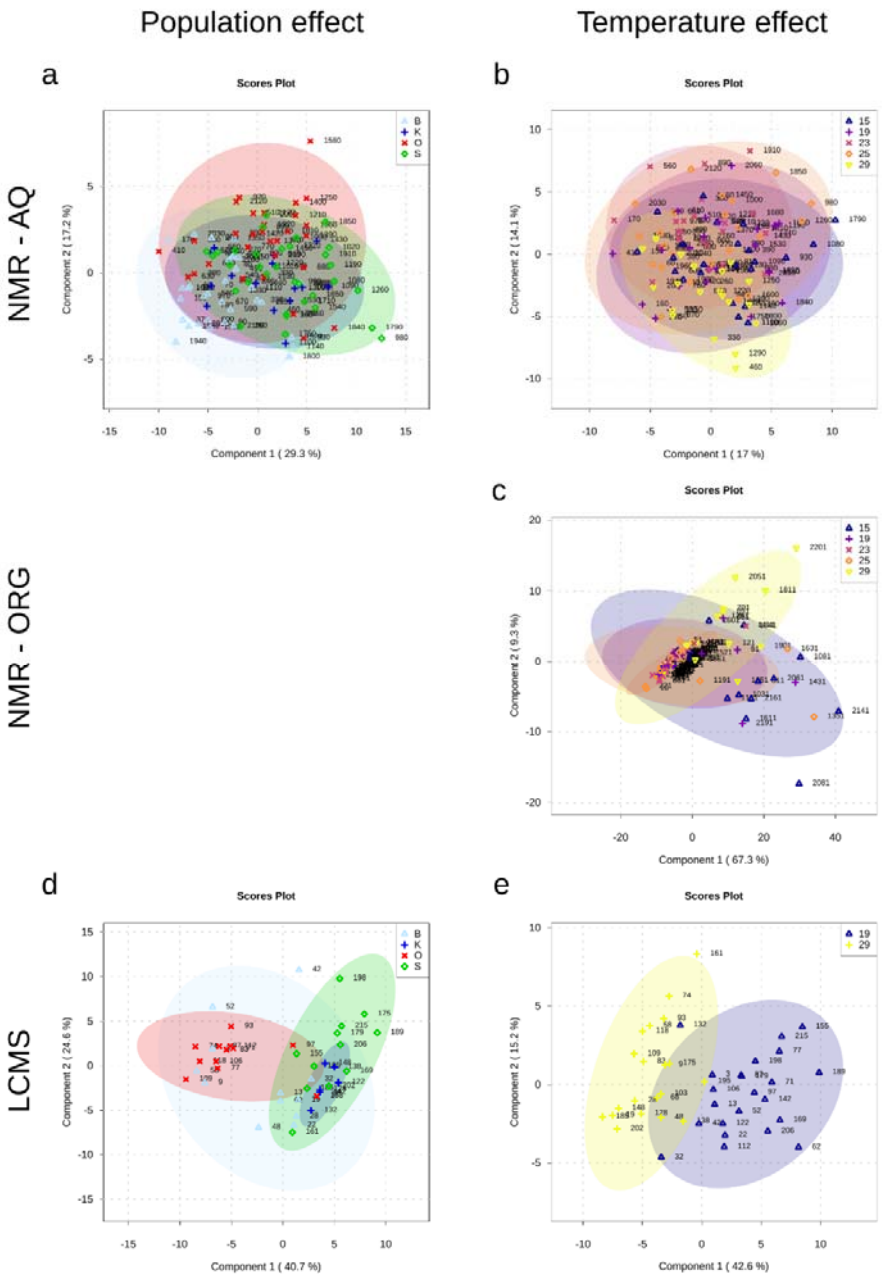

Figure S19: Metabolite intensities for named LC-MS metabolites for CCRTemp tested spiders.

Metabolite intensities of all named LC-MS metabolites in CCRTemp performance tested spiders, giving a visualization of direction of change with temperature and difference between populations. Trendlines have been added for ease of interpretation.

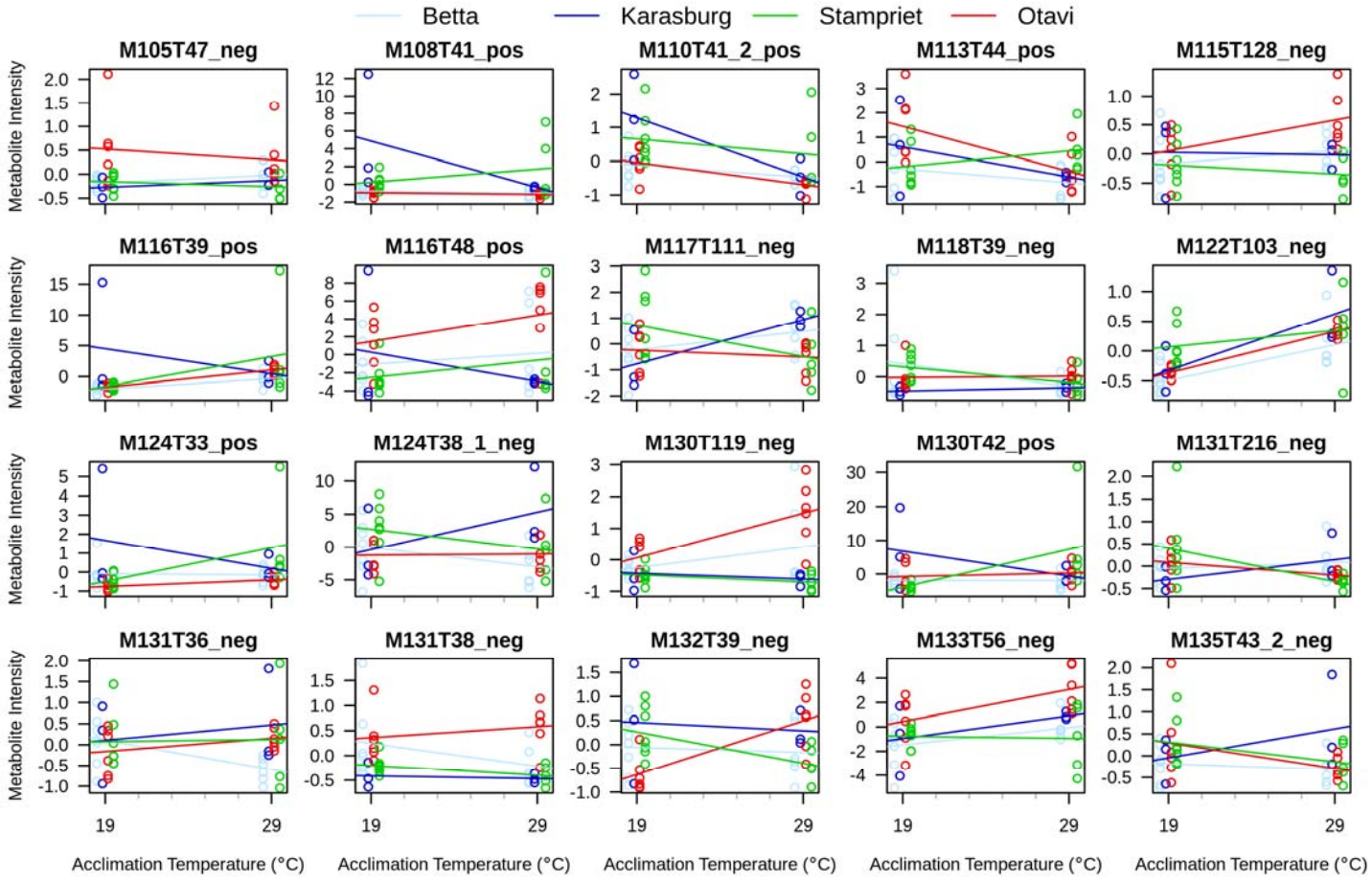

Figure S19 – continued: Metabolite intensities for named LC-MS metabolites for CCRTemp tested spiders.

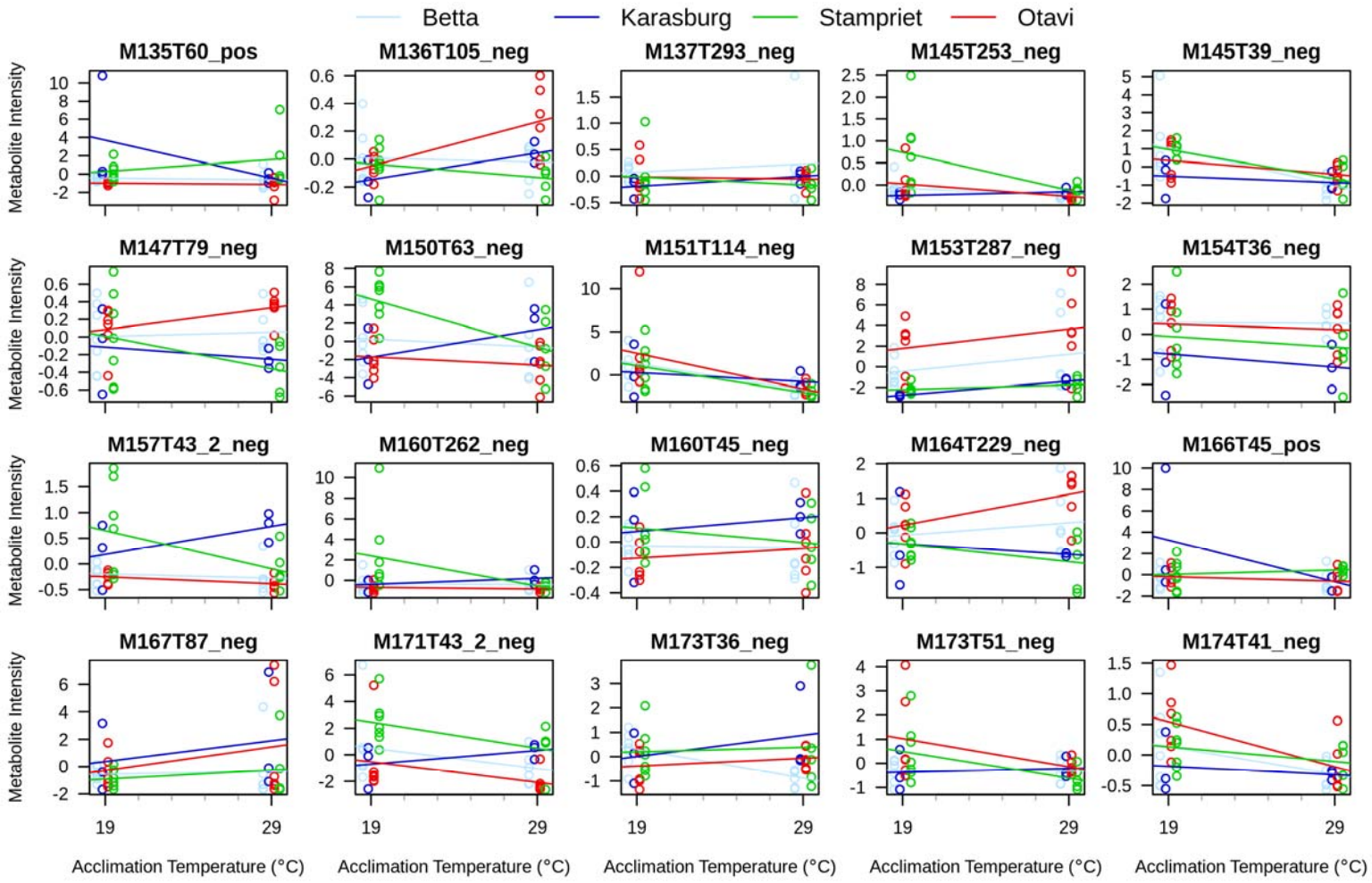

Figure S19 – continued: Metabolite intensities for named LC-MS metabolites for CCRTemp tested spiders.

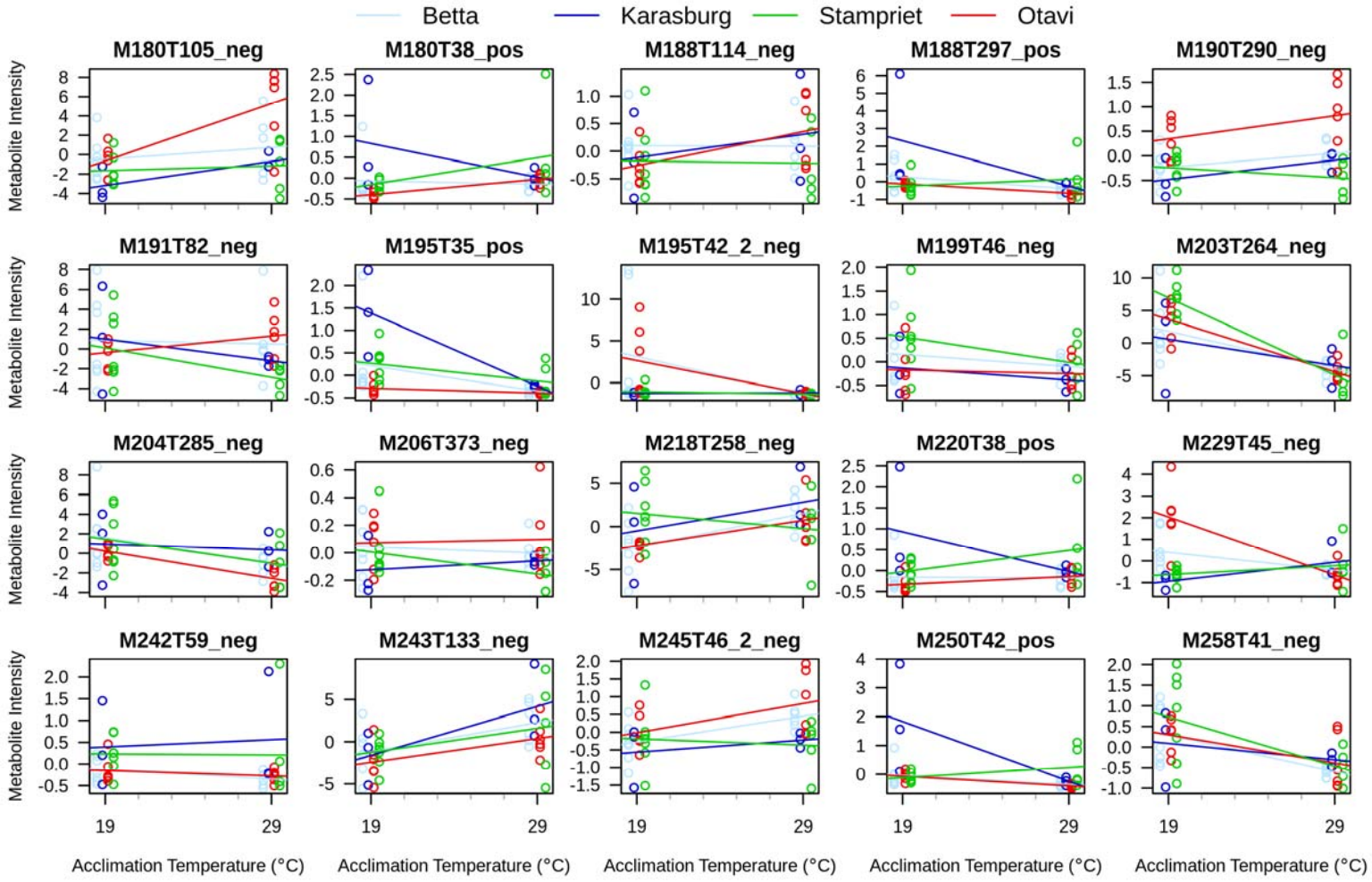

Figure S19 – continued: Metabolite intensities for named LC-MS metabolites for CCRTemp tested spiders.

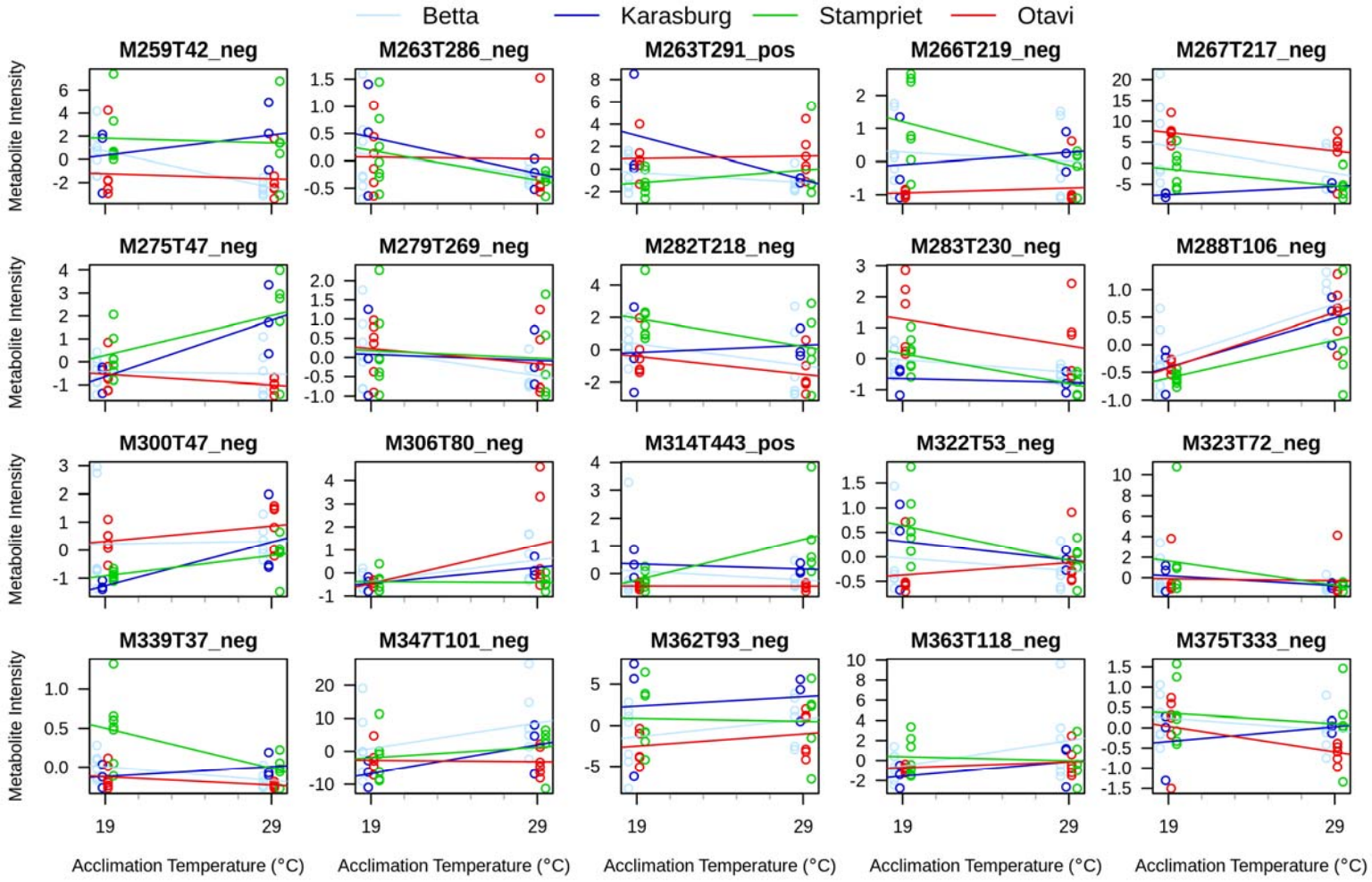

Figure S19 – continued: Metabolite intensities for named LC-MS metabolites for CCRTemp tested spiders.

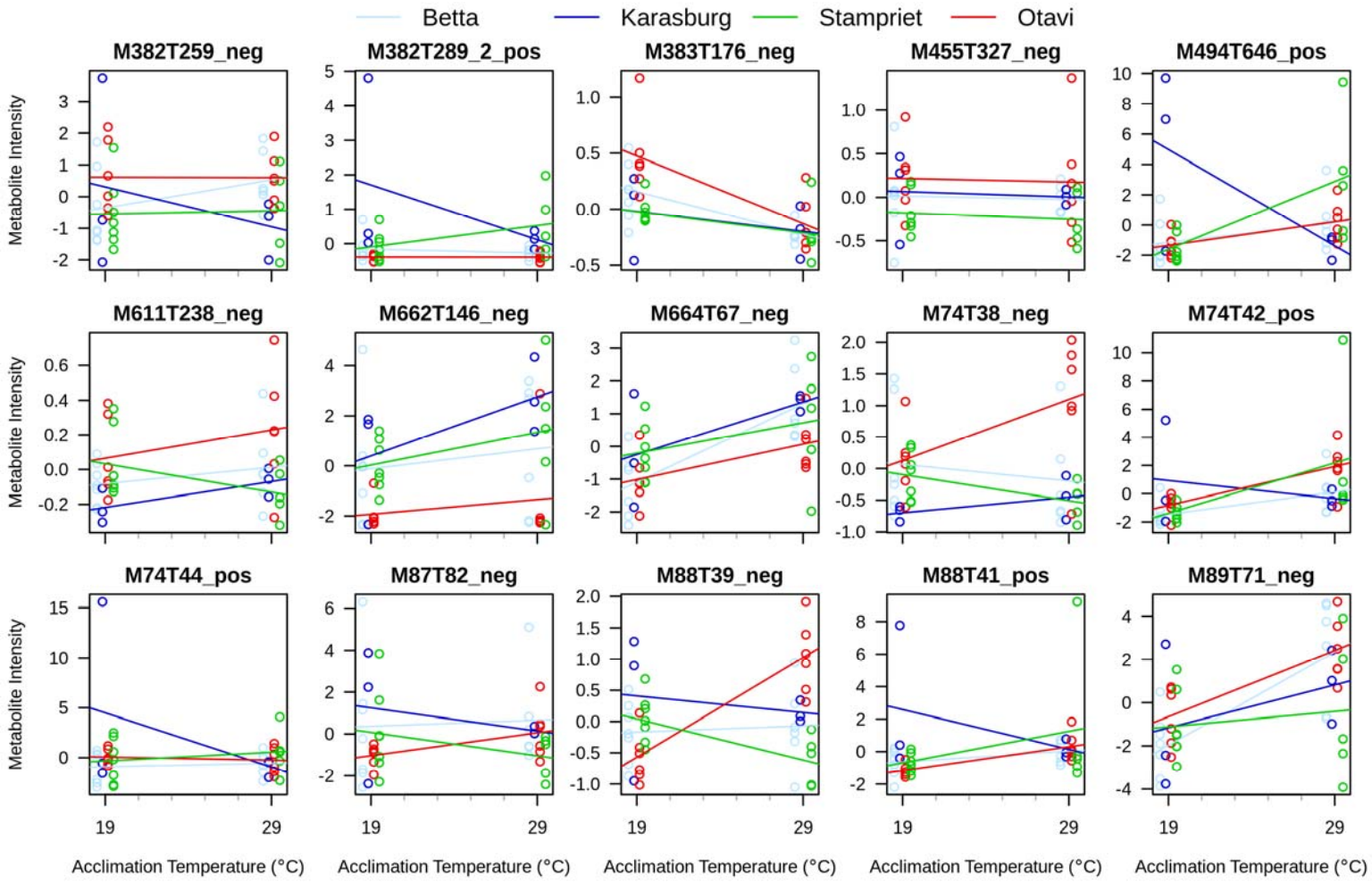

Figure S20: PCA of metabolite NMR-Aq data from the CTmax treatment

Principal Component Analysis of Metabolites from NMR from spiders having gone through CTmax treatment, colored according to population and temperature acclimation. Only metabolites that showed population effects (a, c) or temperature effect (b,d) are plotted. Here the first three principal components are plottet.

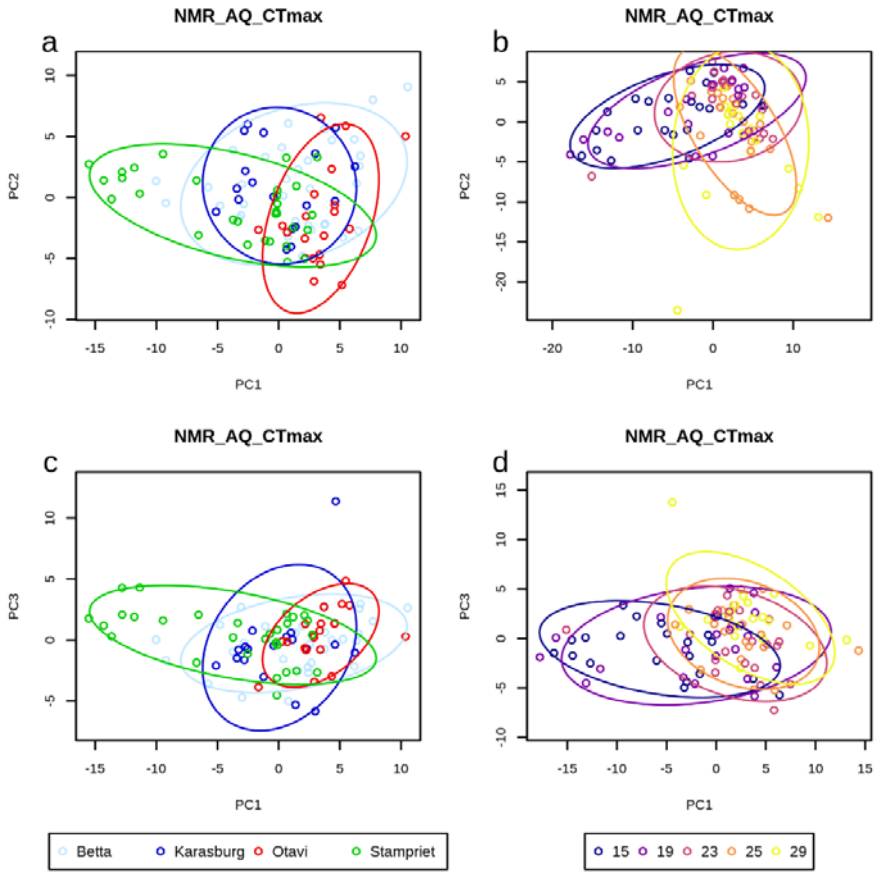

Figure S21: PCA of metabolite NMR-Aq data from the CCRTemp treatment

Principal Component Analysis of Metabolites from NMR from spiders having gone through CCR treatment, colored according to population and temperature acclimation. Only metabolites that showed population effects (a, c) or temperature effect (b,d) are plotted. Here the first three principal components are plottet.

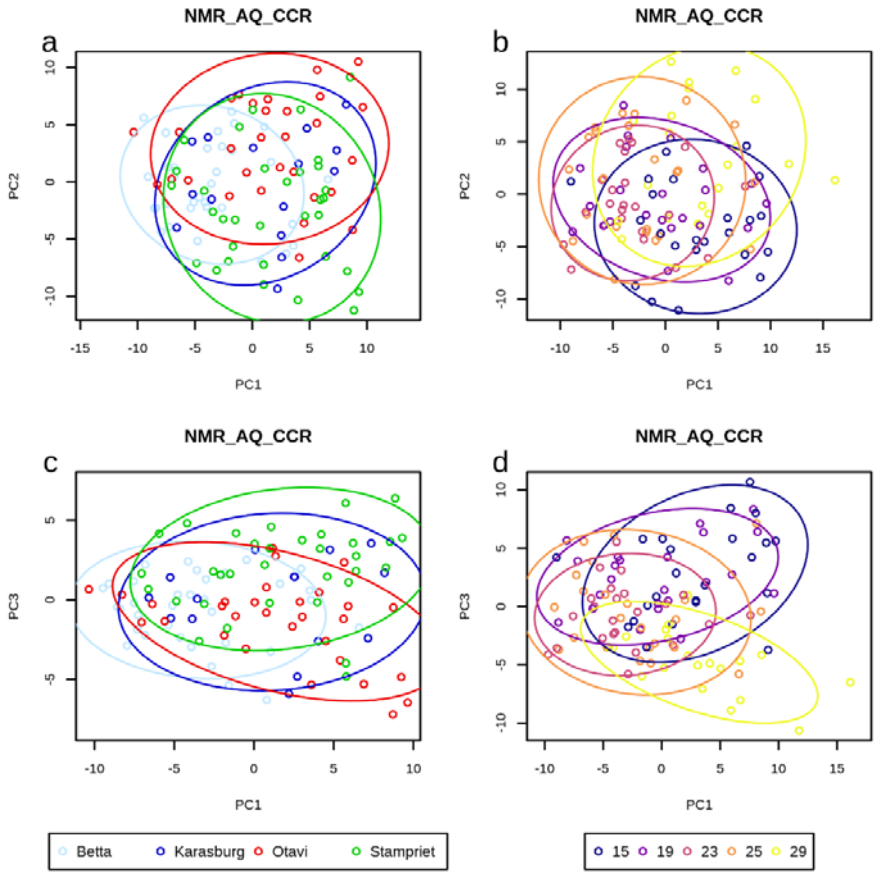

Figure S22: Number of ASVs with responses to population and temperature in microbiome

Barplot with the number of microbial ASVs showing population and temperature responses in S. dumicola. The total number of ASVs passing the filtering criterion is 78.

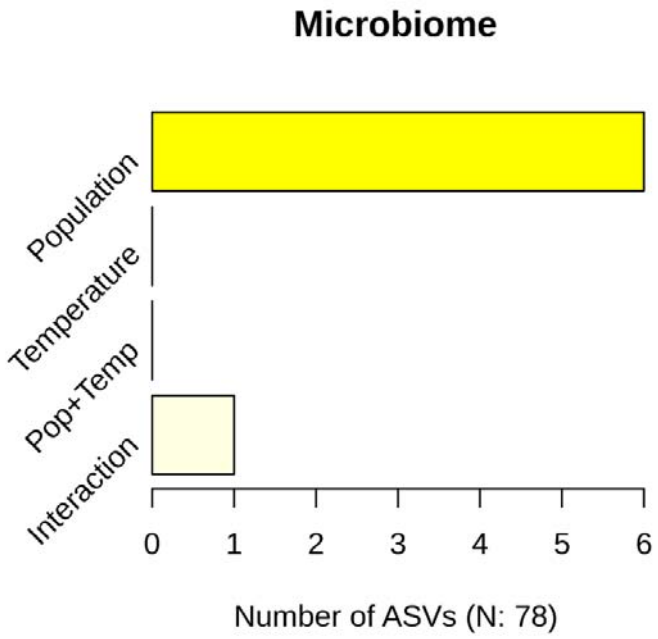

Figure S23: Gene expression with similar population specific acclimation responses as the heat tolerance phenotype

Genes with expression levels showing similar population-specific trends as that of Heat tolerance (CTmax). Genes presented in these graphs show a response suggesting an involvement in the observed population dependent heat tolerance, thus linking gene expression to the expressed phenotype.

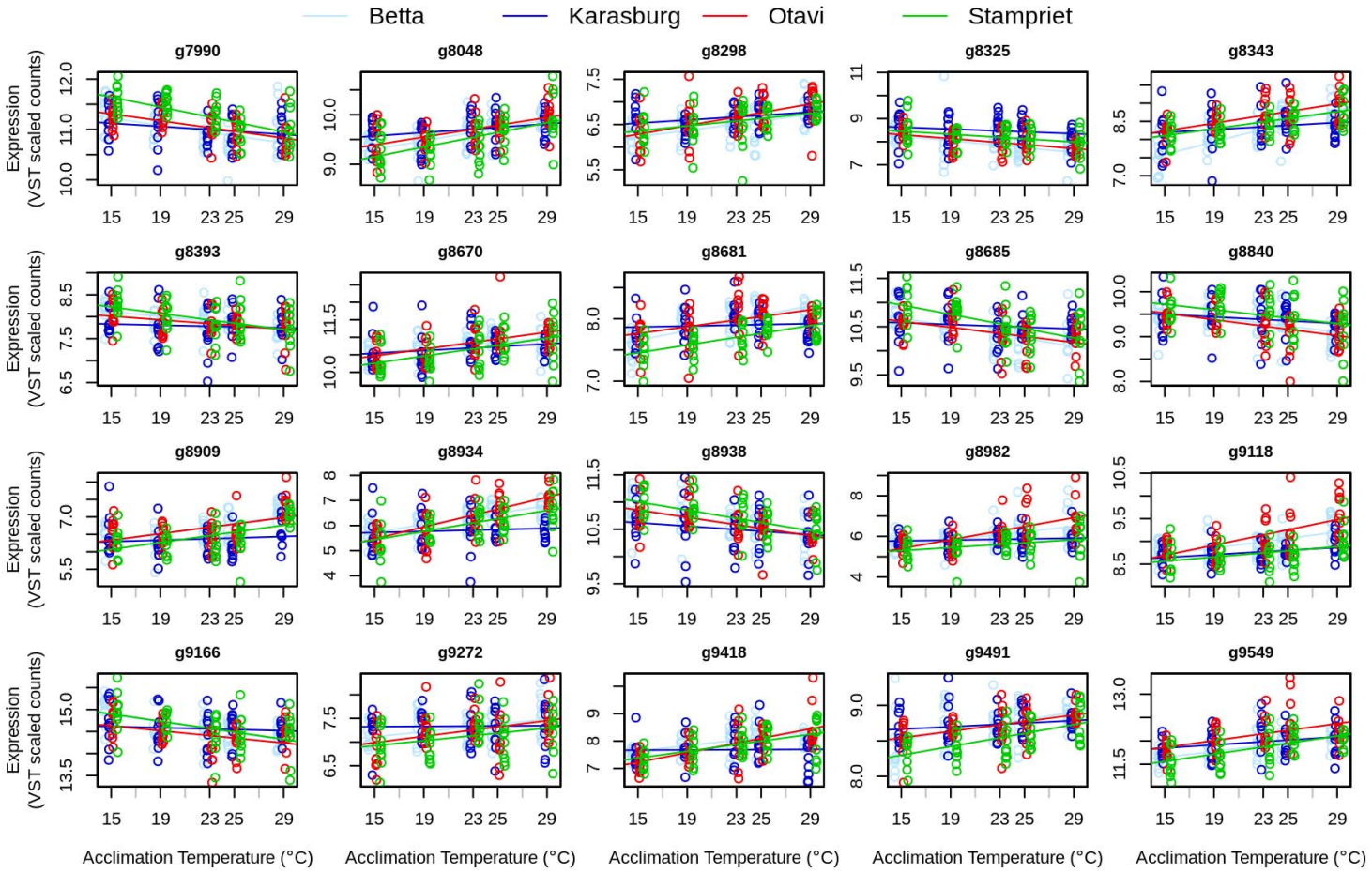

Figure S23 – continued: Gene expression with similar population specific acclimation responses as the heat tolerance phenotype

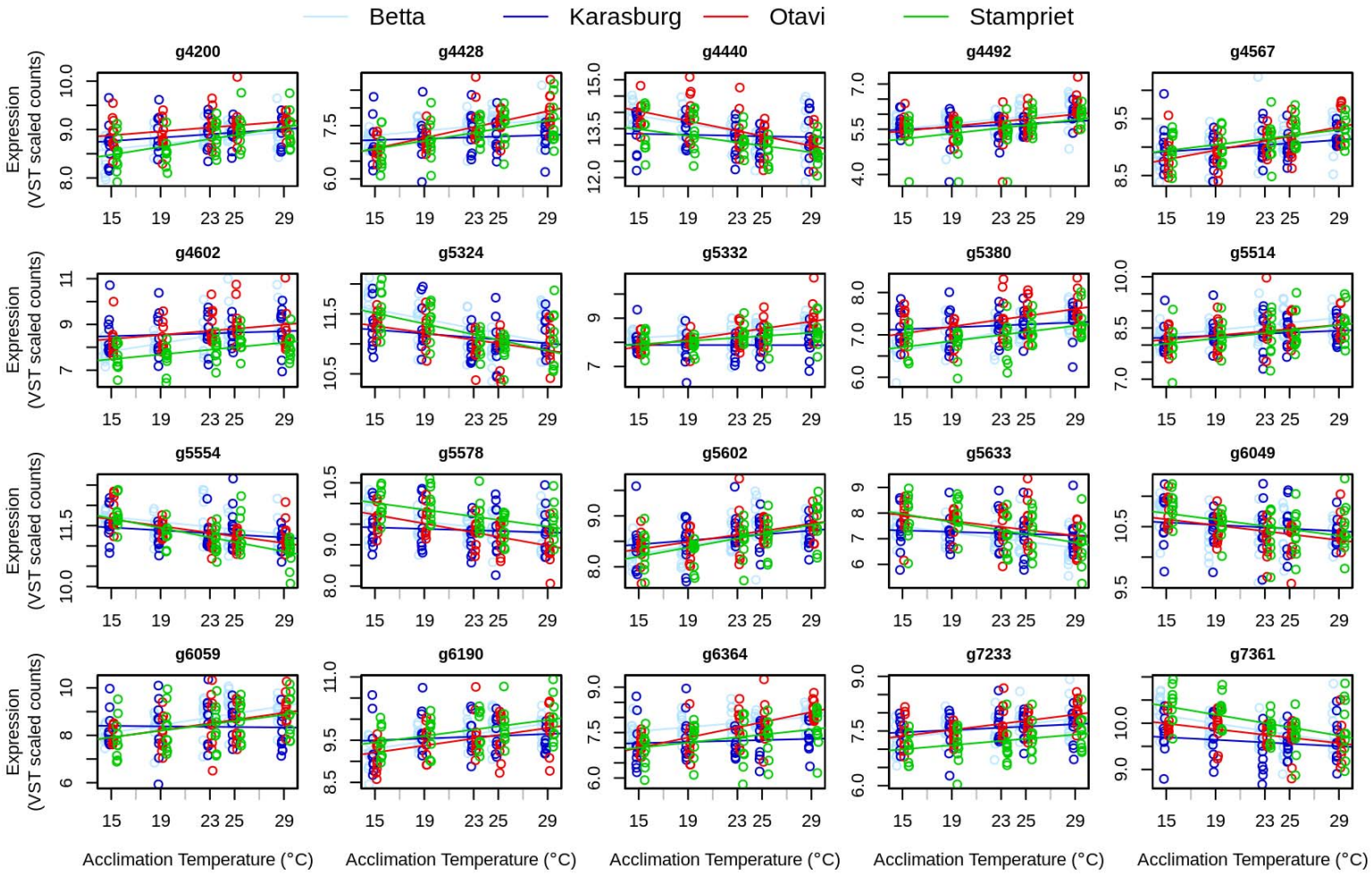

Figure S23 – continued: Gene expression with similar population specific acclimation responses as the heat tolerance phenotype

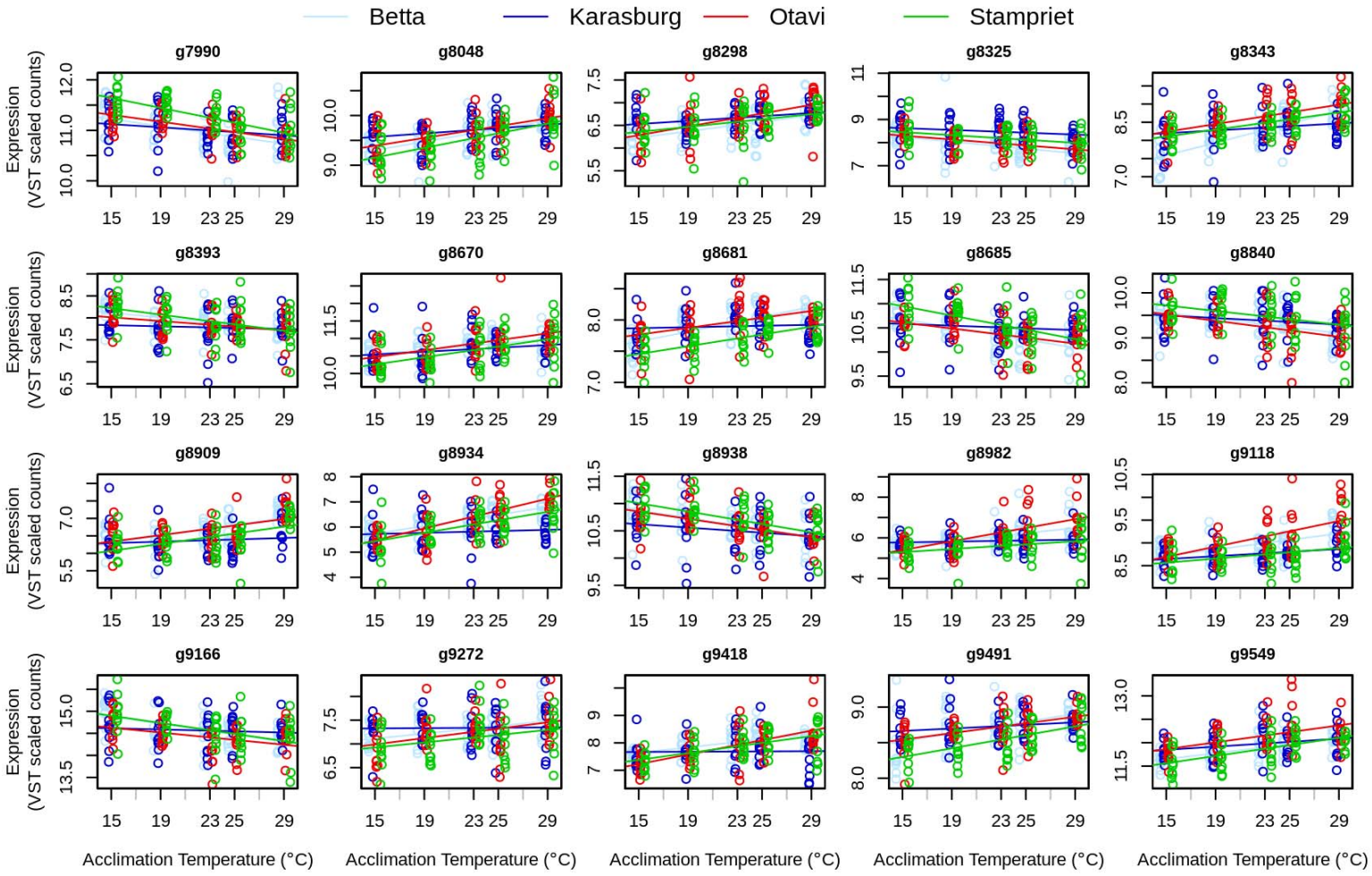

Figure S23 – continued: Gene expression with similar population specific acclimation responses as the heat tolerance phenotype

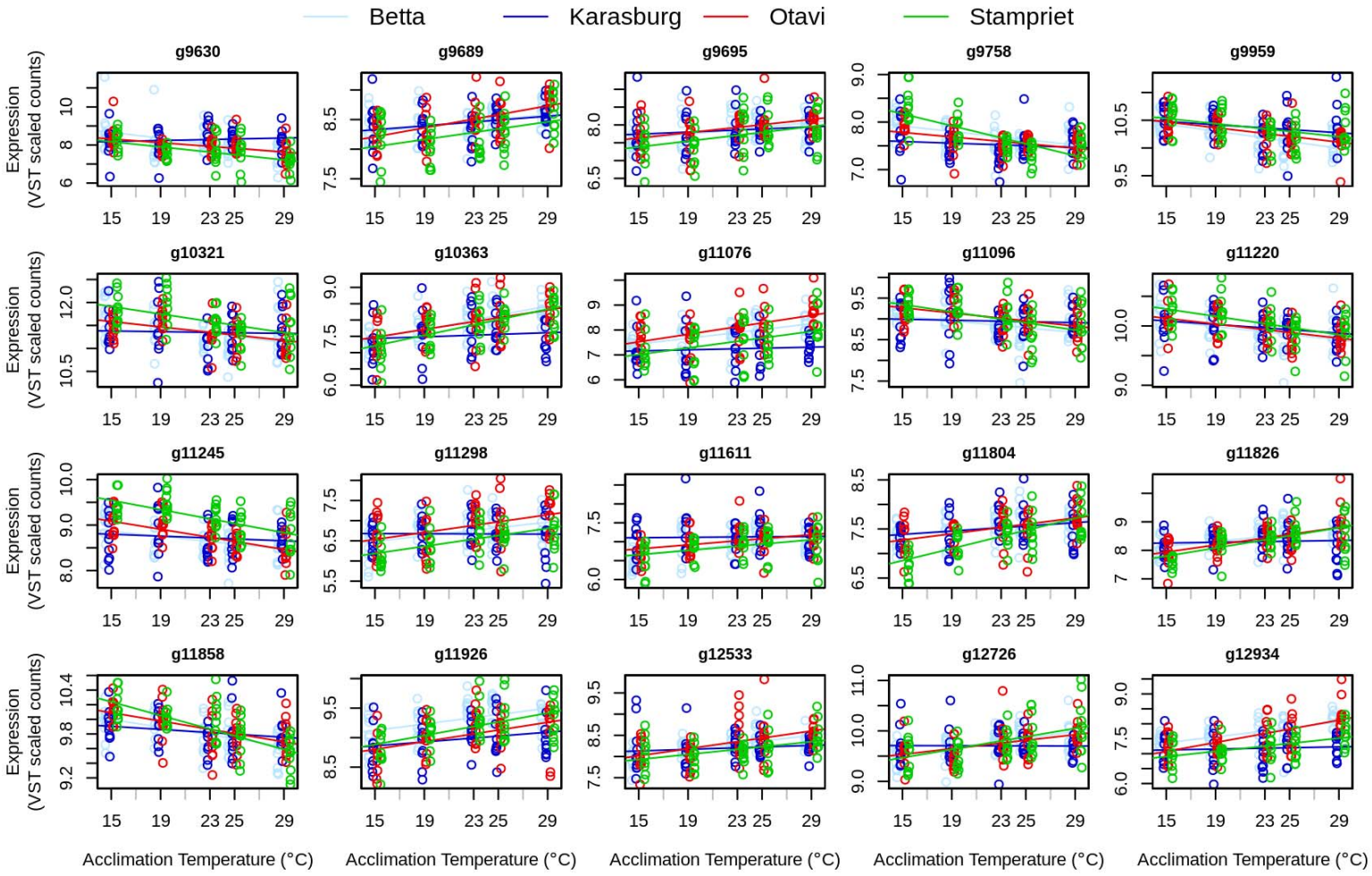

Figure S23 – continued: Gene expression with similar population specific acclimation responses as the heat tolerance phenotype

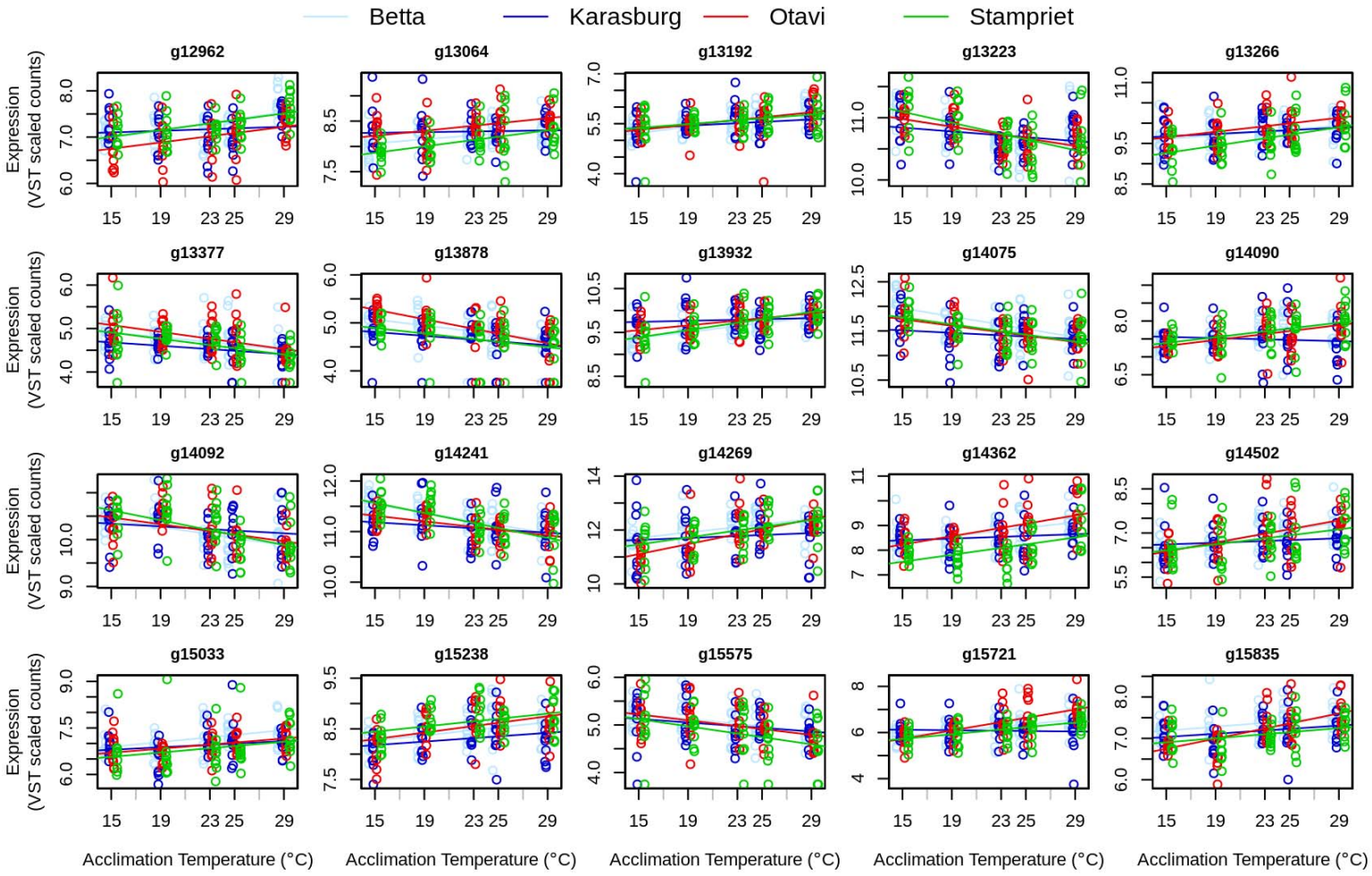

Figure S23 – continued: Gene expression with similar population specific acclimation responses as the heat tolerance phenotype

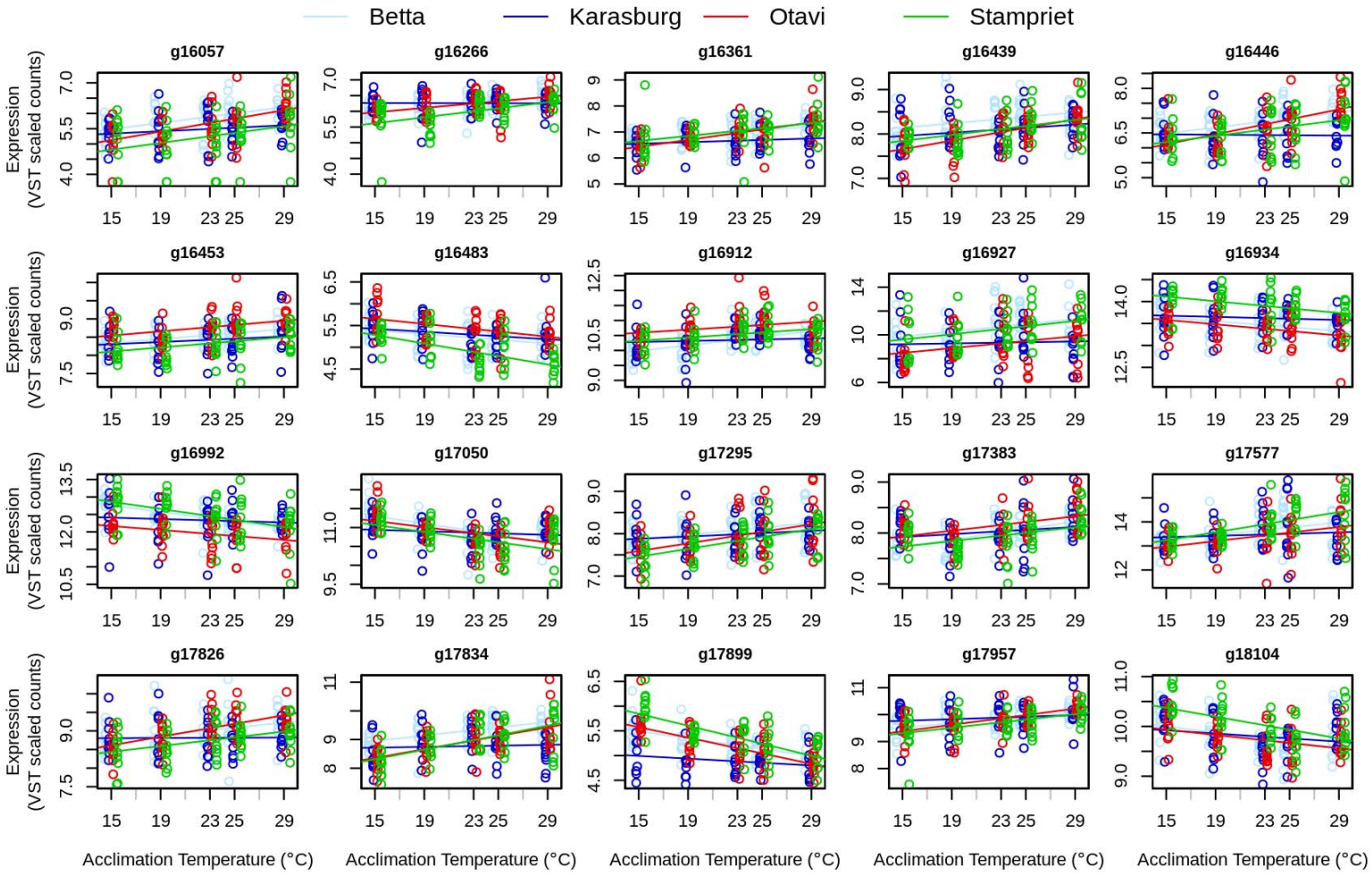

Figure S23 – continued: Gene expression with similar population specific acclimation responses as the heat tolerance phenotype

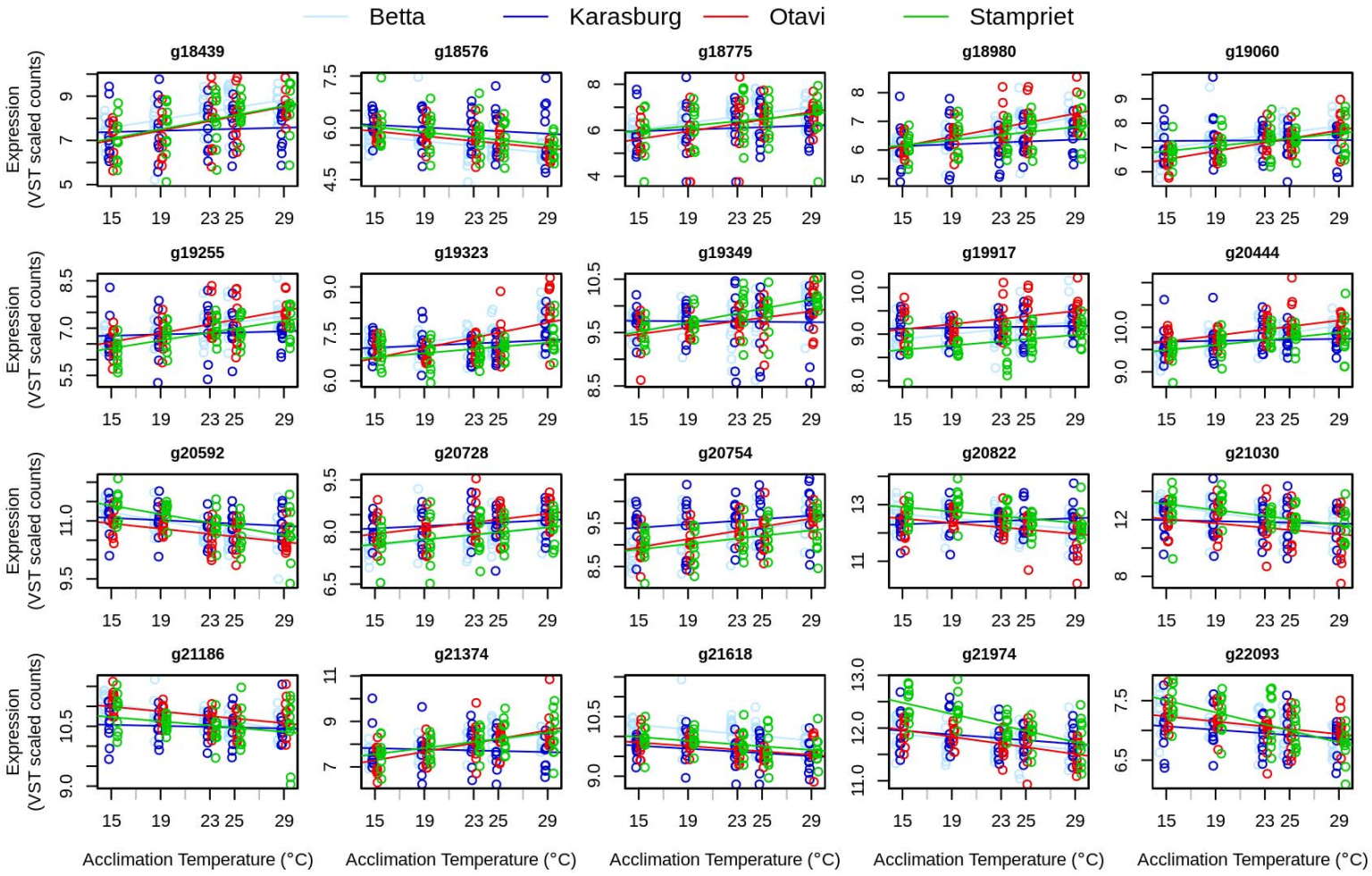

Figure S23 – continued: Gene expression with similar population specific acclimation responses as the heat tolerance phenotype

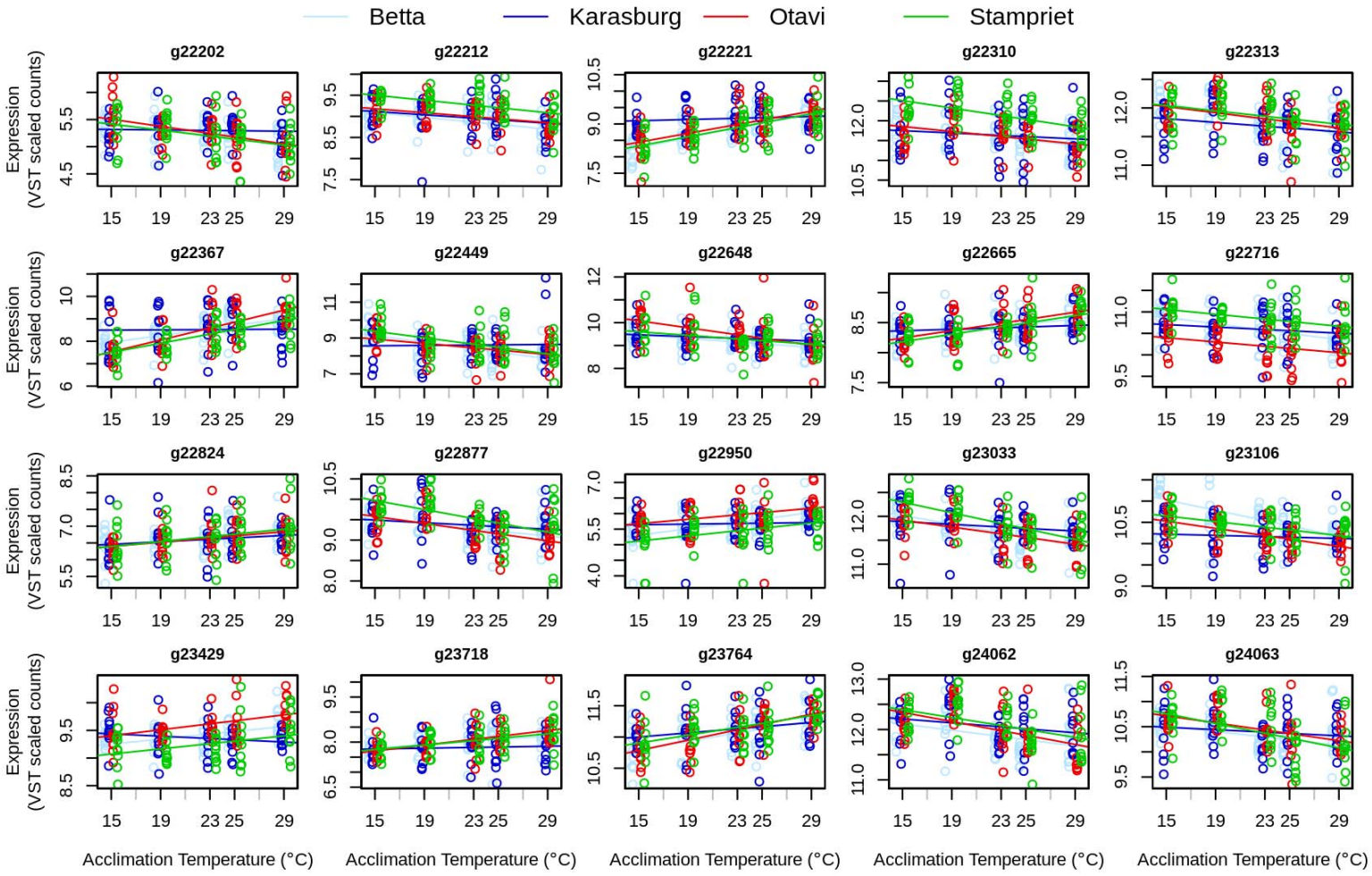

Figure S23 – continued: Gene expression with similar population specific acclimation responses as the heat tolerance phenotype

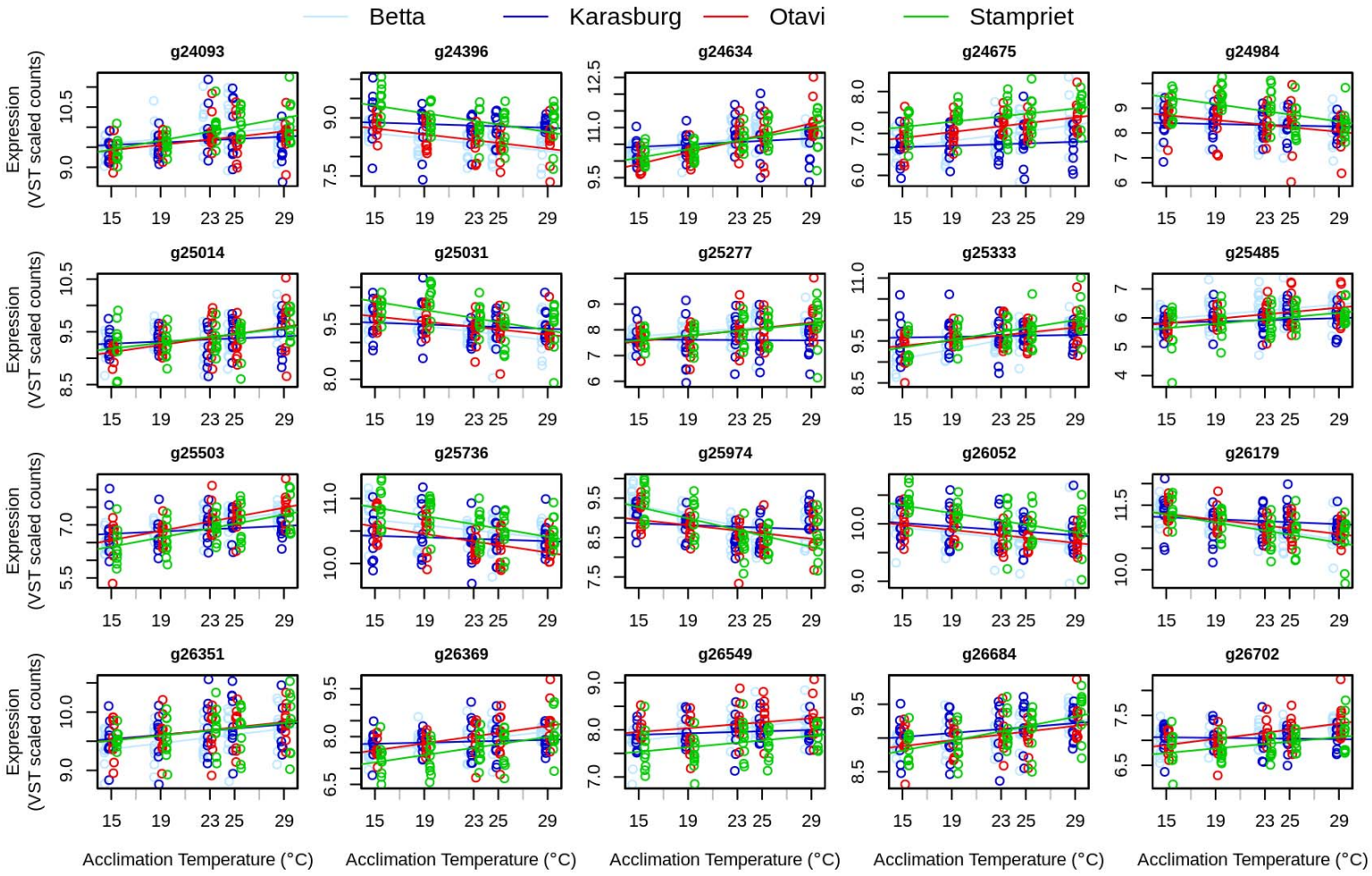

Figure S23 – continued: Gene expression with similar population specific acclimation responses as the heat tolerance phenotype

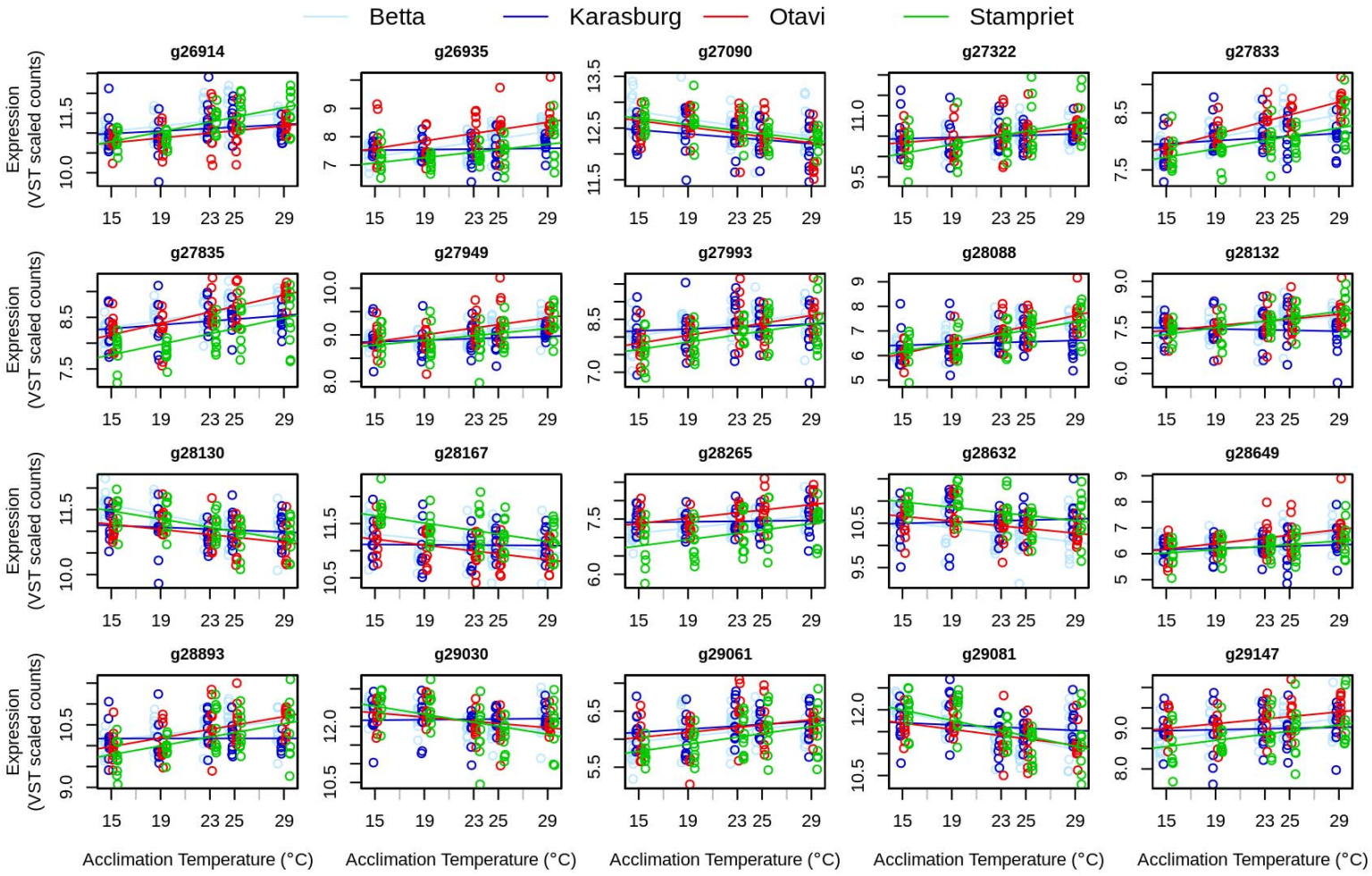

Figure S23 – continued: Gene expression with similar population specific acclimation responses as the heat tolerance phenotype

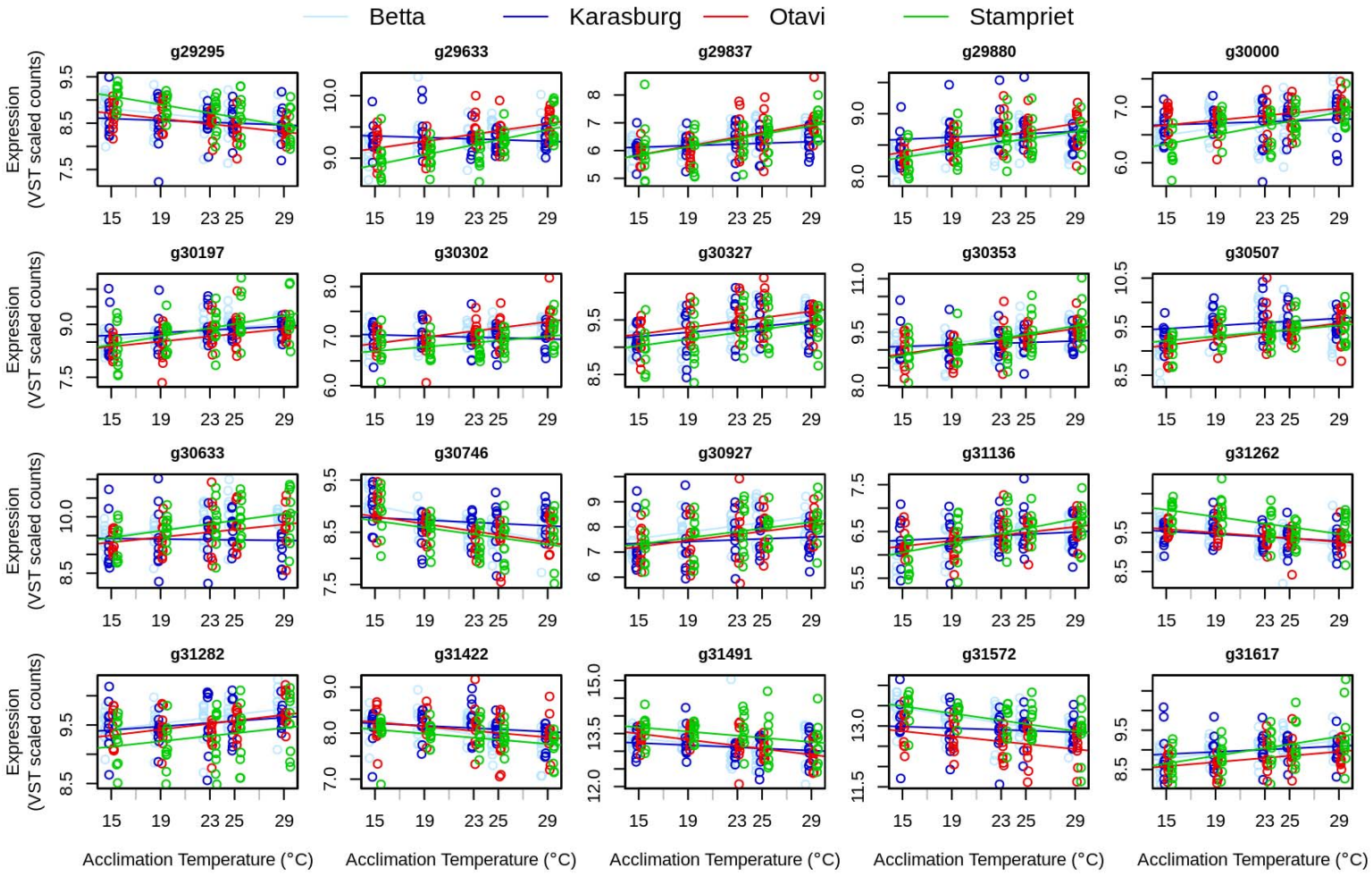

Figure S23 – continued: Gene expression with similar population specific acclimation responses as the heat tolerance phenotype

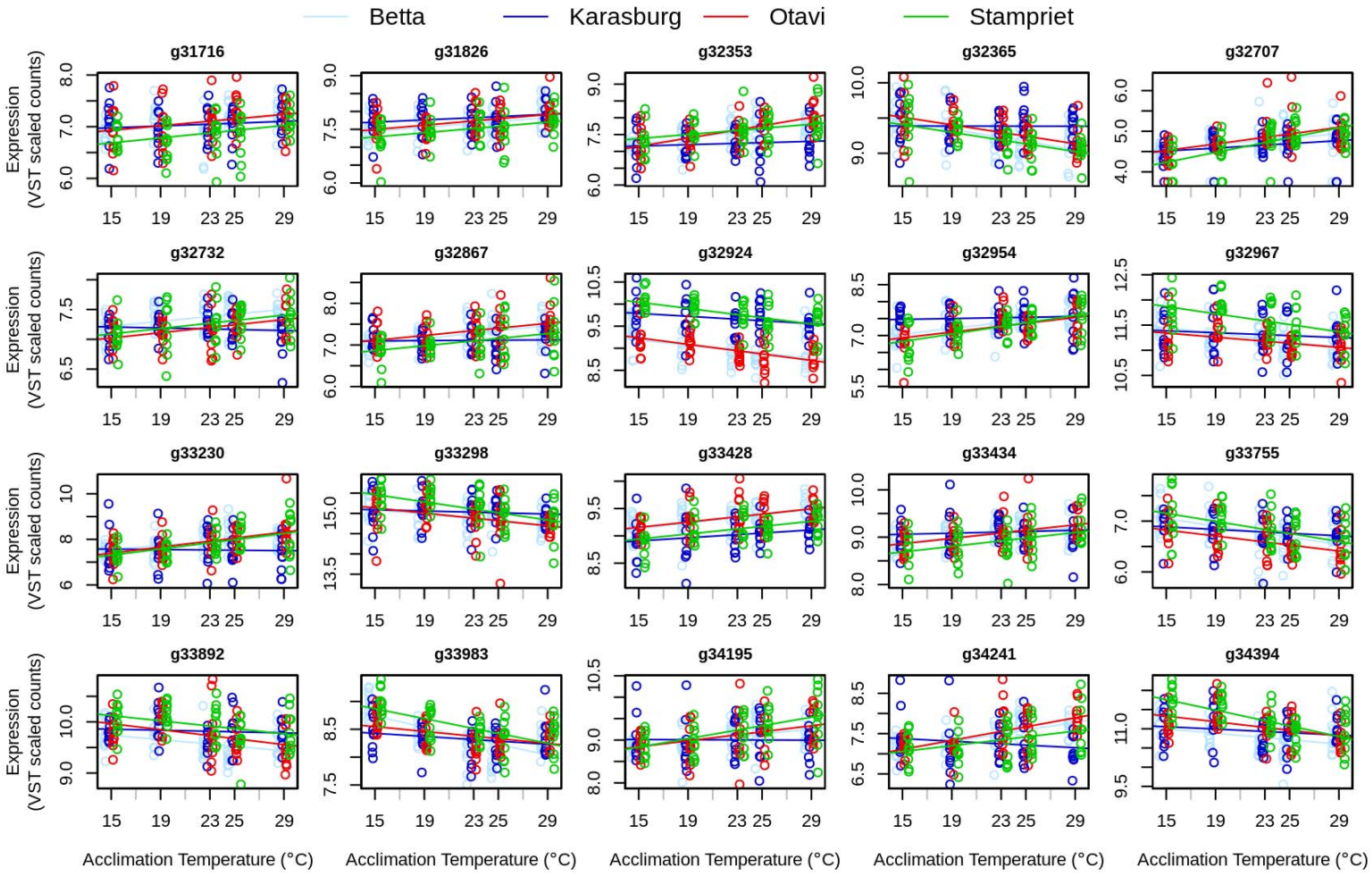

Figure S23 – continued: Gene expression with similar population specific acclimation responses as the heat tolerance phenotype

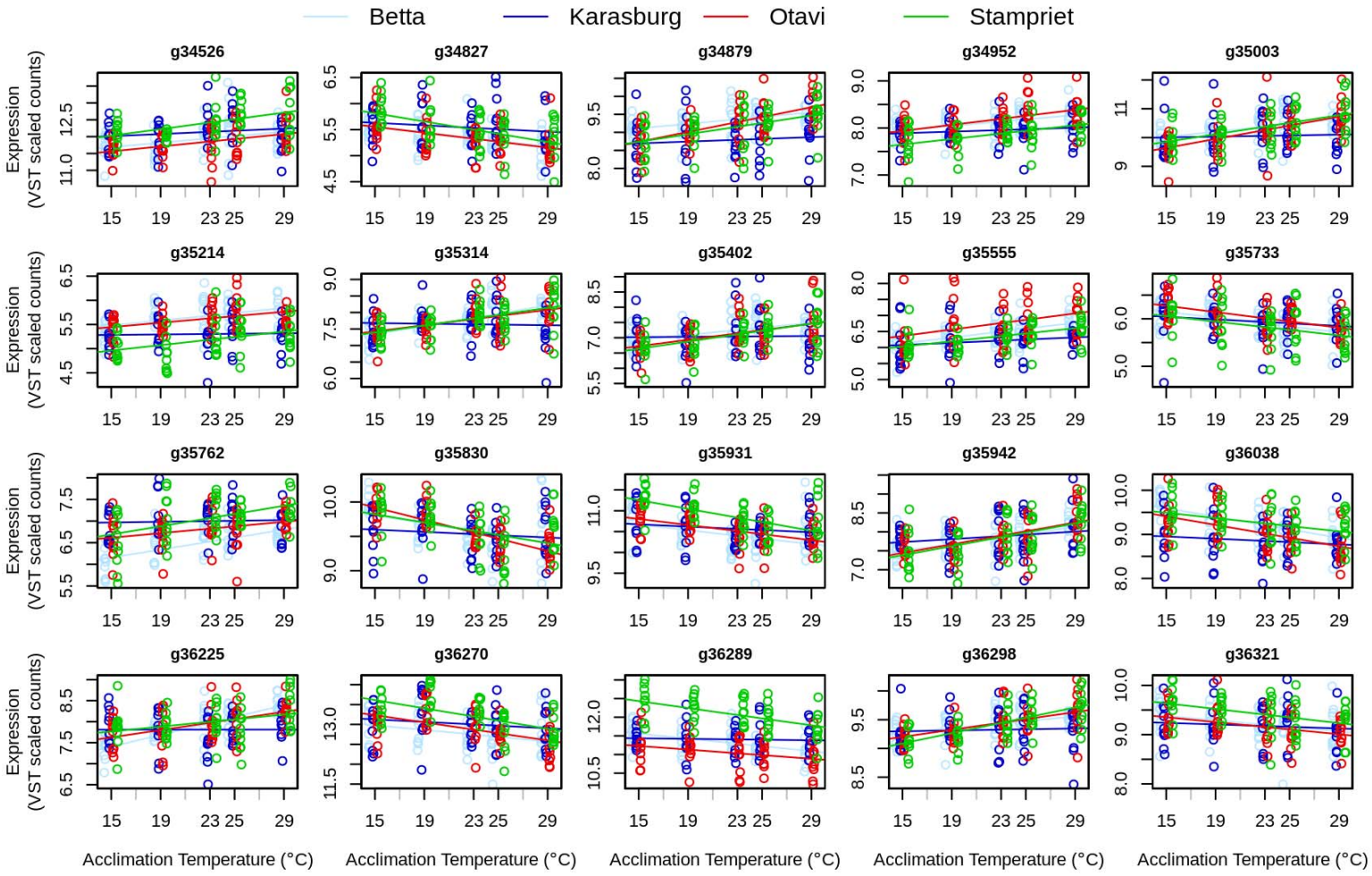

Figure S23 – continued: Gene expression with similar population specific acclimation responses as the heat tolerance phenotype

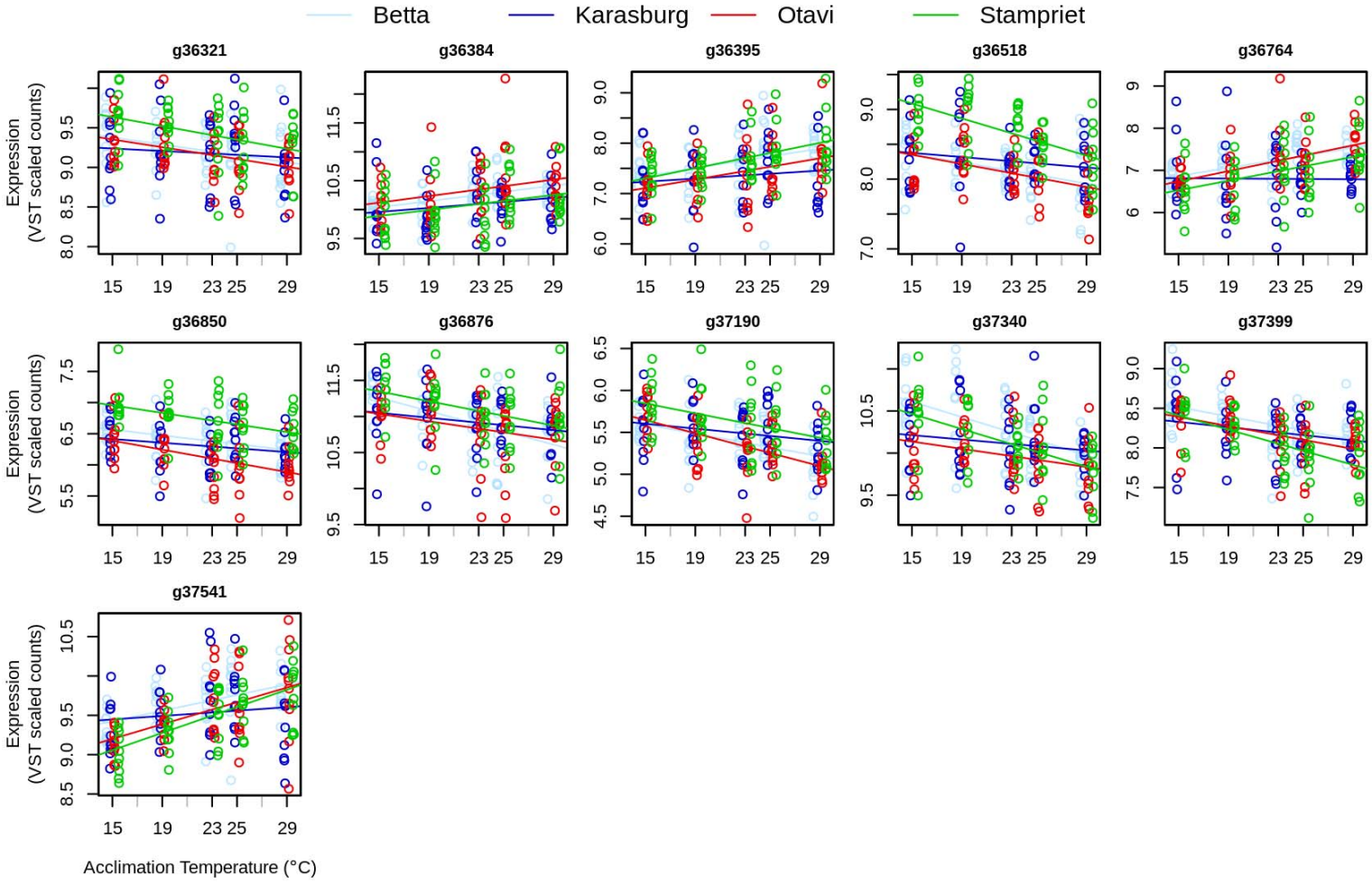

Figure S24: Gene expression with similar population specific acclimation responses as the cold tolerance phenotype

Genes with expression levels showing similar population-specific trends as that of cold tolerance (CCRTemp). Genes presented in these graphs show a response suggesting a clearer involvement in the observed population dependent cold tolerance, linking gene expression to the expressed phenotype.

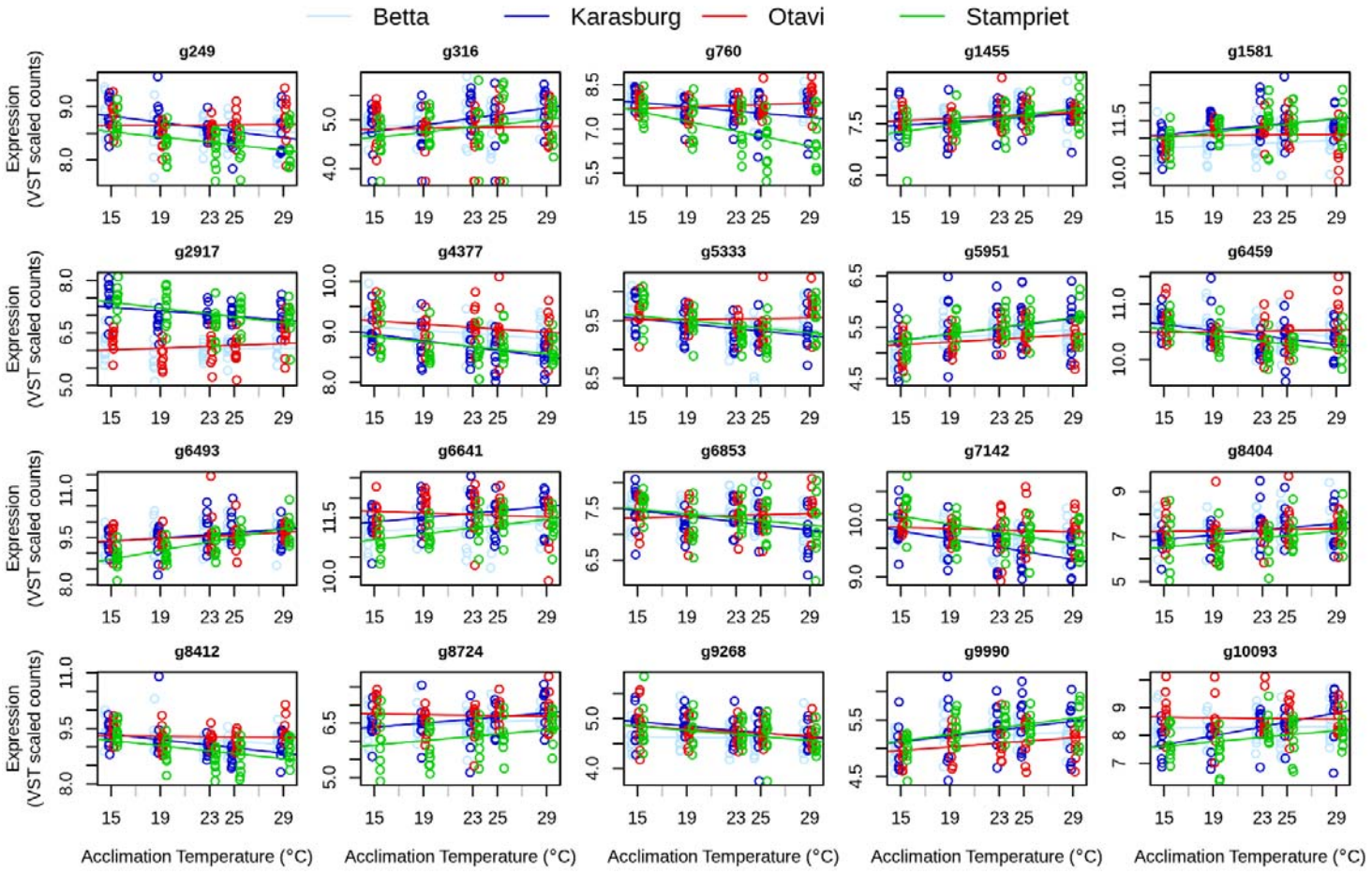

Figure S24 - continued: Gene expression with similar population specific acclimation responses as the cold tolerance phenotype

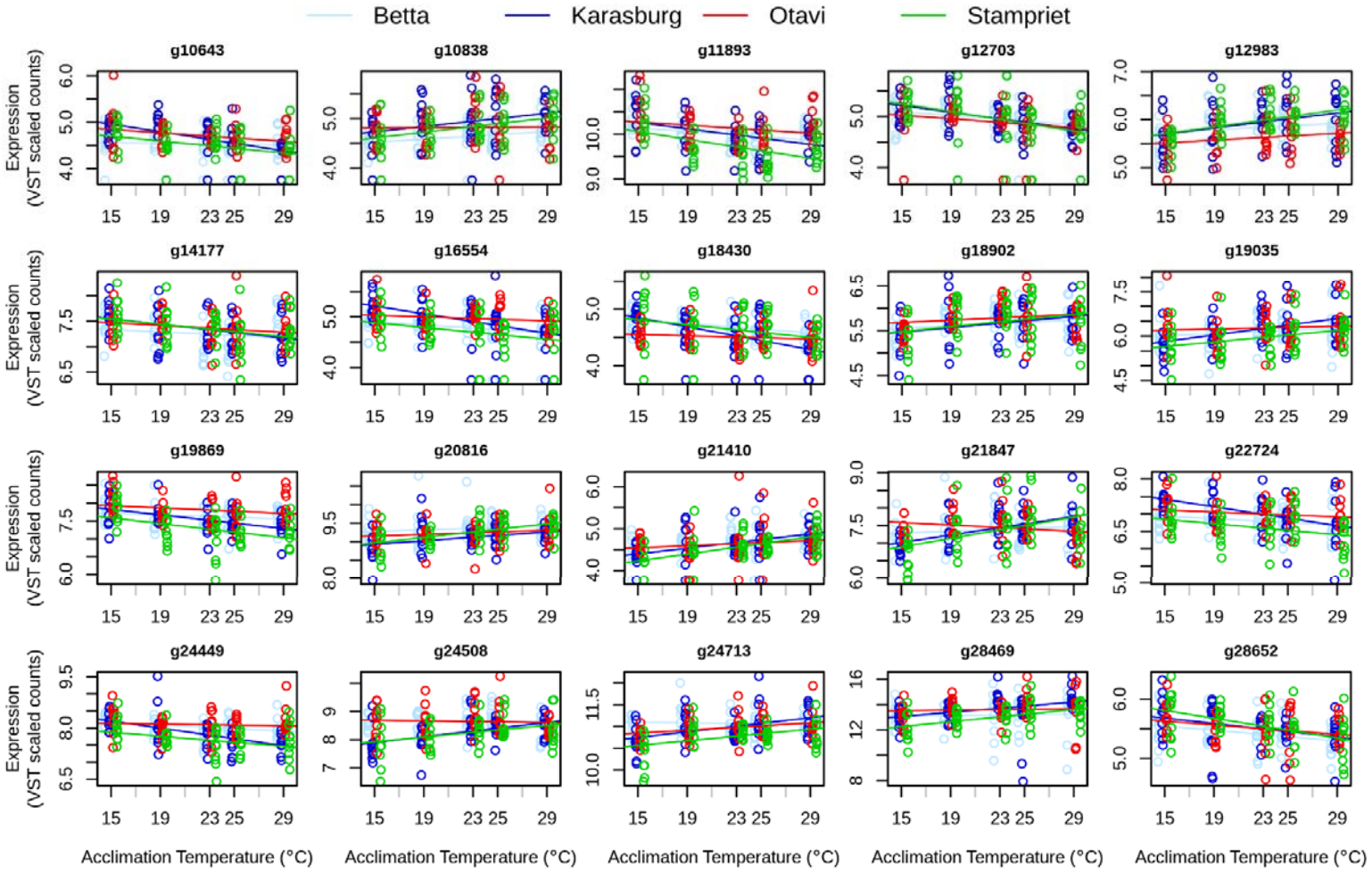

Figure S24 - continued: Gene expression with similar population specific acclimation responses as the cold tolerance phenotype

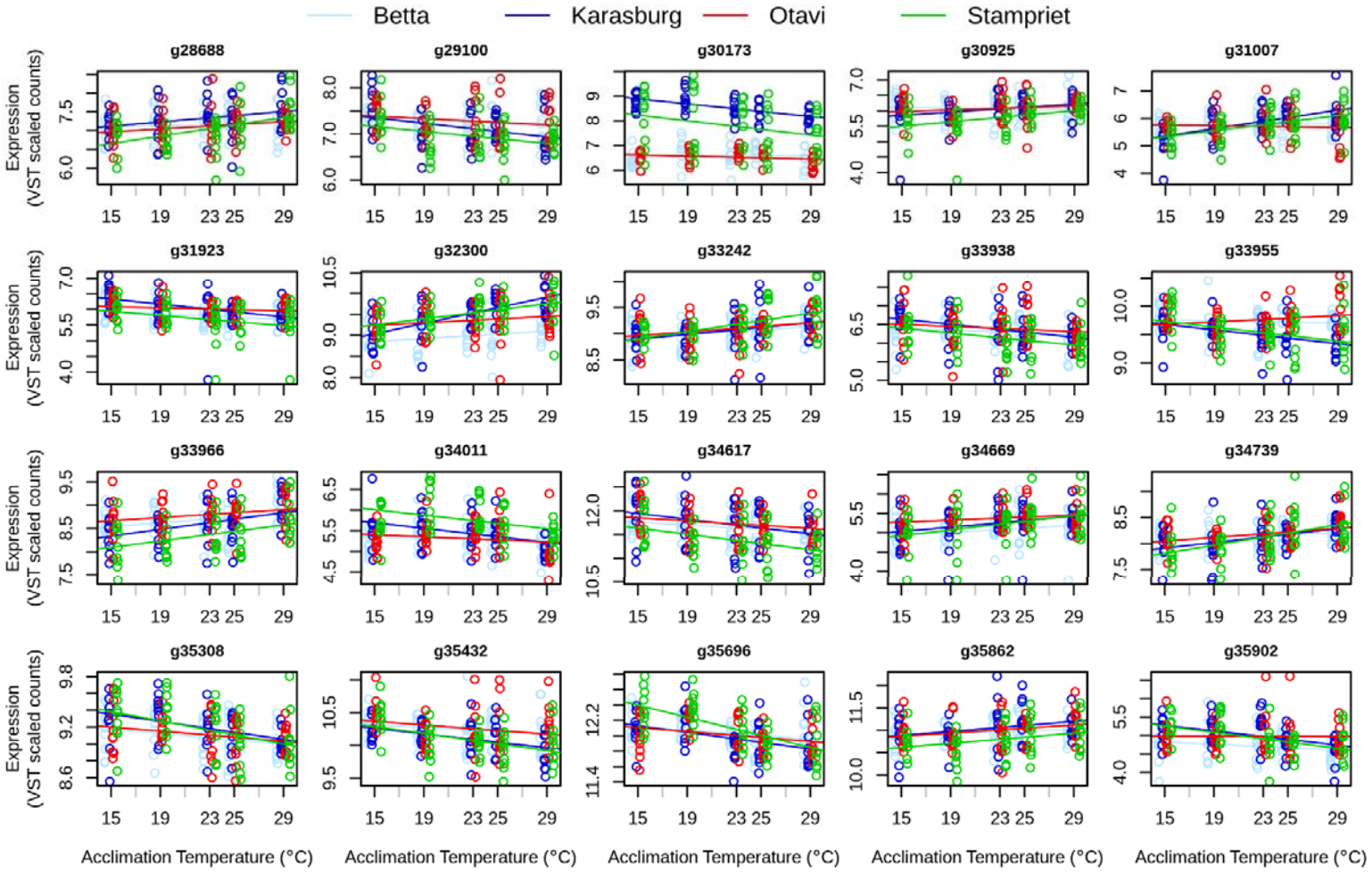

Figure S24 - continued: Gene expression with similar population specific acclimation responses as the cold tolerance phenotype

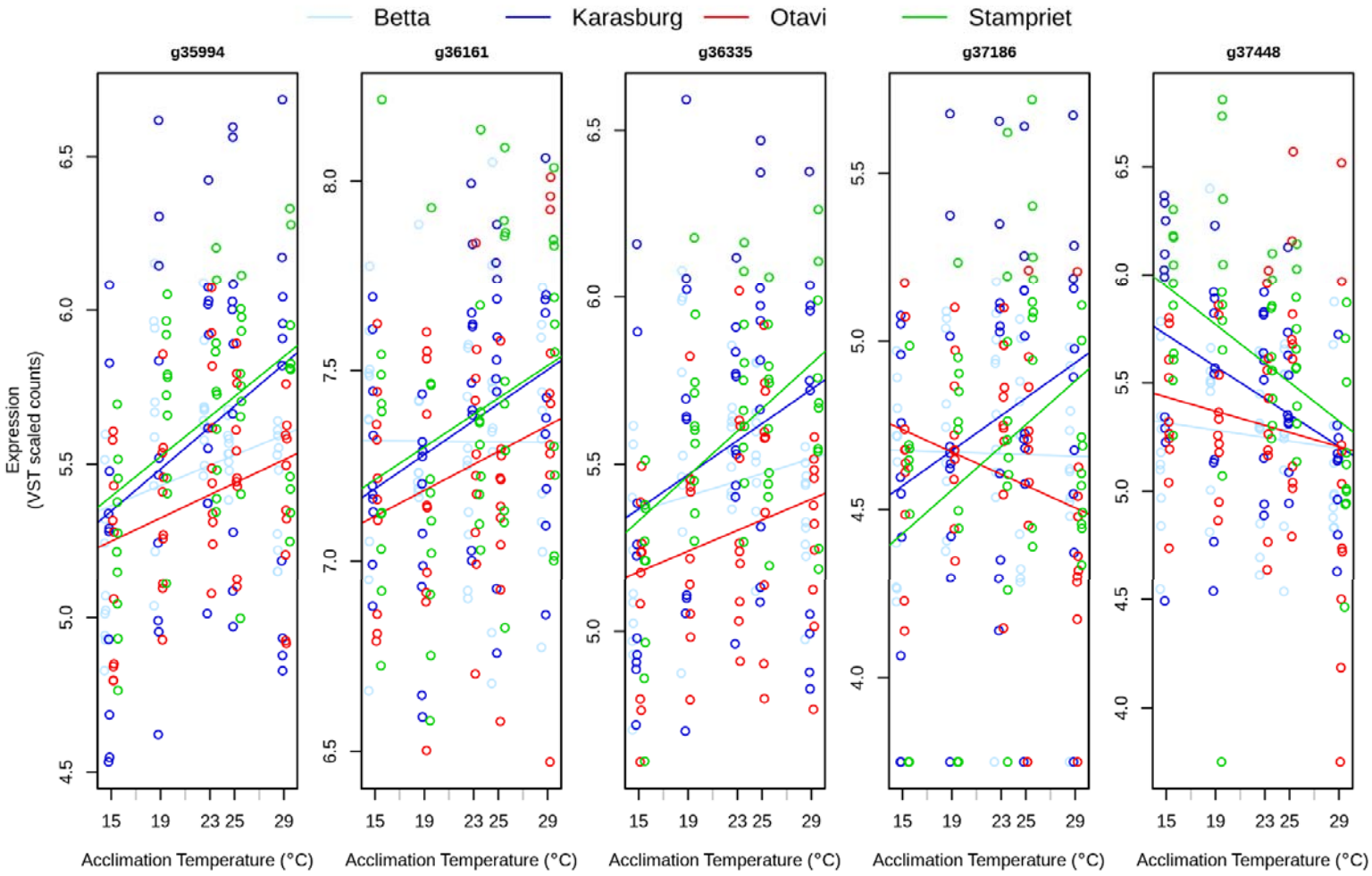

Figure S25: Hydrophilic metabolites with similar population specific acclimation responses as the heat tolerance phenotype

Metabolites with intensity levels showing similar population-specific trends as that of Heat tolerance (CTmax). These 4 metabolites were identified using NMR on spiders in aquatic solution. Metabolites presented in these graphs show a response suggesting an involvement in the observed population dependent heat tolerance, thus linking metabolites to the expressed phenotype.

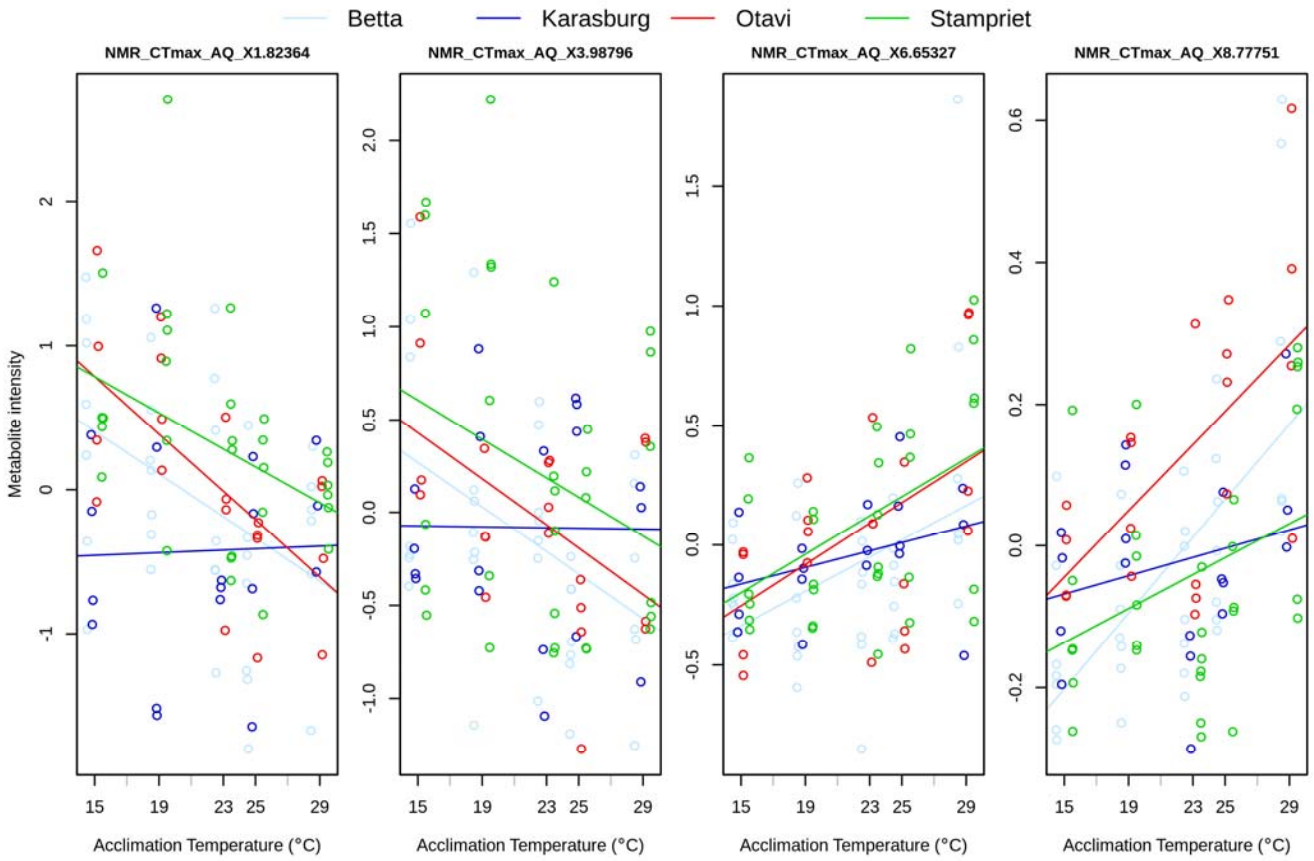

Figure S26: Hydrophobic metabolites with similar population specific acclimation responses as the heat tolerance phenotype

Metabolites with intensity levels showing similar population-specific trends as that of Heat tolerance (CTmax). These 2 metabolites were identified using NMR on spiders in organic solution. Metabolites presented in these graphs show a response suggesting an involvement in the observed population dependent heat tolerance, thus linking metabolites to the expressed phenotype.

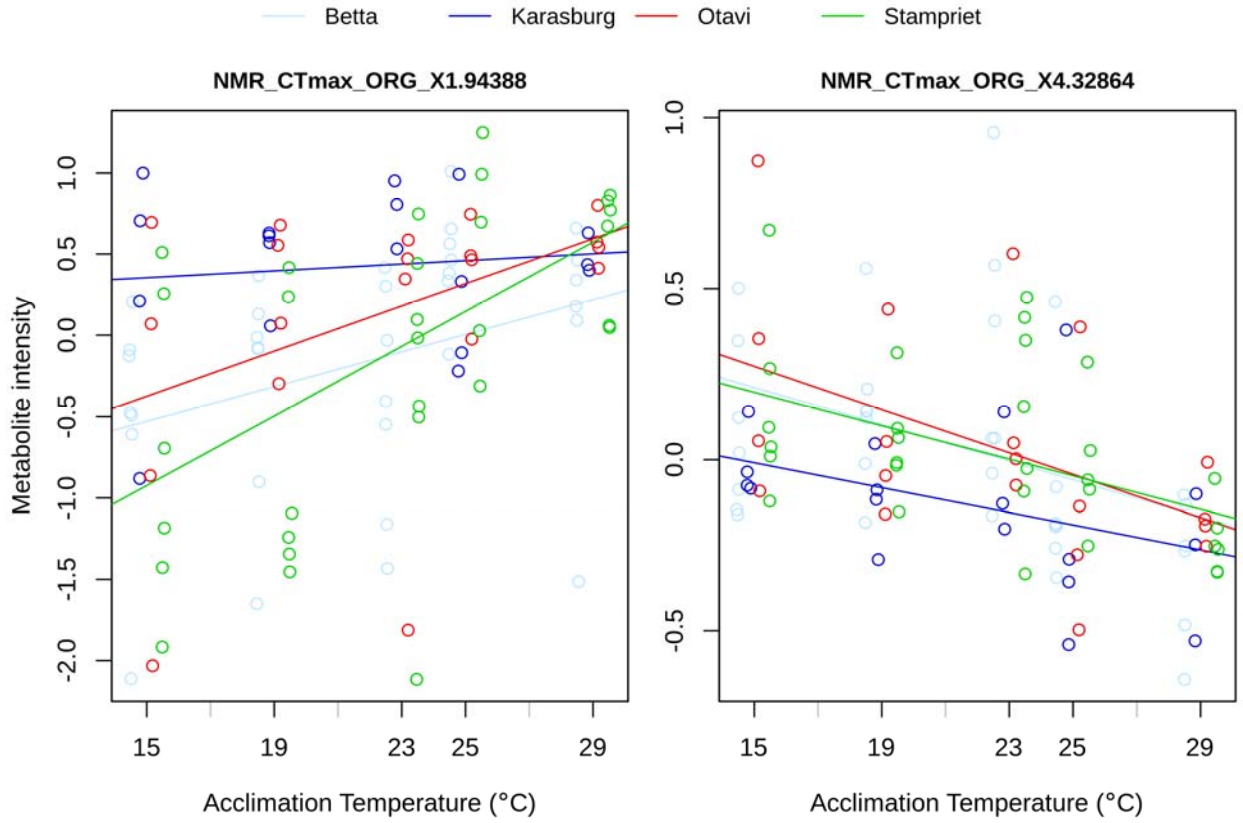

Figure S27: Hydrophilic metabolites with similar population specific acclimation responses as the cold tolerance phenotype

Metabolites with intensity levels showing similar population-specific trends as that of Cold tolerance (CCRTemp). This metabolite was identified using NMR on spiders in aquatic solution. The metabolite presented in here show a response suggesting an involvement in the observed population dependent cold tolerance, thus potentially linking metabolite to the expressed phenotype.

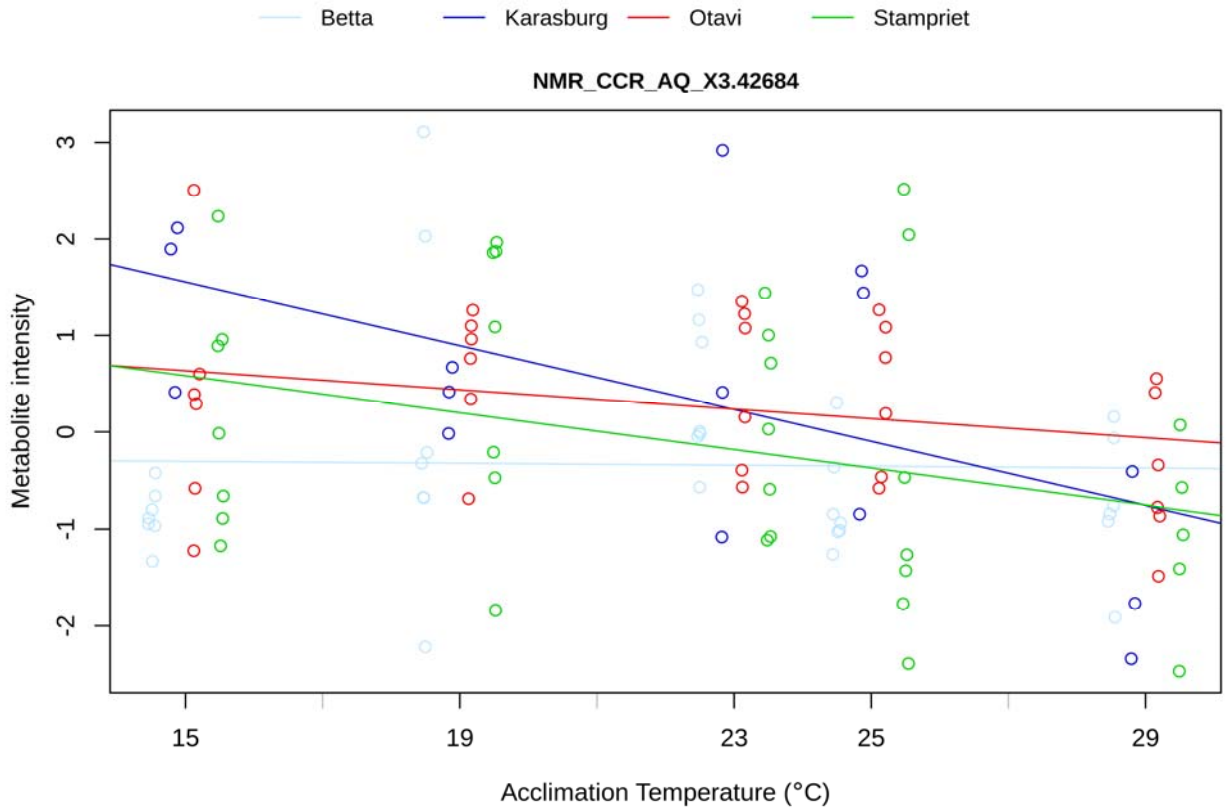

Figure S28: Phylogenies with scenarios for gain/loss of plasticity in heat and cold tolerance

Phylogenetic relationships showing the possible scenarios for ancestral loss or gain of plasticity for temperature tolerances in *S. dumicola* spiders.

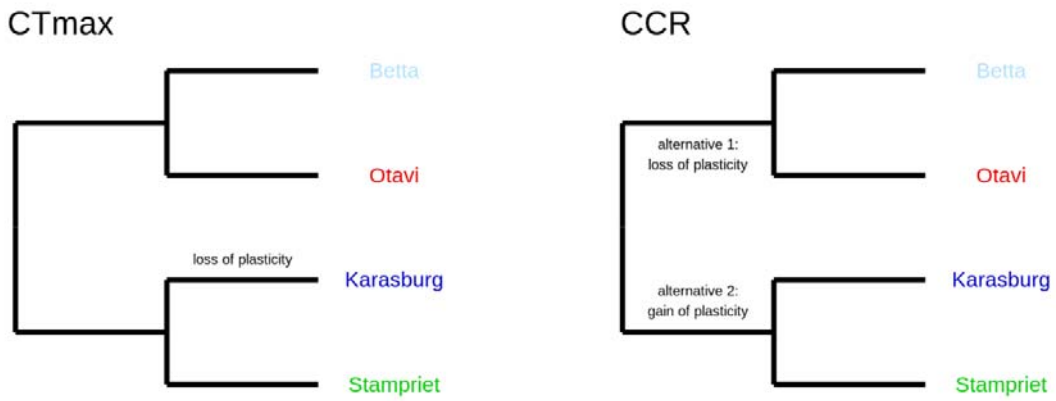

Figure S29: PCA of microbiomic data

Principal component analyses of microbiome ASVs with population effects. PCA analysis on differential microbiome ASV abundances with population effect. Three principal components are plotted, along with a screeplot and a biplot. Karasburg (blue) separates clearly from Otavi (red), Betta (light blue) and Stampriet (green).

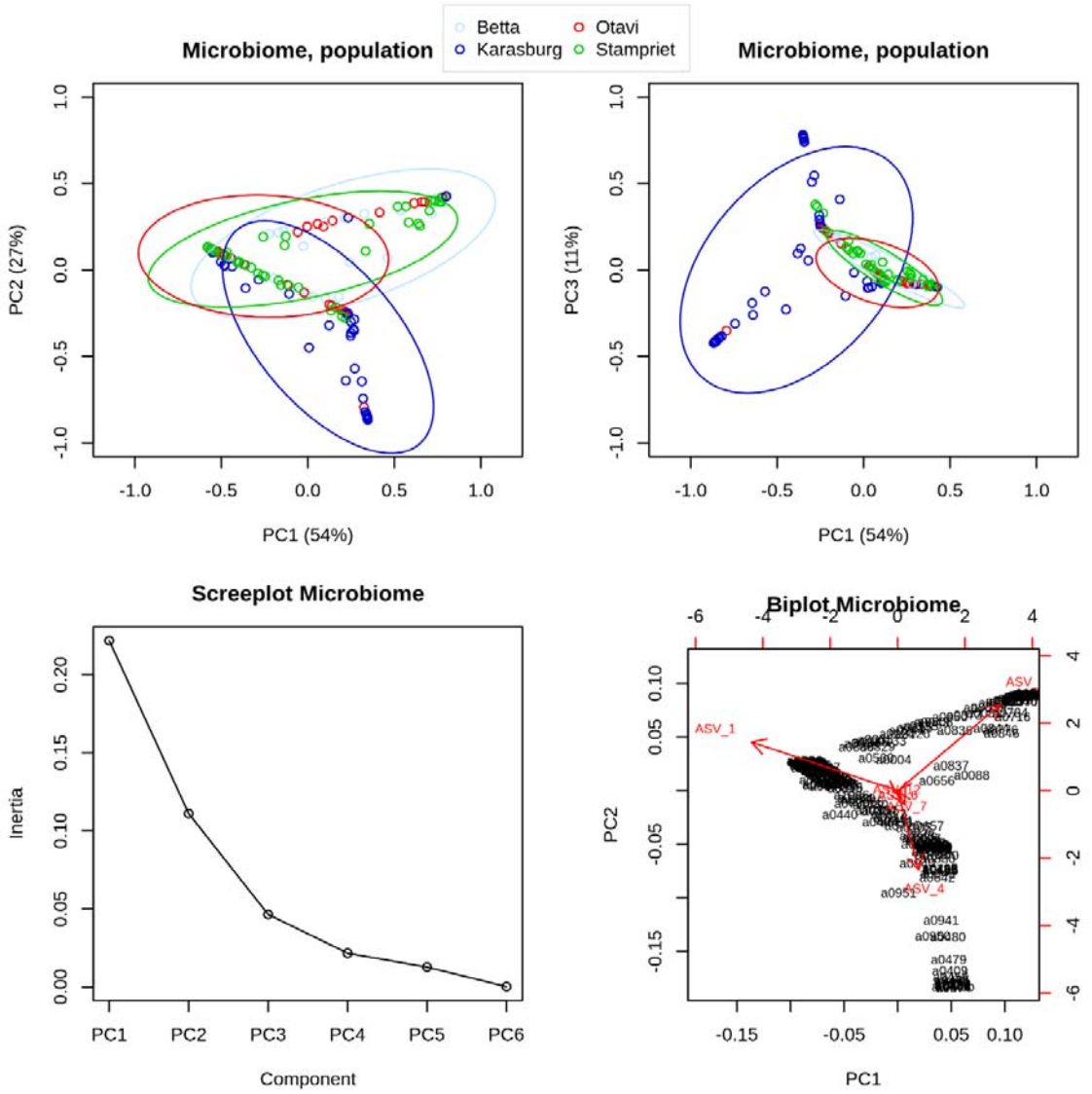

Figure S30: Plots of microbiomic ASVs with population effect

Reaction norms for microbiome ASV abundances for two acclimation temperatures. The graphs show relative abundance as a function of temperature acclimation for each of the ASVs showing population effects.

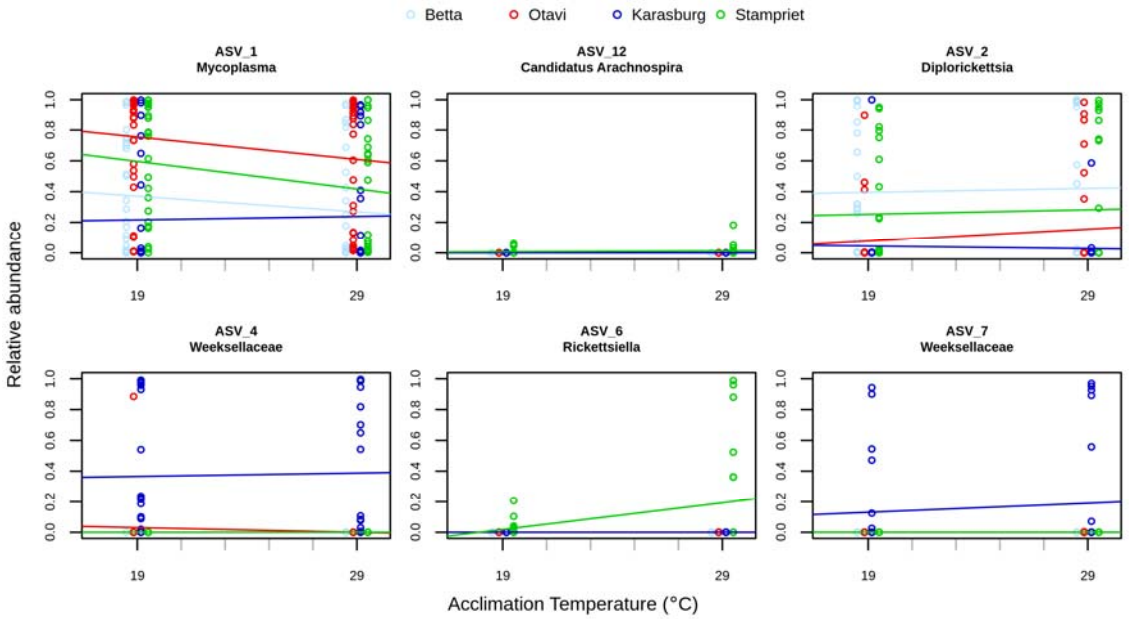

ASV_1 in this study corresponds to ASV_4 in Busck et al., (2020).
ASV_2 in this study corresponds to ASV_9 in Busck et al., (2020).
ASV_12 *Candidatus* Arachnospira was formerly classified as *Borrelia.*

Figure S31: Coverage plot for methylation data

Plot of the coverage distribution for the methylation data. The maximum coverage threshold of 32x were determined by estimating the top one percent of the distribution, and confirmed via visual inspection.

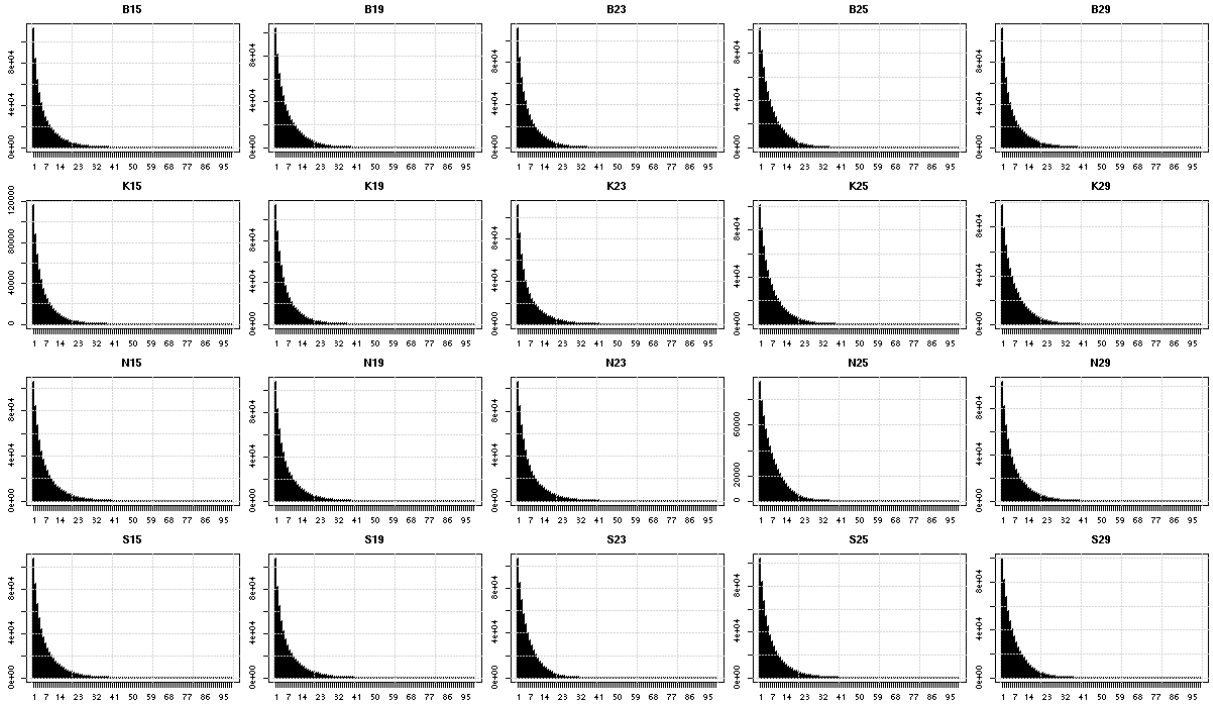

Figure S32: PCA of metabolite NMR-Org data from the CTMax and CCRTemp treatment

Principal Component Analysis of Metabolites from NMR from spiders having gone through CTmax (a, c) or CCR (b, d) treatment. Only metabolites that showed temperature effect are plotted. No metabolites extracted using organic solution showed population responses, thus there is no graph colored by population. Here the first three principal components are plottet.

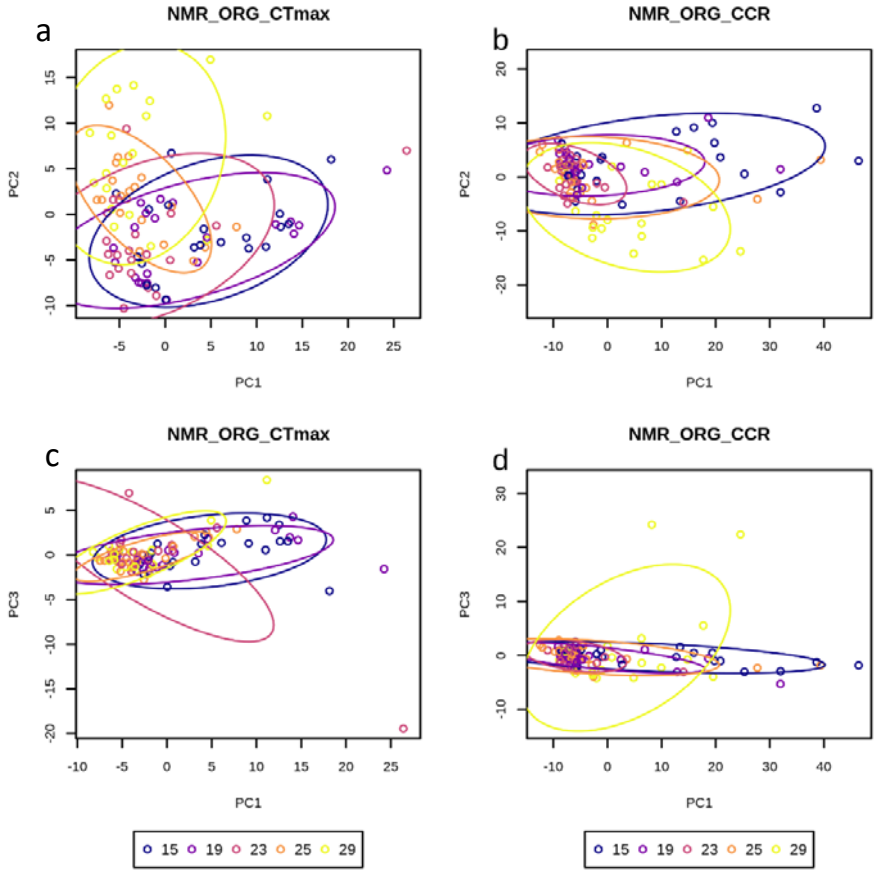

Figure S33: Methylation in plastically expressed genes in response to temperature acclimation

Violin plots of weighted methylation level in three categories of genes: genes that are not plastically expressed in our study, genes that are plastically expressed, or plastically expressed genes with similar population patterns as temperature tolerance phenotypes. Plastic genes show a highly bimodal pattern (middle), which means that a subset of plastic genes have low methylation level, whereas other genes are plastic despite the potential inhibition from methylation, and may thus be regulated by other means than methylation. Plastic genes more likely to be involved in temperature tolerances (right) are generally highly methylated.

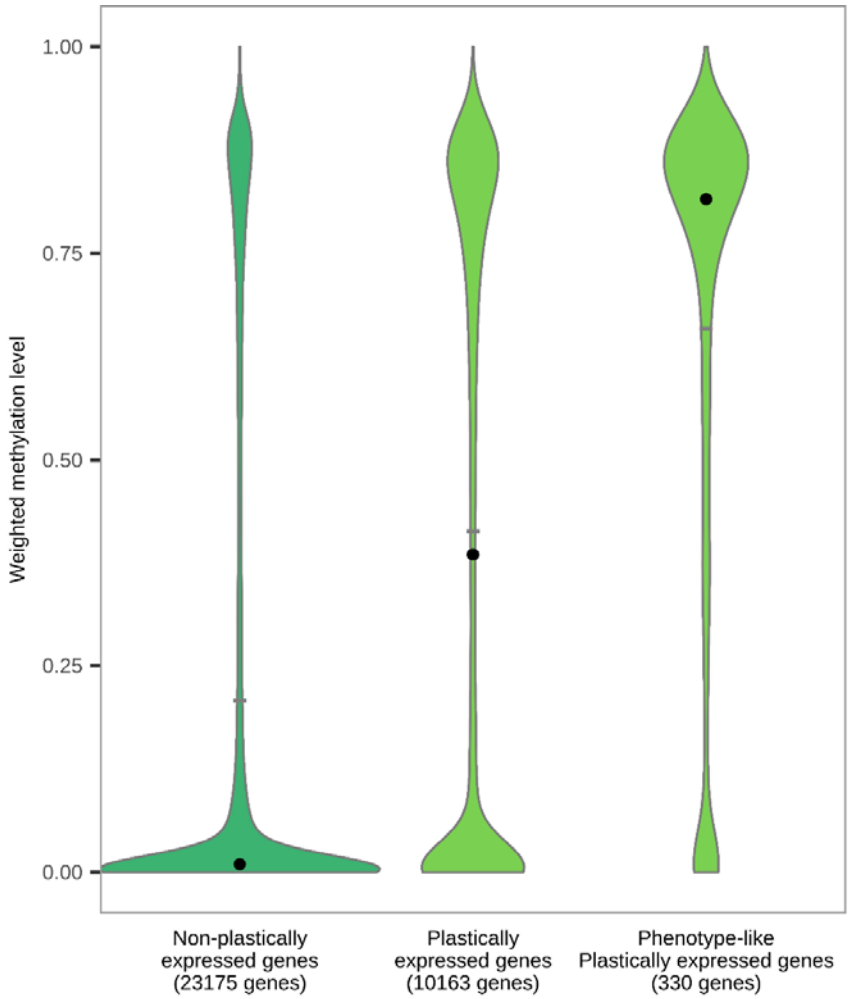

Table S1: Number of social spider *S. dumicola* nest replicates per population/acclimation group

	Count of Nests/boxes
Betta	**101**
15	20
19	20
23	20
25	20
29	21
Karasburg	**65**
15	13
19	13
23	13
25	13
29	13
Otavi	**111**
15	22
19	22
23	22
25	22
29	23
Stampriet	**94**
15	19
19	18
23	18
25	19
29	20
Grand Total	**371**

Table S2: Table of LCMS metabolites and their effects

Metabolites identified by Liquid Chromatography coupled Mass Spectrometer (LC-MS) that were significantly different between treatments or populations. Suffix "_neg" means feature retrieved using negative ionization; Suffix "_pos" means feature retrieved using positive ionization.

Feature ID	Metabolite	Group	Assay	Significance	ID Level*
M229T45_neg	D-Ribulose 5-phosphate	sugar	CCR	interaction	2
M250T42_pos	2'-Deoxyadenosine	nucleoside precursor/ degradation product	CCR	interaction	2
M88T39_neg	L-Alanine	amino acid	CCR	interaction	1
M494T646_pos	L-α-Lysophosphatidyl-choline; 16:0	lipid derivative	CCR	interaction	1
M145T39_neg	L-glutamine	amino acid	CCR	plastic	1
M180T105_neg	Tyrosine	amino acid	CCR	plastic	1
M258T41_neg	D-Glucosamine 6-phosphate	hexose phosphate	CCR	plastic	2
M243T133_neg	Uridine	nucleoside	CCR	plastic	1
M110T41_2_pos	Cytosine	nucleotide	CCR	plastic	2
M229T45_neg	D-Ribulose 5-phosphate	sugar	CCR	plastic	2
M339T37_neg	Fructose 1,6-bisphosphate	hexose phosphate	CCR	plastic	2
M145T253_neg	2-Methylglutaric acid	TCA degradation product	CCR	plastic	2
M383T176_neg	5-Adenosyl-L-homocysteine	amino acid derivative, metabolic intermediate	CCR	plastic	2
M89T71_neg	D-Lactate	fermentation product	CCR	plastic	1
M195T35_pos	Gluconate	sugar derivative	CCR	plastic	2
M306T80_neg	Glutathione reduced	tripeptide, antioxidant	CCR	plastic	1
M174T41_neg	L-Citrulline	amino acid	CCR	plastic	2
M203T264_neg	L-Tryptophane	amino acid	CCR	plastic	1
M664T67_neg	NADH	redox carrier	CCR	plastic	2
M122T103_neg	Nicotinic acid (niacin)	acid, vitamin	CCR	plastic	2
M288T106_neg	Ophthalmic acid	oligopeptide	CCR	plastic	2
M74T42_pos	Trimethylamine N-oxide	amine oxide	CCR	plastic	2
M151T114_neg	Xanthine	nucleoside precursor/ degradation product	CCR	plastic	1
M283T230_neg	Xanthosine	nucleoside	CCR	plastic	1

M204T285_neg	Xanthurenic acid	carboxylic acid	CCR	plastic	1
M74T38_neg	Glycine	amino acid	CCR	population	1
M131T38_neg	L-Asparagine	amino acid	CCR	population	1
M130T119_neg	L-Leucine	amino acid	CCR	population	1
M164T229_neg	Phenylalanine	amino acid	CCR	population	2
M180T105_neg	Tyrosine	amino acid	CCR	population	2
M157T43_2_neg	Allantoin	metabolic intermediate	CCR	population	2
M133T56_neg	Malic acid	metabolic intermediate	CCR	population	1
M110T41_2_pos	cytosine	nucleotide	CCR	population	2
M171T43_2_neg	Glycerol 3-phosphate	polyol	CCR	population	1
M229T45_neg	D-Ribulose 5-Phosphate	sugar	CCR	population	2
M339T37_neg	Fructose 1,6-bisphosphate	hexose phosphate	CCR	population	2
M259T42_neg	Fructose 6-phosphate	hexose phosphate	CCR	population	2
M153T287_neg	2,3-Dihydroxybenzoic acid	phenolic compound	CCR	population	2
M250T42_pos	2'-Deoxyadenosine	nucleoside precursor/ degradation product	CCR	population	2
M266T219_neg	2'-Deoxyguanosine	nucleoside	CCR	population	2
M267T217_neg	2-Deoxyxanthosine	nucleoside	CCR	population	2
M145T253_neg	2-Methylglutaric acid	TCA degradation product	CCR	population	2
M275T47_neg	6-Phosphogluconic acid	pentose phosphate pathway metabolic intermediate	CCR	population	2
M105T47_neg	D-Glyceric Acid	organic acid	CCR	population	1
M195T35_pos	Gluconate	sugar derivative	CCR	population	2
M150T63_neg	Guanine	nucleotide	CCR	population	1
M108T41_pos	Hypotaurine	osmolyte, antioxidant	CCR	population	2
M190T290_neg	N-acetyl-DL-methionine	amino acid derivative	CCR	population	1
M662T146_neg	NAD+	redox carrier	CCR	population	2
M382T289_2_pos	Succinyladenosine	nucleoside derivative	CCR	population	1
M283T230_neg	Xanthosine	nucleoside	CCR	population	1
M190T290_neg	N-acetyl-DL-methionine	amino acid derivative	Ctmax	interaction	1
M383T176_neg	5-adenosyl-L-homocysteine	amino acid derivative, metabolic intermediate	Ctmax	interaction	2

M136T105_neg	Tyramine	amino acid derivative	Ctmax	interaction	2
M130T42_pos	Hydroxyproline	amino acid	Ctmax	interaction	2
M160T45_neg	L-2-aminoadipic acid	metabolic intermediate	Ctmax	interaction	2
M173T36_neg	L-Arginine	amino acid	Ctmax	interaction	2
M131T38_neg	L-Asparagine	amino acid	Ctmax	interaction	1
M145T39_neg	L-Glutamine	amino acid	Ctmax	interaction	1
M131T36_neg	L-Ornithine	amino acid	Ctmax	interaction	2
M118T39_neg	L-Threonine	amino acid	Ctmax	interaction	2
M180T38_pos	Tyrosine	amino acid	Ctmax	interaction	1
M258T41_neg	D-Glucosamine 6-phosphate	hexose phosphate	Ctmax	interaction	2
M220T38_pos	N-acetyl-D-glucosamine	amino sugar	Ctmax	interaction	2
M137T293_neg	4-Hydroxybenzoic acid	aromatic acid	Ctmax	interaction	2
M263T286_neg	Phe-Val	dipeptide	Ctmax	interaction	2
M89T71_neg	D-Lactate	fermentation product	Ctmax	interaction	1
M157T43_2_neg	Allantoin	metabolic intermediate	Ctmax	interaction	2
M115T128_neg	Fumaric acid	TCA cycle intermediate	Ctmax	interaction	1
M117T111_neg	Succinic acid	TCA cycle intermediate	Ctmax	interaction	1
M122T103_neg	Nicotinic acid (niacin)	acid, vitamin	Ctmax	interaction	2
M250T42_pos	2'-Deoxyadenosine	nucleoside precursor/ degradation product	Ctmax	interaction	2
M242T59_neg	Cytidine	nucleoside	Ctmax	interaction	2
M150T63_neg	Guanine	nucleoside	Ctmax	interaction	1
M243T133_neg	Uridine	nucleoside	Ctmax	interaction	1
M135T43_2_neg	Hypoxanthine	nucleoside precursor/ degradation product	Ctmax	interaction	2
M347T101_neg	Inosine 5'-monophosphate	nucleoside precursor/ degradation product	Ctmax	interaction	2
M363T118_neg	Xanthosine 5' monophosphate	nucleoside precursor/ degradation product	Ctmax	interaction	2
M275T47_neg	6-Phosphogluconic acid	pentose phosphate pathway metabolic intermediate	Ctmax	interaction	2
M131T216_neg	Glutaric acid	carboxylic acid	Ctmax	interaction	2
M108T41_pos	Hypotaurine	osmolyte, antioxidant	Ctmax	interaction	2
M124T33_pos M124T38_1_neg	Taurine	osmolyte	Ctmax	interaction	1

M455T327_neg	Flavin mononucleotide (FMN)	redox carrier	Ctmax	interaction	1
M147T79_neg	L-2-Hydroxyglutaric acid	short chain hydroxy acid	Ctmax	interaction	2
M199T46_neg	D-Erythrose 4-phosphate	pentose phosphate pathway intermediate	Ctmax	interaction	2
M339T37_neg	Fructose 1,6-bisphosphate	hexose phosphate	Ctmax	interaction	2
M133T56_neg	Malic acid	TCA cycle intermediate	Ctmax	interaction	2
M145T253_neg	2-Methylglutaric acid	TCA degradation product	Ctmax	interaction	2
M611T238_neg	Glutathione oxidized	tripeptide	Ctmax	interaction	1
M218T258_neg	Pantothenic acid	vitamin B5	Ctmax	interaction	1
M188T114_neg	N-Acetyl-L-glutamic acid	metabolic intermediate	Ctmax	plastic	2
M113T44_pos	3-amino-2-piperidone	amino acid derivative	Ctmax	plastic	2
M204T285_neg	Xanthurenic acid	carboxylic acid	Ctmax	plastic	1
M188T297_pos	Kynurenic acid	amino acid derivative	Ctmax	plastic	2
M160T45_neg	L-2-Aminoadipic acid	metabolic intermediate	Ctmax	plastic	2
M173T36_neg	L-Arginine	amino acid	Ctmax	plastic	2
M174T41_neg	L-Citrulline	amino acid	Ctmax	plastic	2
M130T119_neg	L-Leucine	amino acid	Ctmax	plastic	1
M203T264_neg	L-Tryptophane	amino acid	Ctmax	plastic	2
M164T229_neg	Phenylalanine	amino acid	Ctmax	plastic	2
M180T105_neg M180T38_pos	Tyrosine	amino acid	Ctmax	plastic	1
M258T41_neg	D-Glucosamine 6-phosphate	hexose phosphate	Ctmax	plastic	2
M220T38_pos	N-acetyl-D-glucosamine	amino sugar	Ctmax	plastic	2
M160T262_neg	Indole-3-carboxylic acid	amino acid derivative	Ctmax	plastic	2
M263T291_pos	Phe-Val	dipeptide	Ctmax	plastic	2
M494T646_pos	L-α-Lysophosphatidyl-choline; 16:0	lipid derivative	Ctmax	plastic	1
M191T82_neg	Citric acid	TCA cycle intermediate	Ctmax	plastic	1
M116T48_pos	N,N-dimethylalanine	amino acid derivative	Ctmax	plastic	2
M122T103_neg	nicotinic acid (niacin)	acid, vitamin	Ctmax	plastic	2
M242T59_neg	Cytidine	nucleoside	Ctmax	plastic	2
M243T133_neg	Uridine	nucleoside	Ctmax	plastic	1

M135T43_2_neg	Hypoxanthine	nucleoside precursor/ degradation product	Ctmax	plastic	2
M347T101_neg	Inosine 5'-monophosphate	nucleoside precursor/ degradation product	Ctmax	plastic	2
M151T114_neg	Xanthine	nucleoside precursor/ degradation product	Ctmax	plastic	1
M283T230_neg	Xanthosine	nucleoside	Ctmax	plastic	1
M322T53_neg	Cytidine 5-monophosphate	nucleotide	Ctmax	plastic	2
M282T218_neg	Guanosine	nucleotide	Ctmax	plastic	2
M323T72_neg	Uridine 5-monophosphate	nucleotide	Ctmax	plastic	1
M275T47_neg	6-Phosphogluconic acid	pentose phosphate pathway metabolic intermediate	Ctmax	plastic	2
M195T42_2_neg	Gluconate	sugar derivative	Ctmax	plastic	2
M87T82_neg	Pyruvic acid	organic acid	Ctmax	plastic	2
M116T39_pos	Betaine	osmolyte	Ctmax	plastic	2
M108T41_pos	Hypotaurine	osmolyte, antioxidant	Ctmax	plastic	2
M124T33_pos M124T38_1_neg	Taurine	osmolyte	Ctmax	plastic	1
M171T43_2_neg	Glycerol 3-phosphate	polyol	Ctmax	plastic	1
M199T46_neg	D-Erythrose 4-phosphate	pentose phosphate pathway intermediate	Ctmax	plastic	2
M339T37_neg	Fructose 1,6-bisphosphate	hexose phosphate	Ctmax	plastic	2
M259T42_neg	Fructose 6-phosphate	hexose phosphate	Ctmax	plastic	2
M133T56_neg	Malic acid	TCA cycle intermediate	Ctmax	plastic	2
M306T80_neg	Glutathione reduced	tripeptide, antioxidant	Ctmax	plastic	1
M288T106_neg	Ophthalmic acid	oligopeptide	Ctmax	plastic	2
M375T333_neg	Riboflavin	vitamin B2	Ctmax	plastic	1
M245T46_2_neg	1-(3-sn-phosphatidyl)-rac-glycerol	lipid derivative	Ctmax	plastic	2
M136T105_neg	Tyramine	amino acid derivative	Ctmax	population	2
M188T297_pos	Kynurenic acid	amino acid derivative	Ctmax	population	2
M74T42_pos	Trimethylamine N-oxide	amine oxide	Ctmax	population	2
M74T44_pos	Glycine	amino acid	Ctmax	population	1
M173T36_neg	L-Arginine	amino acid	Ctmax	population	2
M131T38_neg	L-Asparagine	amino acid	Ctmax	population	1
M132T39_neg	L-Aspartic acid	amino acid	Ctmax	population	2

M130T119_neg	L-Leucine	amino acid	Ctmax	population	1
M164T229_neg	Phenylalanine	amino acid	Ctmax	population	2
M258T41_neg	D-Glucosamine 6-phosphate	hexose phosphate	Ctmax	population	2
M137T293_neg	4-Hydroxybenzoic acid	aromatic acid	Ctmax	population	2
M263T286_neg	Phe-Val	dipeptide	Ctmax	population	2
M157T43_2_neg	Allantoin	metabolic intermediate	Ctmax	population	2
M115T128_neg	Fumaric acid	TCA cylce intermediate	Ctmax	population	1
M122T103_neg	nicotinic acid (niacin)	acid, vitamin	Ctmax	population	2
M250T42_pos	2'-Deoxyadenosine	nucleoside precursor/ degradation product	Ctmax	population	2
M267T217_neg	2-Deoxyxanthosine	nucleoside	Ctmax	population	2
M135T43_2_neg	Hypoxanthine	nucleoside precursor/ degradation product	Ctmax	population	2
M347T101_neg	Inosine 5'-monophosphate	nucleoside precursor/ degradation product	Ctmax	population	2
M151T114_neg	Xanthine	nucleoside precursor/ degradation product	Ctmax	population	1
M282T218_neg	Guanosine	nucleotide	Ctmax	population	2
M105T47_neg	D-Glyceric Acid	organic acid	Ctmax	population	1
M131T216_neg	Glutaric acid	carboxylic acid	Ctmax	population	2
M108T41_pos	Hypotaurine	osmolyte, antioxidant	Ctmax	population	2
M124T38_1_neg	Taurine	osmolyte	Ctmax	population	1
M171T43_2_neg	Glycerol 3-phosphate	polyol	Ctmax	population	1
M664T67_neg	NADH	redox carrier	Ctmax	population	2
M147T79_neg	L-2-Hydroxyglutaric acid	short chain hydroxy acid	Ctmax	population	2
M199T46_neg	D-Erythrose 4-phosphate	pentose phosphate pathway intermediate	Ctmax	population	2
M145T253_neg	2-Methylglutaric acid	TCA degradation product	Ctmax	population	2
M166T45_pos	Pyridoxal	vitamin B6	Ctmax	population	2
M245T46_2_neg	1-(3-sn-phosphatidyl)-rac-glycerol	lipid derivative	Ctmax	population	2

* According to Sumner et al., (2007): 1 = verified by authentic standard, 2 = putatively annotated compounds verified by MS spectral libraries.

Table S3: Model summary output for growth rate model

Best model summary output for growth rate data of *S. dumicola* spiders. The analysis was based on grand mean centered treatment data (acclimation temperature).

Linear model: growth rate ~ Population * Treatment

	Growth rate				
Predictors	*Estimates*	*std. Error*	*CI*	*Statistic*	*p*
(Intercept)	1.53 ***	0.05	1.43 – 1.62	31.10	**<0.001**
Population [Karasburg]	-0.05	0.08	-0.21 – 0.11	-0.64	0.525
Population [Otavi]	-0.11	0.07	-0.25 – 0.02	-1.62	0.106
Population [Stampriet]	-0.07	0.09	-0.25 – 0.11	-0.76	0.447
Treatment	0.10 ***	0.01	0.08 – 0.12	10.29	**<0.001**
Population [Karasburg] * Treatment	0.01	0.02	-0.03 – 0.04	0.30	0.762
Population [Otavi] * Treatment	-0.03 *	0.01	-0.06 – -0.00	-2.01	**0.045**
Population [Stampriet] * Treatment	0.00	0.02	-0.03 – 0.04	0.23	0.817
Observations	304				
R^2 / R^2 adjusted	0.490 / 0.478				
AIC	439.668				
F-statistic	40.66 on 7 and 296 DF				
p-value	< 2.2e-16				

** p < 0.05 ** p < 0.01 *** p < 0.001*

Table S4: ANOVA output for model on growth rate

ANOVA output from the best model on growth rate of *S. dumicola* spiders. The analysis was based on grand mean centered treatment data (acclimation temperature).

Linear model: Growth rate ~ Population * Treatment

ANOVA on Growth rate model

Row	*Df*	*Sum Sq*	*Mean Sq*	*F value*	*Pr(>F)*	
Population	3	0.84	0.28	1.16	0.33	
Treatment	1	66.11	66.11	274.65	0.00	***
Population:Treatment	3	1.56	0.52	2.16	0.09	
Residuals	296	71.25	0.24			

** p < 0.05 ** p < 0.01 *** p < 0.001*

Table S5: ANOVA output for model on survival

Anova() output from the best model on survival of *S. dumicola* spiders compared to the null model. The analysis was based on grand mean centered treatment data (acclimation temperature).

General linear model, binomial, logit link: Survival ~ Population + Treatment.

Analysis of deviance on Survival model

Row	*Df*	*Deviance*	*Resid. Df*	*Resid. Dev*	*Pr(>Chi)*	
Null			303	1325.39		
Population	3	17.99	300	1307.39	0.00	***
Treatment	1	233.25	299	1074.15	0.00	***

** p < 0.05 ** p < 0.01 *** p < 0.001*

Table S6: Model summary for survival model

Best model summary output for survival data of *S. dumicola* spiders. The analysis was based on grand mean centered treatment data (acclimation temperature).

General linear model, binomial, logit link: Survival ~ Population + Treatment.

			Survival data		
Predictors	*Log-Odds*	*std. Error*	*CI*	*Statistic*	*p*
(Intercept)	2.11 ***	0.06	1.99 – 2.22	35.75	**<0.001**
Population [Karasburg]	0.42 ***	0.10	0.22 – 0.63	4.02	**<0.001**
Population [Otavi]	0.06	0.08	-0.10 – 0.22	0.73	0.466
Population [Stampriet]	0.12	0.11	-0.09 – 0.33	1.10	0.274
Treatment	0.11 ***	0.01	0.09 – 0.12	14.82	**<0.001**
Observations	304				
R^2 Tjur	0.010				
R^2 McFadden (adj)	0.125				
AIC	1754.826				
p-value (to null model)	< 2.2e-16				

** p < 0.05 ** p < 0.01 *** p < 0.001*

Table S7: Test output on whether CTmax population trends differ from zero

Table of the summary from the emtrends() function, testing whether the population trends are significantly different from zero. The linear model tested were based on CTmax temperature tolerance data.

CTmax - Trendlines diverging from zero

Population	*Treatment.trend*	*SE*	*df*	*lower.CL*	*upper.CL*	*t.ratio*	*p.value*
Betta	0.104	0.010	298	0.084	0.124	10.057	0.000
Karasburg	0.022	0.013	298	-0.004	0.048	1.690	0.092
Otavi	0.086	0.011	298	0.064	0.108	7.674	0.000
Stampriet	0.042	0.013	298	0.017	0.066	3.319	0.001

Table S8: Test output on whether CCRTemp population trends differ from zero

Table of the summary from the emtrends() function, testing whether the population trends are significantly different from zero. The linear model tested were based on CCRTemp temperature tolerance data.

CCRTemp - Trendlines diverging from zero

Population	*Treatment.trend*	*SE*	*df*	*lower.CL*	*upper.CL*	*t.ratio*	*p.value*
Betta	0.028	0.047	320	-0.065	0.121	0.589	0.557
Karasburg	0.201	0.059	320	0.085	0.316	3.408	0.001
Otavi	0.033	0.047	320	-0.060	0.125	0.695	0.488
Stampriet	0.138	0.055	320	0.029	0.247	2.494	0.013

Table S9: Best model summary on CTmax data

Best model summary output from analyses of CTmax data of *S. dumicola* spiders. The analysis was based on grand mean centered treatment data (acclimation temperature).

Linear model: CTmax ~ Population * Treatment + Body mass + Time since feeding + Preacclimation duration.

	CTmax – heat tolerance				
Predictors	*Estimates*	*std. Error*	*CI*	*Statistic*	*p*
(Intercept)	50.42 ***	0.13	50.17 – 50.67	397.71	**<0.001**
Population [Karasburg]	-0.29 ***	0.09	-0.46 – -0.13	-3.42	**0.001**
Population [Otavi]	0.07	0.08	-0.08 – 0.22	0.92	0.358
Population [Stampriet]	-0.18	0.10	-0.36 – 0.01	-1.85	0.065
Treatment	0.10 ***	0.01	0.08 – 0.12	10.06	**<0.001**
Body mass	-0.01 *	0.01	-0.02 – -0.00	-1.97	**0.050**
Time since feeding	0.05 *	0.02	0.00 – 0.10	2.09	**0.037**
Preacclimation duration	0.00 *	0.00	0.00 – 0.01	2.24	**0.026**
Population [Karasburg] *	-0.08 ***	0.02	-0.11 – -0.05	-5.35	**<0.001**
Population [Otavi] *	-0.02	0.01	-0.05 – 0.01	-1.28	0.202
Population [Stampriet] *	-0.06 ***	0.02	-0.09 – -0.03	-4.07	**<0.001**
Observations	309				
R^2 / R^2 adjusted	0.409 / 0.389				
AIC	407.455				
F-statistic	20.61 on 10 and 298 DF				
p-value	< 2.2e-16				

** p < 0.05 ** p < 0.01 *** p < 0.001*

Table S10: ANOVA output from CTmax model

ANOVA output from the best model on CTmax of *S. dumicola* spiders. The analysis was based on grand mean centered treatment data (acclimation temperature).

Linear model: CTmax ~ Population * Treatment + Body mass + Time since feeding + preacclimation duration.

ANOVA on CTmax model

Row	*Df*	*Sum Sq*	*Mean Sq*	*F value*	*Pr(>F)*	
Population	3	3.82	1.27	6.07	0.00	***
Treatment	1	27.67	27.67	131.78	0.00	***
Body mass	1	1.81	1.81	8.63	0.00	**
Time since feeding	1	1.13	1.13	5.40	0.02	*
Preacclimation duration	1	1.09	1.09	5.19	0.02	*
Population:Treatment	3	7.74	2.58	12.29	0.00	***
Residuals	298	62.58	0.21			

** p < 0.05 ** p < 0.01 *** p < 0.001*

Table S11: Test output on whether CTmax population trends differ

Table showing the output from the emtrends() function on the CTmax model, testing whether trends are different from each other. Significance groups have been added by the MultComp cld() function.

CTmax - Trendlines significance groups

Population	*Treatment.trend*	*SE*	*df*	*lower.CL*	*upper.CL*	*group*
Karasburg	0.022	0.013	298	-0.004	0.048	a
Stampriet	0.042	0.013	298	0.017	0.066	a
Otavi	0.086	0.011	298	0.064	0.108	b
Betta	0.104	0.010	298	0.084	0.124	b

Table S12: Model summary output for CCRTemp model

Best model summary output from analyses of CCRTemp data of *S. dumicola* spiders. The analysis was based on grand mean centered treatment data (acclimation temperature).

Linear model: CCRTemp ~ Population * Treatment + Body mass mean + Time since feeding.

	CCRTemp – cold tolerance				
Predictors	*Estimates*	*std. Error*	*CI*	*Statistic*	*p*
(Intercept)	12.93 ***	0.54	11.86 – 13.99	23.78	**<0.001**
Population [Karasburg]	-0.83 *	0.35	-1.53 – -0.13	-2.33	**0.020**
Population [Otavi]	0.58	0.33	-0.06 – 1.23	1.79	0.075
Population [Stampriet]	-0.50	0.34	-1.16 – 0.17	-1.47	0.141
Treatment	0.03	0.05	-0.07 – 0.12	0.59	0.557
Body mass mean	-0.04	0.03	-0.10 – 0.01	-1.50	0.134
Feding time	-0.31 **	0.11	-0.52 – -0.10	-2.93	**0.004**
Population [Karasburg] *	0.17 *	0.07	0.04 – 0.31	2.50	**0.013**
Population [Otavi] *	0.00	0.06	-0.11 – 0.12	0.08	0.935
Population [Stampriet] *	0.11	0.07	-0.02 – 0.24	1.62	0.105
Observations	330				
R^2 / R^2 adjusted	0.098 / 0.073				
AIC	1427.653				
F-statistic	3.862 on 9 and 320 DF				
p-value	0.0001159				

** p < 0.05 ** p < 0.01 *** p < 0.001*

Table S13: ANOVA output from CCRTemp model

ANOVA output from the best model on CCRTemp of *S. dumicola* spiders. The analysis was based on grand mean centered treatment data (acclimation temperature).

Linear model: CCRTemp ~ Population * Treatment + Body mass + Time since feeding.

ANOVA on CCRTemp model

Row	*Df*	*Sum Sq*	*Mean Sq*	*F value*	*Pr(>F)*	
Population	3	48.43	16.14	3.78	0.01	*
Treatment	1	22.64	22.64	5.30	0.02	*
Body mass	1	2.77	2.77	0.65	0.42	
Time since feeding	1	36.79	36.79	8.61	0.00	**
Population:Treatment	3	37.91	12.64	2.96	0.03	*
Residuals	320	1367.54	4.27			

** p < 0.05 ** p < 0.01 *** p < 0.001*

Table S14: Test output on whether CCRTemp population trends differ

Table showing the output from the emtrends() function on the CCRTemp model, testing whether trends are different from each other. Significance groups have been added by the MultComp cld() function.

CCRTemp - Trendlines significance groups

Population	*Treatment.trend*	*SE*	*df*	*lower.CL*	*upper.CL*	*group*
Betta	0.028	0.047	320	-0.065	0.121	a
Otavi	0.033	0.047	320	-0.060	0.125	a
Stampriet	0.138	0.055	320	0.029	0.247	a
Karasburg	0.201	0.059	320	0.085	0.316	a

Table S15: Gene ontology enrichment analysis results

Functional enrichment results of genes expressed with similar population-dependent responses as was found in temperature tolerances (CTmax and CCRTemp). Ontology types investigated: Biological Process (BP) and Molecular Function (MF).

Ontology type	Data type	GOBPID	Pvalue	OddsRatio	ExpCount	Count	Size	Term
BP	CCR	GO:0007369	0.013958	165.3333	0.014	1	2	gastrulation
BP	CCR	GO:0001704	0.013958	165.3333	0.014	1	2	formation of primary germ layer
BP	CCR	GO:0048869	0.013958	165.3333	0.014	1	2	cellular developmental process
BP	CCR	GO:0030154	0.013958	165.3333	0.014	1	2	cell differentiation
BP	CCR	GO:0000002	0.020874	82.58333	0.021	1	3	mitochondrial genome maintenance
BP	CCR	GO:0048598	0.041374	32.93333	0.042	1	6	embryonic morphogenesis
BP	CCR	GO:0043549	0.041374	32.93333	0.042	1	6	regulation of kinase activity
BP	CCR	GO:1904029	0.041374	32.93333	0.042	1	6	regulation of cyclin-dependent protein kinase activity
BP	CCR	GO:0000079	0.041374	32.93333	0.042	1	6	regulation of cyclin-dependent protein serine/threonine kinase activity
BP	CCR	GO:0051338	0.041374	32.93333	0.042	1	6	regulation of transferase activity
BP	CCR	GO:0050790	0.041374	32.93333	0.042	1	6	regulation of catalytic activity
BP	CCR	GO:0065009	0.041374	32.93333	0.042	1	6	regulation of molecular function
BP	CCR	GO:0071900	0.041374	32.93333	0.042	1	6	regulation of protein serine/threonine kinase activity
BP	CCR	GO:0045859	0.041374	32.93333	0.042	1	6	regulation of protein kinase activity
BP	CTmax	GO:0044770	0.00422	7.539683	0.704	4	22	cell cycle phase transition
BP	CTmax	GO:0044772	0.005388	11.02299	0.384	3	12	mitotic cell cycle phase transition
BP	CTmax	GO:0022402	0.011693	5.388571	0.928	4	29	cell cycle process
BP	CTmax	GO:1903047	0.020364	6.155172	0.608	3	19	mitotic cell cycle process
BP	CTmax	GO:0048523	0.021385	3.205917	2.272	6	71	negative regulation of cellular process
BP	CTmax	GO:0044843	0.024638	10.68889	0.256	2	8	cell cycle G1/S phase transition
BP	CTmax	GO:0000082	0.024638	10.68889	0.256	2	8	G1/S transition of mitotic cell cycle
BP	CTmax	GO:0070647	0.031049	9.152381	0.288	2	9	protein modification by small protein conjugation or removal

BP	CTmax	GO:0007049	0.038025	3.594595	1.312	4	41	cell cycle
BP	CTmax	GO:2000113	0.04019	3.015873	1.952	5	61	negative regulation of cellular macromolecule biosynthetic process
BP	CTmax	GO:0010558	0.04019	3.015873	1.952	5	61	negative regulation of macromolecule biosynthetic process
BP	CTmax	GO:0051172	0.04019	3.015873	1.952	5	61	negative regulation of nitrogen compound metabolic process
BP	CTmax	GO:0031324	0.04019	3.015873	1.952	5	61	negative regulation of cellular metabolic process
BP	CTmax	GO:0031327	0.04019	3.015873	1.952	5	61	negative regulation of cellular biosynthetic process
BP	CTmax	GO:0009890	0.04019	3.015873	1.952	5	61	negative regulation of biosynthetic process
BP	CTmax	GO:0000278	0.042428	4.448276	0.8	3	25	mitotic cell cycle
BP	CTmax	GO:0044260	0.044224	2.457778	3.392	7	106	cellular macromolecule metabolic process
BP	CTmax	GO:0009889	0.045356	2.905492	2.016	5	63	regulation of biosynthetic process
BP	CTmax	GO:2000112	0.045356	2.905492	2.016	5	63	regulation of cellular macromolecule biosynthetic process
BP	CTmax	GO:0010556	0.045356	2.905492	2.016	5	63	regulation of macromolecule biosynthetic process
BP	CTmax	GO:0031326	0.045356	2.905492	2.016	5	63	regulation of cellular biosynthetic process
MF	CTmax	GO:0000981	0.010249	4.111559	2.752294	7	100	DNA-binding transcription factor activity, RNA polymerase II-specific
MF	CTmax	GO:0003700	0.010249	4.111559	2.752294	7	100	DNA-binding transcription factor activity
MF	CTmax	GO:0140110	0.010249	4.111559	2.752294	7	100	transcription regulator activity

286

287

Supplementary comment 1: Potential confounding factors:

The spiders from all four populations were sampled over a relatively short period, and due to population differences they do not show entirely synchronized phenology. We made an effort to assay spiders in a size-dependent order, nevertheless they exhibited differences in body mass when their thermal limits were estimated (ANOVA, p-value < 2e-16 in all acclimation regimes in both CTmax and CCRTemp). The spiders from Otawi were the heaviest, followed by spiders from Karasburg, Betta, and Stampriet (Figure S5). In order to test if the body mass difference among populations represents a potential confounding factor regarding their thermal tolerances (Anthony et al., 2021; Oyen et al., 2021), we correlated individual CTmax and CCRTemp with body masses for each population separately. In most tests there were non-significant correlations, and no common trend was observed. On the contrary, sometimes there is a negative trend and sometimes a positive trend.

We included time since feeding, since feeding – for practical reasons – was done on specific days for all spiders, and time since feeding could influence temperature tolerances (Manenti et al., 2018; Nyamukondiwa & Terblanche, 2009). We also included the number of days the spiders had spent in the lab at 21˚C before being separated out into acclimation treatments (Preacclimation duration). However, note that time since feeding and preacclimation duration is not biased among populations. In summary, the size of the spiders, their hunger state, and preacclimation duration, did not seem to influence their thermal tolerances in a biased way.

References for supplement:

Anthony, S. E., Buddle, C. M., Høye, T. T., Hein, N., & Sinclair, B. J. (2021). Thermal acclimation has limited effect on the thermal tolerances of summer-collected Arctic and sub-Arctic wolf spiders. *Comparative Biochemistry and Physiology Part A: Molecular & Integrative Physiology*, *257*, 110974. doi: 10.1016/J.CBPA.2021.110974

Busck, M. M., Settepani, V., Bechsgaard, J., Lund, M. B., Bilde, T., & Schramm, A. (2020). Microbiomes and Specific Symbionts of Social Spiders: Compositional Patterns in Host Species, Populations, and Nests. *Frontiers in Microbiology*, *11*, 1–14. doi: 10.3389/fmicb.2020.01845

Liu, S., Aagaard, A., Bechsgaard, J., & Bilde, T. (2019). DNA methylation patterns in the social spider, *Stegodyphus dumicola*. *Genes*, *10*(2), 1–17. doi: 10.3390/genes10020137

Manenti, T., Cunha, T. R., Sørensen, J. G., & Loeschcke, V. (2018). How much starvation, desiccation and oxygen depletion can *Drosophila melanogaster* tolerate before its upper thermal limits are affected? *Journal of Insect Physiology*, *111*, 1–7. doi: 10.1016/J.JINSPHYS.2018.09.002

Nyamukondiwa, C., & Terblanche, J. S. (2009). Thermal tolerance in adult Mediterranean and Natal fruit flies (*Ceratitis capitata* and *Ceratitis rosa*): Effects of age, gender and feeding status. *Journal of Thermal Biology*, *34*(8), 406–414. doi: 10.1016/J.JTHERBIO.2009.09.002

Oyen, K. J., Jardine, L. E., Parsons, Z. M., Herndon, J. D., Strange, J. P., Lozier, J. D., & Dillon, M. E. (2021). Body mass and sex, not local climate, drive differences in chill coma recovery times in common garden reared bumble bees. *Journal of Comparative Physiology B: Biochemical, Systemic, and Environmental Physiology*, *191*(5), 843–854. doi: 10.1007/s00360-021-01385-7

Sumner, L. W., Amberg, A., Barrett, D., Beale, M. H., Beger, R., Daykin, C. A., … Viant, M. R. (2007). Proposed minimum reporting standards for chemical analysis: Chemical Analysis Working Group (CAWG) Metabolomics Standards Initiative (MSI). *Metabolomics*, *3*(3), 211–221. doi: 10.1007/S11306-007-0082-2/METRICS